SPLICE RESEARCH

Progress Report

YIELD-LINE ANALYSIS OF END-PLATE CONNECTIONS WITH BOLT FORCE PREDICTIONS

by

Ramzi Srouji

and

Anant R. Kukreti

Thomas M. Murray

Co-Principal Investigators

Sponsored by

Metal Building Manufacturing Association

and

American Institute of Steel Construction

Report No. FSEL/MBMA 83-05

December 21, 1983

FEARS STRUCTURAL ENGINEERING LABORATORY

School of Civil Engineering and Environmental Science

University of Oklahoma

Norman, Oklahoma 73019

YIELD-LINE ANALYSIS OF END-PLATE CONNECTIONS WITH BOLT FORCE PREDICTIONS

A THESIS

APPROVED FOR THE SCHOOL OF CIVIL ENGINEERING AND ENVIRONMENTAL SCIENCE

By

_____

_____

_____

TABLE OF CONTENTS

LIST OF FIGURES

LIST OF TABLES

ABSTRACT

This study involves the development of a methodology for the design of four types of end-plate configurations using yield-line analysis. The four types of end-plates are: two-bolt flush, four-bolt flush, unstiffened extended with two bolts on either side of the tension flange, and stiffened extended with two bolts on either side of the tension flange. Prediction equations for the bolt forces, including prying action, are also developed. Finite element analyses were conducted for the two-bolt flush end-plate as part of the study.

Experimental verification of the yield-line analysis and the bolt force prediction method was conducted for the two-bolt flush end-plates and the four-bolt flush end-plates. In addition, existing test data for the unstiffened extended end-plates were compared to the analytical procedures developed. A comparison between the data obtained from the testing of the two-bolt and the four-bolt flush end-plate connections was also conducted.

Based on the experimental results obtained, including both strength and stiffness of the connections, design methods are recommended. Since stiffness data was only available for the two-bolt and the four-bolt flush end-plates, complete design procedures for the extended end-plates are not recommended. However, procedures for strength requirements of the two extended end-plate configurations are explained.

YIELD-LINE ANALYSIS OF END-PLATE CONNECTIONS WITH BOLT FORCE PREDICTIONS

CHAPTER I

INTRODUCTION AND LITERATURE REVIEW

1.1 Background

Bolted end-plate connections of different configurations have been extensively used in the metal building industry for moment-resistant connections in portal frame construction. The popularity of these connections is due to economics, ease of fabrication and the assumption that they provide a rigid moment connection. Typical end-plate configurations are shown in Figure 1.1. Four different types of end-plates are shown. Figures 1.1(a) and (b) show flush end-plate connections with two and four-bolts at the tension flange. Figures 1.1(c) and (d) show stiffened and unstiffened extended end-plate connections with two-bolts on either side of the tension flange. The configuration shown in Figure 1.1(c) is referred to as a stiffened, extended end-plate connection. The end-plate may connect a beam to the end-plate of another beam or to a column flange, as in Figures 1.2(a) and (b). A connection between two beams is usually referred to as a "splice connection".

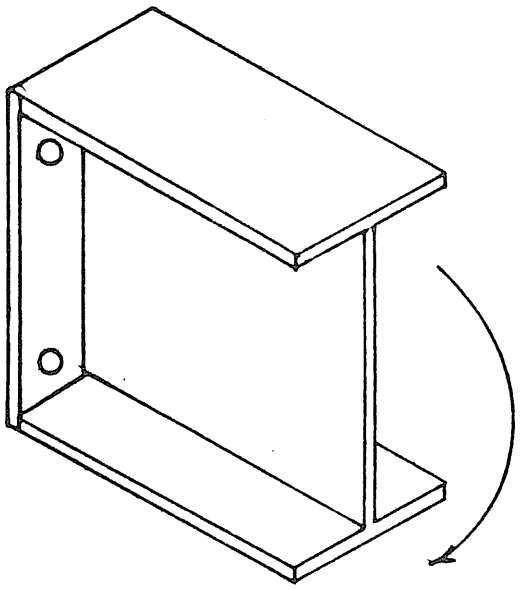

(a) Two-Bolt Flush End-Plate

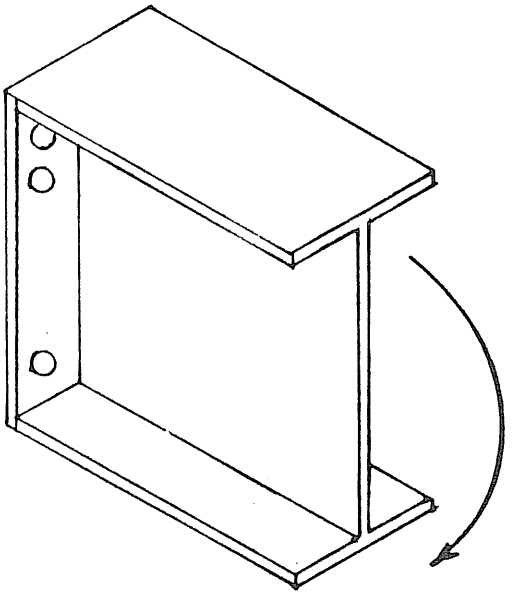

(b) Four-Bolt Flush End-Plate

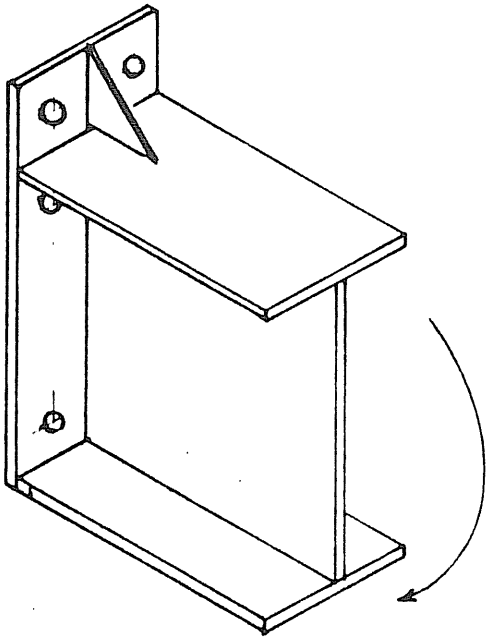

(c) Stiffened Extended End-Plate

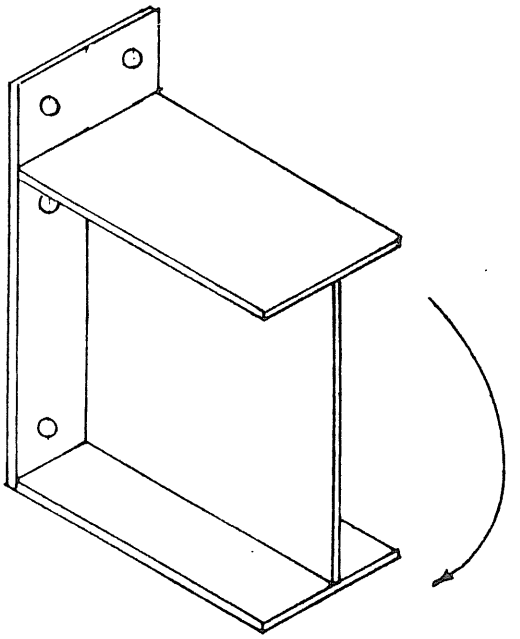

(d) Unstiffened Extended End-Plate

Figure 1.1 Typical End-Plate Configurations

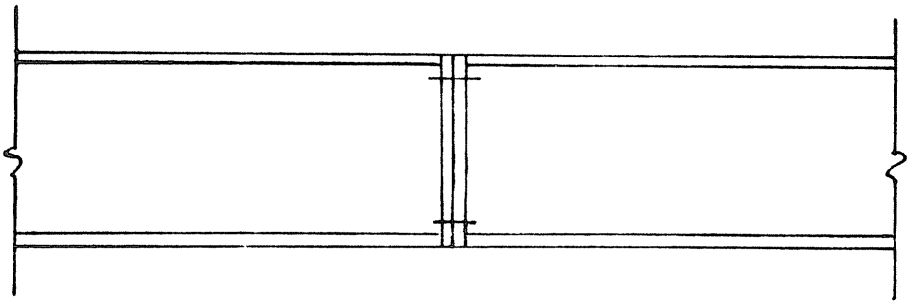

(a) Splice-Plate Connection

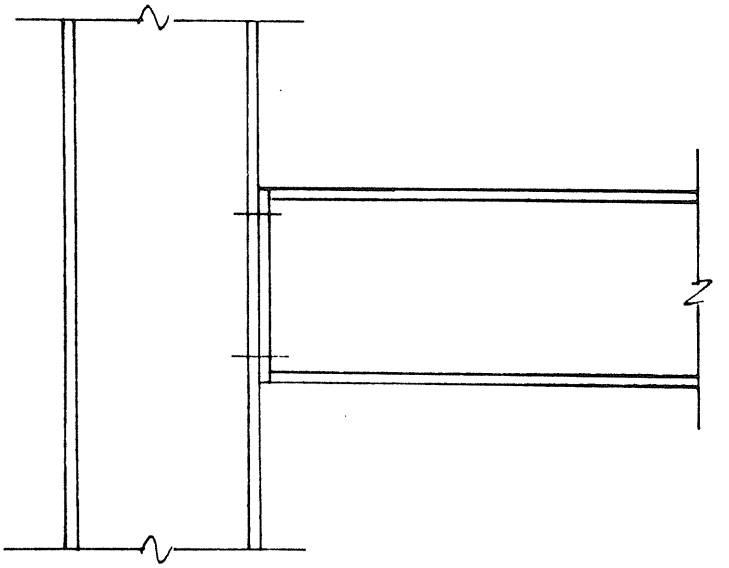

(b) Beam-to-Column Connection

Figure 1.2 Typical Uses of End-Plate Connections

Although design procedures have been suggested to determine end-plate thickness using yield-line theory, the finite-element method, and experimental test data, the variation between the different methods is large. Similarly, a wide variety of methods have been suggested to predict the bolt forces that are developed in end-plates. Some of these methods are based on the assumption that prying action does not exist or, if it does, it can be neglected. While other methods assume that prying action affects the bolt forces that are developed, and therefore cannot be neglected.

The purpose of this study is to develop a rational method of design for the four different types of end-plates that are shown in Figure 1.1 (a-d), a prediction equation for the bolt forces, and to verify the results through comparison with available experimental data and an extensive experimental testing program for the two-bolt flush end-plate and the four-bolt flush end-plate connections.

Current literature dealing with the different design and bolt force prediction methods is first reviewed followed by the development of the yield-line design procedures for the four types of end-plate connections. Both straight and curved yield-line analyses were considered for the two-bolt flush end-plate connection, but only straight yield-line analyses were considered for the other three end-plate types. For the bolt force prediction equations, it was assumed that the prying action is of major importance. Therefore, prediction equations for the prying action are also developed. In Chapter III the testing procedure and the instrumentations that were used are described. In addition, the

test results for the two-bolt flush end-plate and the four-bolt flush end-plate connection tests are presented and compared to the different analytical procedures that are described in Chapter II. Also, some of the available experimental test data dealing with the stiffened and unstiffened extended end-plate connections are presented. In Chapter IV a design procedure is proposed based on the comparison of the analytical and experimental results. Then conclusions and recommendations for further study are presented.

1.2 Literature Review

Douty and McGuire[1] in 1965 suggested that the end-plate should be proportioned to resist a moment equal to the beam flange force times the distance from the center of the beam flange to the nearest row of bolts. This rationalization is based on the assumption that the end-plate is cantilevered from the nearest row of tension bolts under the action of the tension flange forces. They also suggested use of the material yield point as the maximum stress level in the end-plate when the stress at the beam flange is also at the yield point. The required end-plate thickness can then be calculated using the following equation:

$$m_p b_f = b_f t_f F_{by}(p_t - t_f/2) \qquad (1.1)$$

in which m_p = plastic moment capacity of plate per unit length = $F_{py}t_p^2/4$, F_{py} = yield stress of the plate material, t_p = thickness of end-plate, b_f = width of end-plate and of beam flange, t_f = thickness of flange, F_{by} = yield stress of beam material, and p_t = pitch measured from top of flange to centerline of the bolt row. Rearranging Equation 1.1 and assuming $F_{by} = F_{py}$, the required end-plate thickness is

$$t_p = \sqrt{4t_f(p_t - t_f/2)} \tag{1.2}$$

Blockley[2] in a 1970 BCSA Booklet used a yield-line pattern for which the beam web was assumed to deliver the entire bolt force to the end-plate. Again, the end-plate is assumed to act as a cantilever. The resulting required thickness of an end-plate in the case where two rows of tension bolts are used, i.e. four tension bolts, is

$$t_p \geq \sqrt{(2P_p x)/(p_b F_{py})} \tag{1.3}$$

where P_p = bolt proof load, x = distance from the edge of the bolt head to the beam web, and p_b = vertical bolt pitch between upper and lower rows of tension bolts.

The German[3] and French Specifications[4] for steel construction provide formulas to determine the moment capacity of flush end-plate connections with known plate thickness. These formulas can be rearranged to determine the end-plate thickness, if the tension bolts are not allowed to exceed the bolt proof load. In the German Specification it is assumed that the flange force is transferred only to the bolts adjacent to the tension flange. From the German Specification

$$t_p \geq \sqrt{\frac{4}{F_{py}(b_f - 2d_h)} \left[\frac{2P_p h_s c_1}{(h-t_f)} - \frac{b_f F_{by} t_f^2}{4}\right]} \tag{1.4}$$

in which d_h = bolt hole diameter, h_s = distance between bolt center and compression flange, and c_1 = ($p_f - \frac{3}{2}t_f - t_p/2$ - diameter of washer 4). However it is recommended that

$$t_p \geq 1.5d_b \tag{1.5}$$

for two bolt rows. The French Specifications formula was experimentally

determined on the basis of 171 test results. It requires

$$t_p \geq P_p \{(a_2/a_1) + (p_f/2a_5)\}^{-1}/3750 \qquad (1.6)$$

where a_1 = distance from bolt centerline to edge of web root fillet, a_2 = distance from bolt centerline to web, and a_5 = distance from top bolt row centerline to edge of flange root fillet. Equation 1.6 is to be used with metric units only.

Zoetermeijer[5] in 1981 analyzed an infinitely long plate bounded by two fixed edges and one free edge and loaded with a concentrated force using yield-line theory. As a result of this analysis a chart was developed by which the ultimate load of a stiffened column flange or a flush end-plate can be determined once the distance from the bolt to the beam flange and web are known. However, he notes that the analysis was only an approximation. For the bolt proof load to be developed, the end-plate thickness required is

$$t_p \geq \sqrt{(4P_p)/(F_{py}\alpha)} \qquad (1.7)$$

where α = coefficient depending on bolt arrangement (Zoetermeijer).

Packer and Morris[6] (1977) also used curved yield-lines to predict end-plate capacity with testing directed at the failure of the column flange. Due to limited experimental data, the study did not give any conclusive results. Subsequently, Phillips and Packer[7] (1981) conducted a series of tests to determine the influence of the end-plate thickness on moment rotation characteristics and the end-plate collapse mechanism. They also studied end-plate connections with two rows of tension bolts in order to study the influence of the second row on the stiffness of the connection.

They also suggest two failure mechanisms for end-plates with two rows of bolts, by which they determine the required thickness of the end-plate. They concluded that flush end-plates with two rows of two bolts in the tension region are suitable for semi-rigid construction, and that the second row of tension bolts is effective but to a much lesser extent than previously estimated. They also concluded that the French design specifications best predict the connection moment capacity when the bolt proof load can be reached before plate failure.

Mann and Morris[8] reviewed previous research programs and proposed a design procedure for the extended end-plate connection. They suggest that in plastic design, connections must fulfill two basic requirements. First they must be strong enough to withstand hinge moments and second they must provide adequate hinge rotation while sustaining these moments. The end-plate design method was based on the assumption that some form of yield line pattern will develop. The recommended design procedure includes methods to determine both bolt size and end-plate thickness. The bolt force is assumed to be a combination of direct force and induced prying force. In the case of direct force, the lower bolts carry the greater share of load, because of the added stiffness of the end-plate due to the web. However, the prying force in the bolts are distributed in the opposite sense. An increase of 33% onto the direct force is suggested rather than a precise calculation of the prying action. The equation for the tensile bolt load is

$$B = \frac{1.33\ F_f}{4} = \frac{F_f}{3} \qquad (1.8)$$

where F_f = force in the flange = $M_u/(d-t_f)$, B = bolt load. The equation for the end-plate thickness is given as

$$t_p = \left[\frac{F_f\, p_f}{F_{py}\, b_f}\right]^{\frac{1}{2}} \qquad (1.9)$$

where p_f = the distance between the bolt centerline and the face of the flange. If the recommended end-plate dimensions are used with high strength bolts then

$$t_p = 1.2\, d_b \qquad (1.10)$$

Krishnamurthy [9] exhaustively studied, both analytically and experimentally, the unstiffened extended end-plate with two bolts on either side of the tension flange. His resulting design procedure was adopted in the 8-th Edition of the AISC Manual of Steel Construction[10]. The design method suggested was a direct result of a 2-D and/or 3-D finite-elements analysis. From Krishnamurthy's theoretical studies, it was concluded that even though prying action is present, it is overly conservative to consider this action in the design of the end-plate.

Krishnamurthy[11] (1979) investigated the validity of his design procedure by testing nine different specimens. The end-plates were tested as beam-to-beam connections and each of these specimens was able to reach or exceed its theoretical plastic moment capacity of the beam. Most of the specimens, however, failed due to torsion or compression flange buckling at load points. Krishnamurthy[12] (1980) further investigated his suggested design procedure by using thin splice plates to determine how much thinner the plates could get before the connection

became bolt- or plate-critical. The major outcome of this investigation was the conclusion that the prying phenomenon is not critical in end-plate design procedures.

Krishnamurthy[13] (1978) also investigated the behavior of stiffened end-plate connections using two bolts on either side of the tension flange. For this study, the tension region was modeled as a tee-stub. The purpose of the study was to develop information on the effect of the stiffeners on the behavior of tee-stubs, and of end-plates. The prediction equation suggested for the end-plate thickness is given by,

$$t_p = 0.069 \left(\frac{F}{F_{yb}} \frac{F_y}{f_b} \right)^{0.653} \left(\frac{p_f^{0.655} \, e^{(s_t/b_f)}}{d_b^{0.613} \, b_f^{0.348}} \right) \qquad (1.11)$$

where f_b = plate bending stress, s_t = stiffener thickness. The conclusions and design equations presented were based purely on computer analysis. Later, Krishnamurthy[14] (1979) tested stiffened tee-stub specimens to verify the analytical results. The results were reported to be within 25 percent variation with most error on the conservative side. It was found that a reduction of end-plate thickness can be obtained by the use of stiffeners. However, no formal design procedure was recommended.

Kennedy, Vinnakota and sherbourne[15] (1981) used the split-tee analogy for certain bolted splices and beam-column connections. They identified three types of end-plate behavior. The first case, to which all end-plates belong under low applied loads, is identified by the absence of plastic hinges in the end-plate and the end-plate is said to

be "thick". The upper limit on this behavior occurs at a load which causes yielding in the end-plate at the beam flange. Once this load is exceeded, a plastic hinge is formed at the flange and the end-plate is said to be of "itermediate" thickness. As the load is increased, a second plastic hinge forms at the bolt lines. At this load the end-plate is considered to be a "thin" plate. The analytical model for their theory is shown in Figure 1.3.

Kennedy et. al. consider bolt force to be the sum of a portion of the flange force and prying forces. They identify three stages of prying action corresponding to the three phases which the end-plate goes through. For "thick" plates, the prying force is assumed to be zero. When the end-plate is considered as "thin", the prying force is at its maximum. For "intermediate" plates, the prying forces are somewhere between zero and the maximum value. The equation for the maximum prying force is given as

$$Q_{max} = \frac{w' t_p^2}{4a} \sqrt{F_{py}^2 - 3\left(\frac{F'}{w' t_p}\right)^2} \qquad (1.12)$$

where Q_{max} = maximum prying force, w' = width of end-plate per bolt at bolt line minus bolt hole, a = distance from edge of end-plate to bolt line, and F' = flange force per bolt. The value of a is to be limited to $a \geq 2.5d_b$ and $a \leq 2t_p$. For initial design it is suggested that

$$2d_b < a < 3d_b$$

for "intermediate" end-plates, the following equation for prying force is suggested.

$$Q = \frac{F_p}{a} - b_f t_p^2 \sqrt{F_{py}^2 - 3\left(\frac{F}{b_f t_p}\right)^2} - \frac{\pi d_b^3}{32a} F_{yb} \qquad (1.13)$$

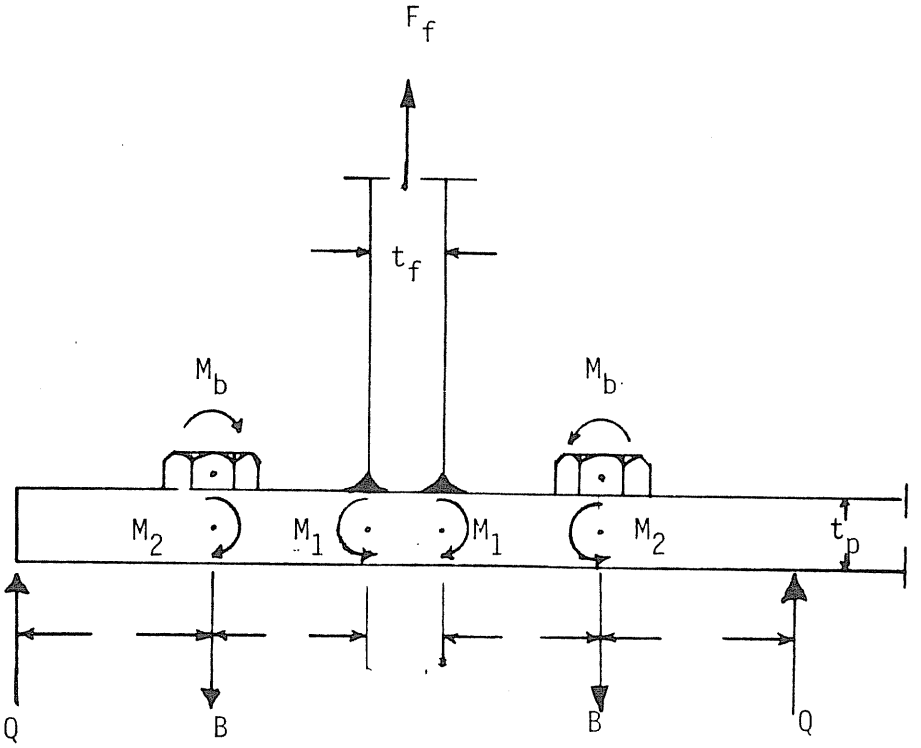

Figure 1.3 Kennedy et. al. Analytical Model

Kennedy et. al. suggest a design method based on their findings, however, the above results are based on only two tests. They suggest that for ideal design, the end-plate should be "thick" under service loads, "intermediate" under factored loads and function as a "thin" plate at ultimate loads.

To evaluate the several design procedures described above for the various end-plate types, the required end-plate thicknesses were determined for a number of configurations. For the one-row flush end-plate connections, Table 1.1 shows the thicknesses determined for the eight specimens tested using five different design methods. Table 1.2 shows the thicknesses determined for the two-row flush end-plate connection specimens that were tested. Six specimens were designed using four different methods. For the extended unstiffened end-plates, the examples in the AISC manual are used for comparison with the Kennedy et. al. [15] and Mann and Morris [8] procedures. The results are shown in Table 1.3. For the stiffened extended end-plate, the only design equation is the one given by Krishnamurthy [13] for the stiffened tee-stub. Therefore, no comparison is possible.

It is evident from Tables 1.1 - 1.3 that the variation between the different methods for the different end-plate types is as large as 100% in some cases. Hence, it is difficult to justify any of the methods for design and additional research is required. Further, no concrete data is available on the moment - curvature ($M - \Phi$) relationships for the two types of flush end-plate connections. Hence,

Table 1.1
Required Thickness for Two-Bolt Flush End-Plate Connections

Case No.	Required End-Plate Thickness (in.)					
	Douty & McGuire	German Specification		French Spec.	Zoetermeijer	Kennedy et al.
		Required	Recommended			
F1-3/4-1/2-16	1.27	0.71	1.13	1.07	0.50	0.68
F1-3/4-3/8-16	1.27	0.71	1.13	1.07	0.50	0.49
F1-5/8-1/2-16	1.41	0.70	0.94	.75	0.43	0.77
F1-5/8-3/8-16	1.25	0.47	0.94	.72	0.38	0.53
F1-5/8-3/8-10	1.17	0.38	0.94	.70	0.36	0.54
F1-5/8-1/2-10	1.27	0.54	0.94	.74	0.39	0.74
F1-3/4-1/2-24A	1.37	0.85	1.13	1.07	0.49	0.77
F1-3/4-1/2-24B	1.22	0.62	1.13	1.04	0.46	0.73

Table 1.2
Required Thickness for two-row Flush End-plate Connection

Case No.	Douty & McGuire	Blockley	German	French
F2-5/8-1/2-16	1.41	0.69	0.94	0.75
F2-5/8-3/8-16	1.25	0.59	0.94	0.72
F2-3/4-3/8-24	1.37	0.78	1.13	1.07
F2-3/4-1/2-24	1.22	0.72	1.13	1.04
F2-3/4-1/2-16	1.27	0.81	1.13	1.07
F2-3/4-3/8-16	1.27	0.81	1.13	1.07

Table 1.3
Extended Unstiffened Design Comparisons

AISC	Mann and Morris P_f = 1.3/8	Kennedy et. al.
0.75	0.72	0.90
0.625	0.58	0.72

the following research program was undertaken.

1.3 Scope of Research

As previously mentioned, the purpose of the research described here is to develop design procedures for the four types of end-plates shown in Figure 1.1. The Design procedure will provide criteria for:

1. Determination of end-plate thickness using given geometry and material yield stress, e.g. strength criterion.
2. Determination of required bolt diameter including prying effects using given end-plate geometry and thickness, and bolt pretension and proof load forces, e.g. bolt force criterion.
3. Determination of the moment-curvature relationship of the entire connection so that possible effects of connection flexibility can be accounted for in the frame design, e.g., stiffness criterion.

The strength criterion is developed using yield-line analysis for the four types of end-plates from which end-plate thickness is determined. The bolt strength requirements are developed using a modified version of the procedure suggested by Kennedy et. al.[15]. Finally, the finite element method is used to develop moment - curvature relationship for the one-row flush end-plate connection. For the two-row flush end-plate connection a simpler method was used, which will be described in chapter II. The analytical developments for the strength and bolt force criteria are described in sections 2.1 and 2.2,

respectively. The basic finite element modeling techniques are discussed in section 2.3.

Eight full-scale one-row flush end-plate connections were tested as well as six two-row flush end-plate connections to verify the analytical results obtained for the two connections. The test specimens, set-up, and procedures are described in chapter III. Comparisons are made with the yield-line strength and bolt force analytical results and with predictions from the finite element analyses. In addition comparisons are made with available test data and the analytical results for the extended end-plates. Finally, design procedures for end-plate thickness and bolt strength are presented for the four end-plate configurations in chapter IV.

CHAPTER II

ANALYTICAL STUDY

2.1 Yield-Line Theory

2.1.1 General

Yield-line theory was first introduced to analyze reinforced concrete slabs. A yield line is a continuous formation of plastic hinges along a straight or curved line. The failure mechanism of the slab is assumed to exist when the yield lines form a Kinematically valid collapse mechanism. Since the elastic deformations are negligible compared to the plastic deformations, it has been proven acceptable to assume that the yield lines divide the slab into rigid plane regions.

Generally, yield-line patterns are assumed to be a series of straight lines, however, some work has been done with curved yield lines. To establish the location of a yield line, the following guidelines should be followed:

1. Axes of rotation generally lie along lines of support.

2. Yield lines pass through the intersection of the axes of rotation of adjacent plate segments.

3. Along every yield line, the bending moment is assumed to be a constant and is taken as the plastic moment of the plate.

The analysis of a yield-line mechanism can be performed by two different methods, the equilibrium method and the virtual work or energy method. The latter method is comparatively simple and straightforward and is preferred.

In this method, the external work done by the applied loads from a small arbitrary virtual deflection is set equal to the internal work done as the plate rotates at the yield lines to accommodate this virtual deflection. For a specified yield-line pattern and loading, a certain plastic moment will be required along the hinge lines. For the same loading, other patterns may result in a larger required plastic moment capacity. Hence, the controlling pattern is the one pattern which requires the largest required plastic moment. Or conversly, for a given plastic moment capacity, the controlling mechanism is the one which produces the lowest failure load. This implies that the yield-line theory is an upper bound procedure and the least upper bound must be found.

To determine the required plastic moment capacity or the failure load, an arbitrary succession of possible yield-line mechanisms must be selected. By equating the internal and external work, the relation between the applied loads and the ultimate resisting moments is obtained. The resulting equation is then solved for either the unknown loads or unknown moments, and by comparing the different values obtained from the various mechanisms the controlling minimum load (or maximum required plastic moment) is obtained.

The internal energy stored in a particular yield-line

mechanism is the sum of the internal energy stored in each yield line forming the mechanism. The internal energy stored in any given yield line is obtained by multiplying the normal moment on the yield line with the normal rotation of the yield line. Thus the energy stored in the n-th yield line of length L_n is

$$W_{in} = \int_{Ln} m_p \, \theta_n \, ds \tag{2.1}$$

where θ_n is the relative rotation of line n, and ds is the elemental length of line n. The internal energy stored by a yield-line mechanism can be written as

$$W_i = \sum_{n=1}^{N} \int_{Ln} m_p \, \theta_n \, ds$$

$$= \sum_{n=1}^{N} m_p \, \theta_n \, Ln \tag{2.2}$$

where N is the number of yield lines in the mechanism.

In complicated yield-line patterns the values of the relative rotation are somewhat tedious to obtain, therefore, it is more convenient to resolve the slopes and moments in the x- and y- directions. This results in the following form of Equation 2.2

$$W_i = \sum_{n=1}^{N} (m_{px} \, \theta_{nx} \, L_x + m_{py} \, \theta_{ny} \, L_y) \tag{2.3}$$

in which m_{px} and m_{py} are the x- and y- components of the normal moment capacity per unit length, L_x and L_y are the x- and y- components of the yield line length, and θ_{nx} and θ_{ny} are the x- and y- components of the relative normal rotation of yield line n.

To calculate the values of θ_{nx} and θ_{ny}, convenient straight

lines parallel to the x- and y- axis in the two segments intersecting at the yield line are selected and their relative rotation calculated by selecting straight lines with known displacements at the ends.

The same method of solution can be used for curved yield lines. However, the internal work must include energy stored along radial lines. Mansfield[16] has shown that the internal energy stored in a segment bounded by a curved yield line, Figure 2.1, is given by

$$W_i = 2m_p \, \delta(\pi - \beta)\mathrm{Sec}^2\phi \qquad (2.4)$$

where δ = normalized displacement of the yield line at point O, Figure 2.1, and β and ϕ are defined in Figure.

2.1.2 Application to End-Plates

A number of yield-line patterns were investigated for each one of the end-plates shown in Figure 1.1. The various mechanisms investigated for the four end-plates are found in Appendix B. For each one of the end-plates, with the range of parameters investigated, one straight yield-line mechanism controls. Curved yield-line mechanisms were used in the analysis of the one-row flush end-plate connections only. The controlling straight yield-line and curved yield-line mechanism for that connection are shown in Figure 2.2 and 2.3, respectively. The geometric parameters are also defined in the figures. The internal energy stored in the straight yield-line mechanism shown in Figure 2.2 is given by

$$W_i = 4m_p \frac{(h - P_t)}{h} \left[\frac{b_f}{2}\left(\frac{1}{P_f} + \frac{1}{s}\right) + (P_f + s)(2/g) \right] \qquad (2.5)$$

where P_f = the distance from the bolt centerline to the face of the

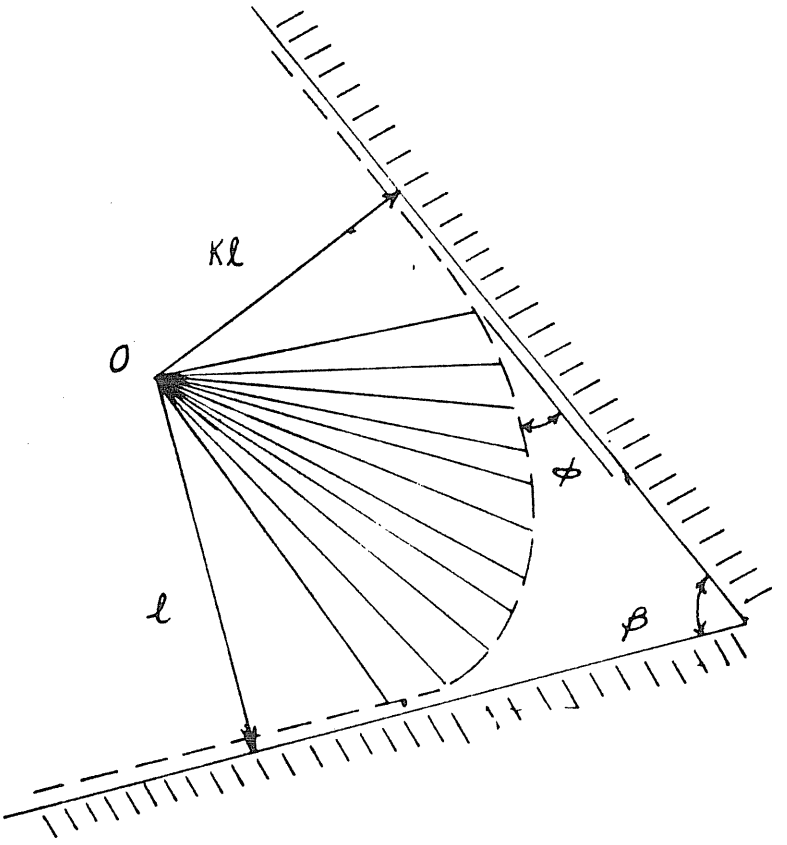

Figure 2.1 Definition for Curved Yield-Line

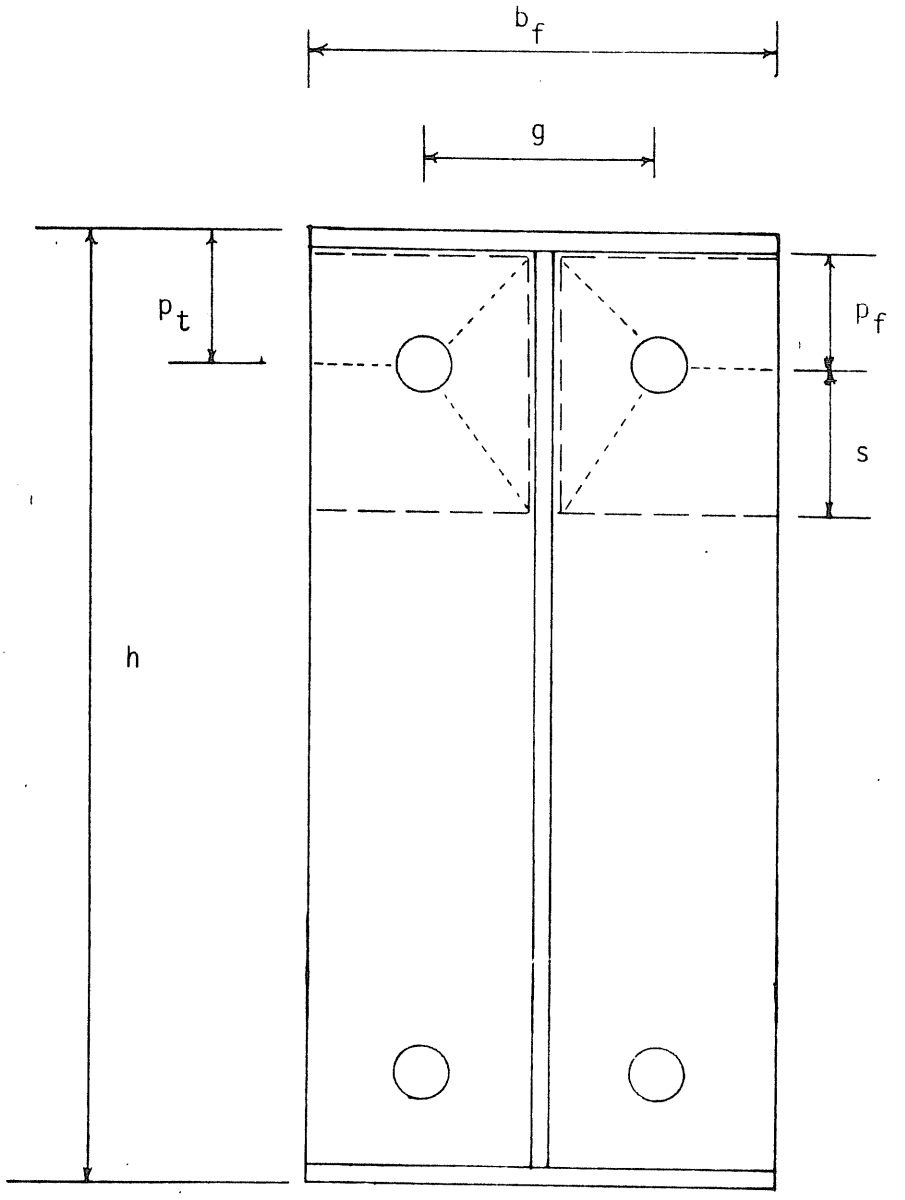

Figure 2.2 Straight Yield-Line Mechanism for Two-Bolt Flush End-Plate

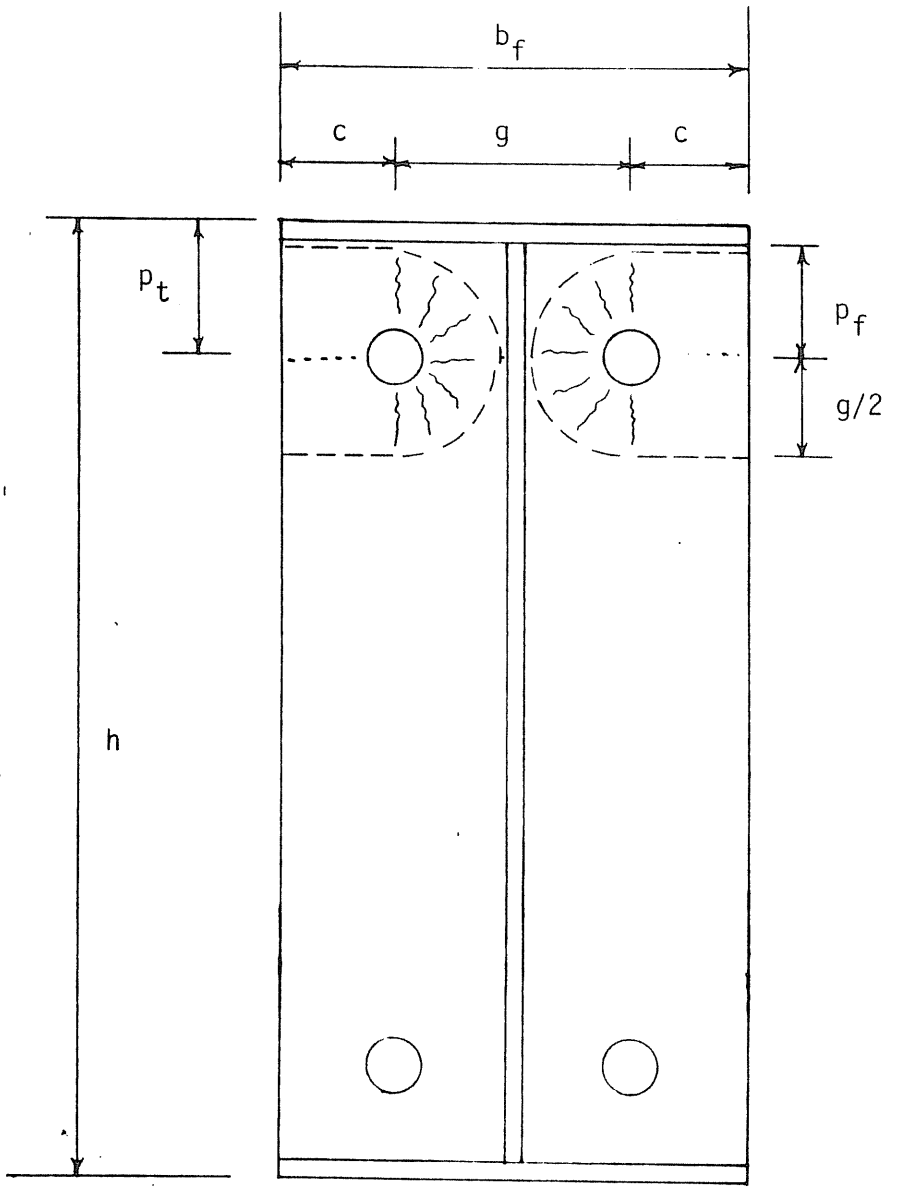

Figure 2.3 Curved Yield-Line Mechanism for Two-Bolt Flush End-Plate

flange, equal to $(P_t - t_f)$, and s = the distance between parallel yield lines, to be determined . The unknown quantity s in Equation 2.5 is obtained by differentiating the internal work equation with respect to s and equating to zero, resulting in

$$s = \frac{1}{2}\sqrt{b_f g} \tag{2.6}$$

The internal energy stored in the yield-line pattern show in Figure 2.3 is calculated using Equation 2.4 with the following: $\delta = 1 - P_t\theta$, $\beta = \pi/2$ and

$$\phi = \tan^{-1}\{(\ln\kappa)/(\pi - \beta)\} \tag{2.7}$$

where $\kappa = 2P_f/g$

Adding up the internal energy stored in all yield lines in the mechanism, the total internal energy is

$$W_i = 4m_p/h \left[c\left(\frac{h - P_t}{P_f} + 2\left(\frac{h - P_t - P_f}{g}\right) + 1\right) + \frac{(h - P_t)\pi}{2} + (h - t_f)\frac{\pi}{2}\sec^2 \tan^{-1} 2\,\mathrm{Ln}\left(\frac{2P_t/g}{\pi}\right)\right] \tag{2.8}$$

The controlling mechanism for the two-row flush end-plate is shown in Figure 2.4. The internal energy stored in this mechanism is given by

$$W_i = \frac{4m_p}{h}\left[\frac{b_f}{2}\left(\frac{h-p_t}{p_f} + \frac{h-p_{t2}}{u}\right) + 2(p_f+p_b+u)\left(\frac{h-p_t}{g}\right)\right] \tag{2,9}$$

where P_{t2} = the distance from the top of the tension flange to the second bolt row, P_b = pitch between bolt rows, and u = the distance between parallel yield lines, to be determined. The unknown quantity u is determined in the same manner as s, e.g., by differentiating the internal work equation with respect to u and equating to zero,

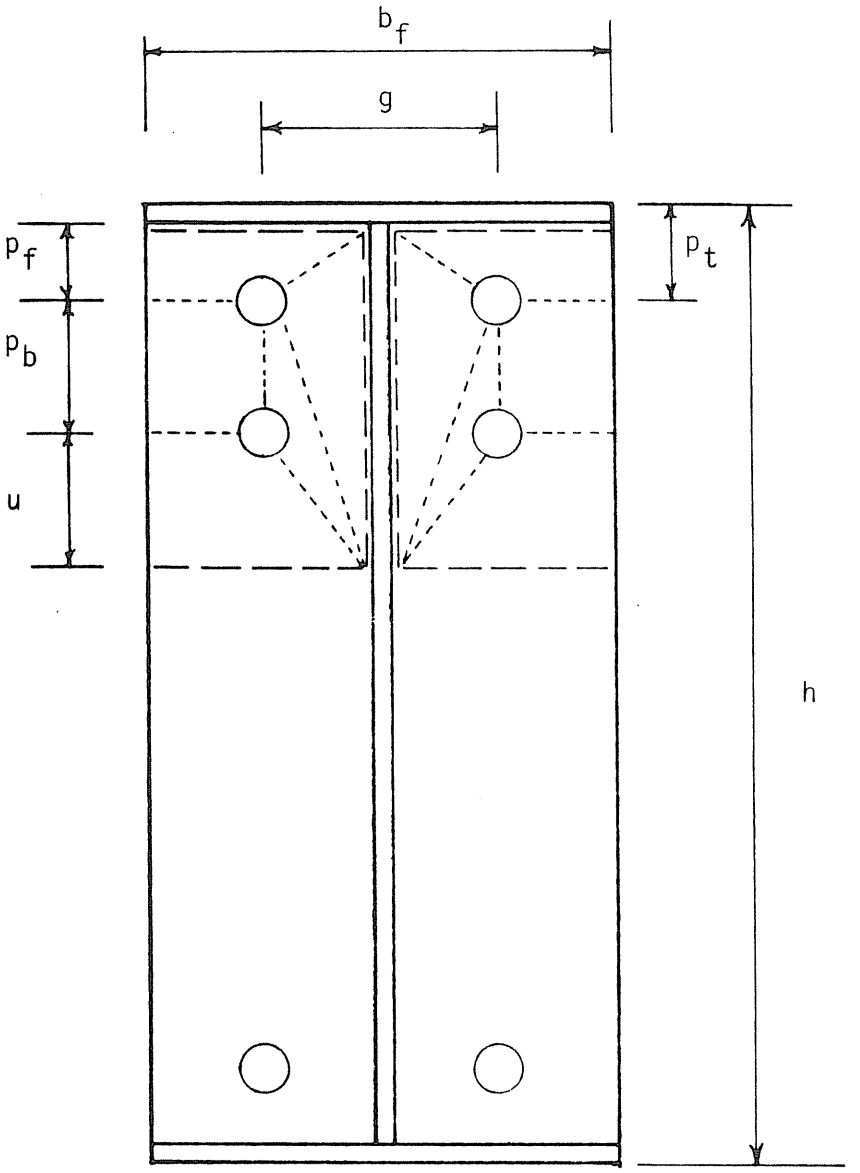

Figure 2.4 Yield-Line Mechanism for Four-Bolt Flush End-Plate

resulting in

$$u = \frac{1}{2}\sqrt{b_f g \frac{h - P_{t_2}}{h - P_t}} \tag{2.10}$$

For the unstiffened extended end-plate, the controlling mechanism is shown is Figure 2.5. Using the above procedures, the internal energy stored in the yield lines of this mechanism is

$$W_i = \frac{4m_p}{h}\left[\left(\frac{b_f}{2}\left(\frac{1}{P_f} + \frac{1}{s}\right) + (P_f + s)(2/g)\right)(h - P_t) + \frac{b_f}{2}\left(\frac{1}{2} + \frac{h}{P_f}\right)\right] \tag{2.11}$$

The controlling mechanism for the stiffened extended end-plate is shown in Figure 2.6. The internal energy stored in this mechanism is given by

$$W_i = \frac{4m_p}{h}\left[\left(\frac{b_f}{2}\left(\frac{1}{P_f} + \frac{1}{s}\right) + (P_f + s)(2/g)\right)\left((h - P_t) + (h + P_f)\right)\right] \tag{2.12}$$

However, if s is greater than d_e, the distance from the bolt line above the tension flange to the edge of the plate, the equation for the mechanism becomes

$$W_i = \frac{4m_p}{h}\left[\left(\frac{b_f}{2}\left(\frac{1}{P_f} + \frac{1}{2s}\right) + (P_f + d_e)(2/g)\right)\left((h - P_t) + (h + P_f)\right)\right] \tag{2.13}$$

For all the end-plates, the external work done due to a unit displacement at the top of the tension beam flange, resulting in a rotation of the beam cross-section about the outside of the compression flange is given by

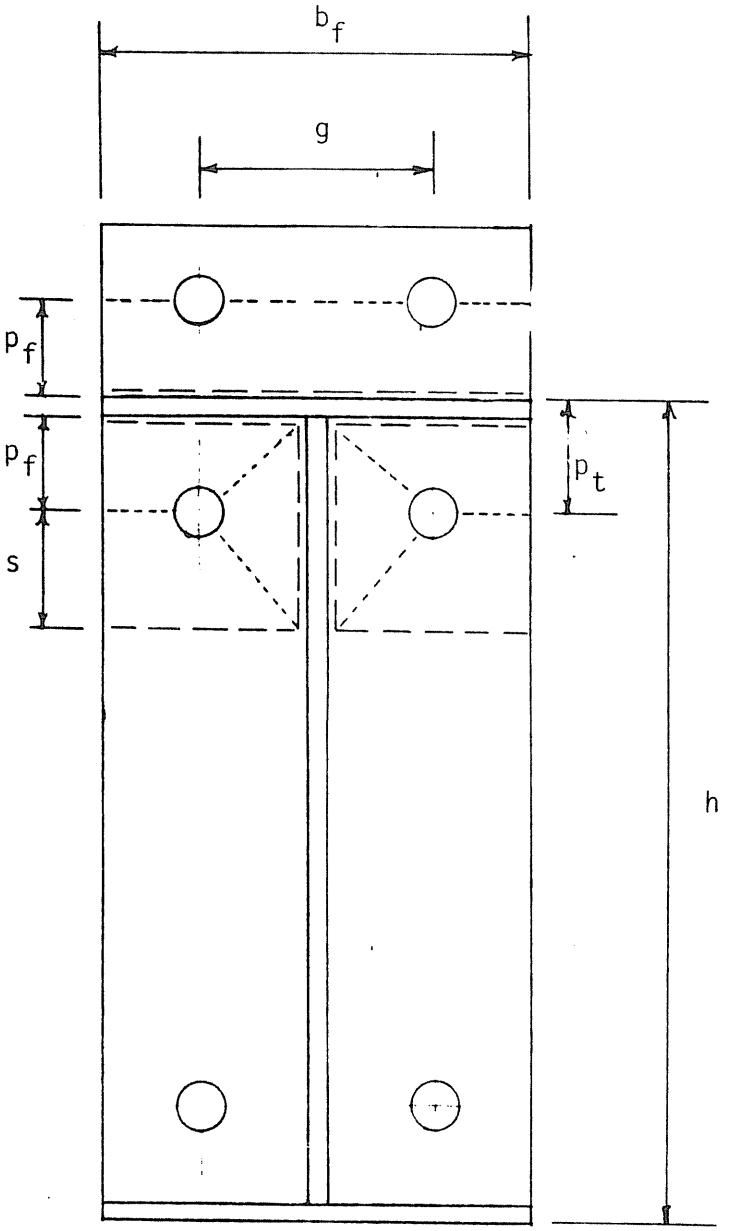

Figure 2.5 Yield-Line Mechanism for Unstiffened Extended End-Plate

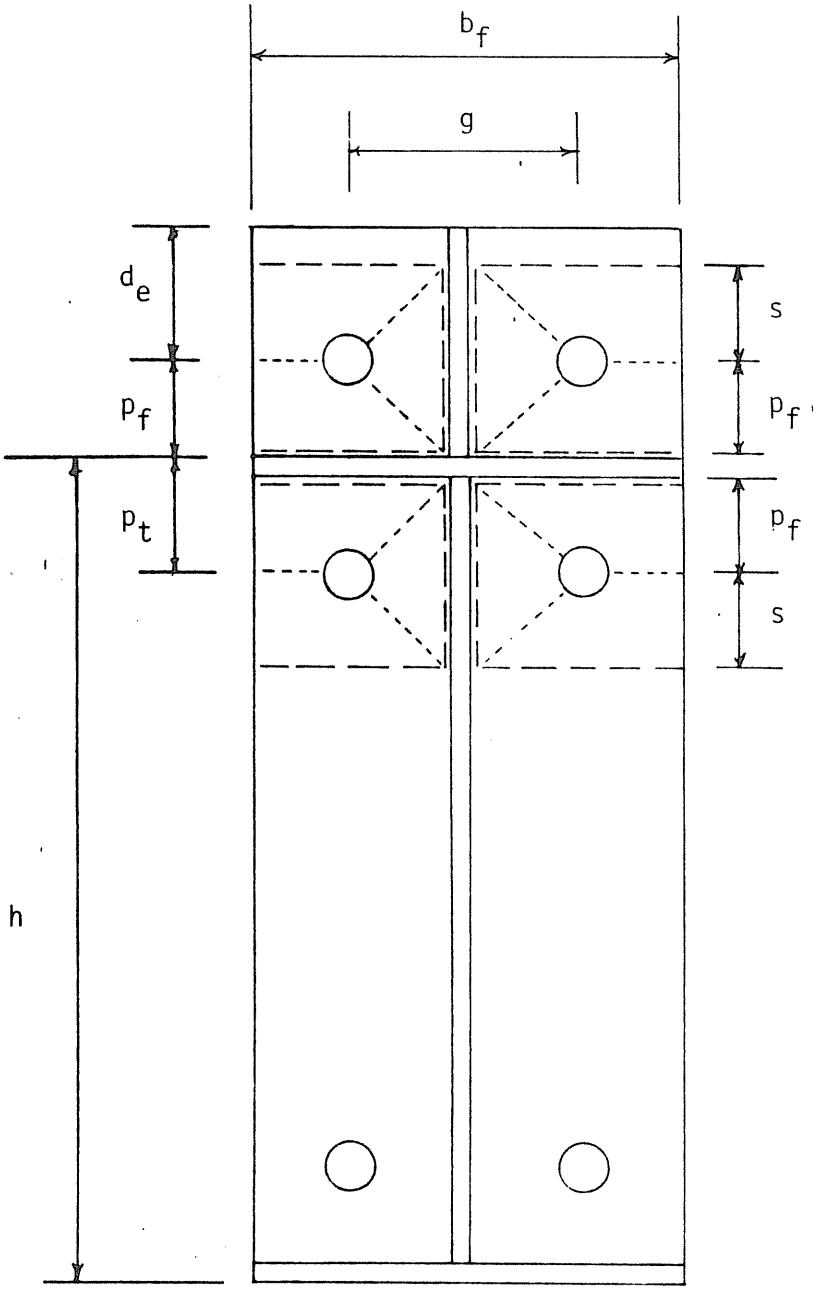

Figure 2.6 Yield-Line Mechanism for Stiffened Extended End-Plate

$$W_e = M_u \theta \tag{2.14}$$

where Mu = factored beam moment at the end-plate, and θ = the rotation at the connection, equal to 1/h, where h = beam depth.

On equating the internal and external work terms and cancelling θ, the expression for the ultimate moment, Mu, can be obtained. Then by rearranging the expression for Mu, the equation for t_p, the end-plate thickness, can be written in terms of Mu. The equations for both Mu and t_p for the four types of end-plates follow.

One-Row Flush End-Plate

Straight Yield-Line Solution

$$M_u = 4m_p(h-p_t)\left[\frac{b_f}{2}\left(\frac{1}{p_f}+\frac{1}{s}\right)+(p_f+s)(2/g)\right] \tag{2.15}$$

$$t_p = \left[\frac{M_u/F_{py}}{(h-p_t)\left[\frac{b_f}{2}\left(\frac{1}{p_f}+\frac{1}{s}\right)+(p_f+s)(2/g)\right]}\right]^{\frac{1}{2}} \tag{2.16}$$

Curved Yield-Line Solution

$$M_u = 4m_p\left[c\left(\frac{h-p_t}{p_f}+2\left(\frac{h-p_t-p_f}{g}\right)+1\right)+\left(\frac{h-p_t}{2}\right)\pi + (h-t_f)\frac{\pi}{2}\sec^2\tan^{-1}2\,\mathrm{Ln}\left(\frac{2p_t/g}{\pi}\right)\right] \tag{2.17}$$

$$t_p = \left[\frac{M_u/F_{py}}{c\left(\frac{h-p_t}{p_f}+2\left(\frac{h-p_t-p_f}{g}\right)+1\right)+\left(\frac{h-p_t}{2}\right)\pi+X}\right]^{\frac{1}{2}} \tag{2.18}$$

where $X = (h-t_f)\frac{\pi}{2}\sec^2\tan^{-1}2\,\mathrm{Ln}\left(\frac{2p_t/g}{\pi}\right)$

Two-Row Flush End-Plate

$$M_u = 4m_p\left[\frac{b_f}{2}\left(\frac{h-p_t}{p_f} + \frac{h-p_{t2}}{u}\right) + 2(p_f+p_b+u)\left(\frac{h-p_t}{g}\right)\right] \tag{2.19}$$

$$t_p = \left[\frac{M_u/F_{py}}{\frac{b_f}{2}\left(\frac{h-p_t}{p_f} + \frac{h-p_{t2}}{u}\right) + 2(p_f+p_b+u)\left(\frac{h-p_t}{g}\right)}\right]^{\frac{1}{2}} \tag{2.20}$$

Unstiffened Extended End-Plate

$$M_u = 4m_p\left[\left(\frac{b_f}{2}\left(\frac{1}{p_f} + \frac{1}{s}\right) + (p_f+s)(2/g)\right)(h-p_t) + \frac{b_f}{2}\left(\frac{1}{2} + \frac{h}{p_f}\right)\right] \tag{2.21}$$

$$t_p = \left[\frac{M_u/F_{py}}{(h-p_t)\left[\frac{b_f}{2}\left(\frac{1}{p_f} + \frac{1}{s}\right)+(p_f+s)(2/g)\right] + \frac{b_f}{2}\left(\frac{1}{2} + \frac{h}{p_f}\right)}\right]^{\frac{1}{2}} \tag{2.22}$$

Stiffened Extended End-Plate

If $s<d_e$

$$M_u = 4m_p\left[\left(\frac{b_f}{2}\left(\frac{1}{p_f} + \frac{1}{s}\right)+(p_f+s)(2/g)\right)\left((h-p_t)+(h+p_f)\right)\right] \tag{2.23}$$

$$t_p = \left[\frac{M_u/F_{py}}{\left(\frac{b_f}{2}\left(\frac{1}{p_f} + \frac{1}{s}\right)+(p_f+s)(2/g)\right)\left((h-p_t)+(h+p_f)\right)}\right]^{\frac{1}{2}} \tag{2.24}$$

If $s>d_e$

$$M_u = 4m_p\left[\left(\frac{b_f}{2}\left(\frac{1}{p_f} + \frac{1}{2s}\right)+(p_f+d_e)(2/g)\right)\left((h-p_t)+(h+p_f)\right)\right] \tag{2.25}$$

$$t_p = \left[\frac{M_u / F_{py}}{\left[\frac{b_f}{2}\left(\frac{1}{p_f} + \frac{1}{2s}\right) + (p_f + d_e)(2/g)\right]\left[(h - p_t) + (h + p_f)\right]} \right]^{\frac{1}{2}} \qquad (2.26)$$

Results from the above analyses are compared, in Chapter III, to experimental data obtained from the testing program conducted as well as available experimental results.

2.2 Estimation of Bolt Forces

Basic yield-line analysis procedures do not result in bolt forces if prying action is to be considered. Therefore, it was necessary to use a different method to obtain the desired bolt forces. A method suggested by Kennedy et. al. can be used to estimate the bolt forces due to both applied force and prying action. This method was discussed in Chapter I. The basic assumption in the method is that the end-plate goes through three different stages of behavior. During the first stage, plastic hinges have not developed and the plate is referred to as "thick". The prying force is taken as zero in this stage. When the plastic hinge forms at the beam flange, the plate becomes "intermediate" and the prying force is somewhere between zero and the maximum prying force that can occur. The last stage begins when a second plastic hinge forms at the bolt line. The end-plate in that stage is called "thin" and the prying force is at its maximum. The original Kennedy model, shown in Figure 1.3, can be used to obtain the bolt forces for both stiffened and unstiffened extended end-plates. The model used for the analysis of the one-row

flush end-plates is shown in Figure 2.7. This model is essentially one-half of the original model. Therefore, the equations used for obtaining the bolt forces for the one-row flush end-plate and the extended end-plates are the same. However, for the two-row flush end-plate, the model was changed to that shown in Figure 2.8. Assumptions had to be made in order to obtain the bolt forces for this particular end-plate configuration. The basic assumptions used by Kennedy are still valid for this model, i.e. the end-plate still goes through three stages of prying action corresponding to the three plate thicknesses. The prying action is still assumed to be zero when the end-plate is thick, at a maximum when the end-plate is thin, and somewhere between the two values when the end-plate is considered as intermediate. It was further assumed that the inner bolt force, B_2, is a function of the flange force, F_f. For thick end-plates, B_2 is assumed to be zero. For intermediate end-plates, the inner bolt force, $B_2 = F_f/10$, and for thin end-plates, $B_2 = F_f/6$.

The analysis of this model exhibited the fact that the two-row flush end-plate changes from thick to intermediate and from intermediate to thin at the same load levels as a one-row flush end-plate.

Following are the steps used for bolt force predictions:

1. Select the load level, or end-plate moment, at which the bolt forces are to be determined. Calculate the resulting flange force, F_f, and flange stress, σ_f.
2. Find the thick plate limit, t_1, for this load level using the following approximate equation:

$$t_1 = \sqrt{2.11\ p_f t_f \sigma_f / F_{py}} \qquad (2.27)$$

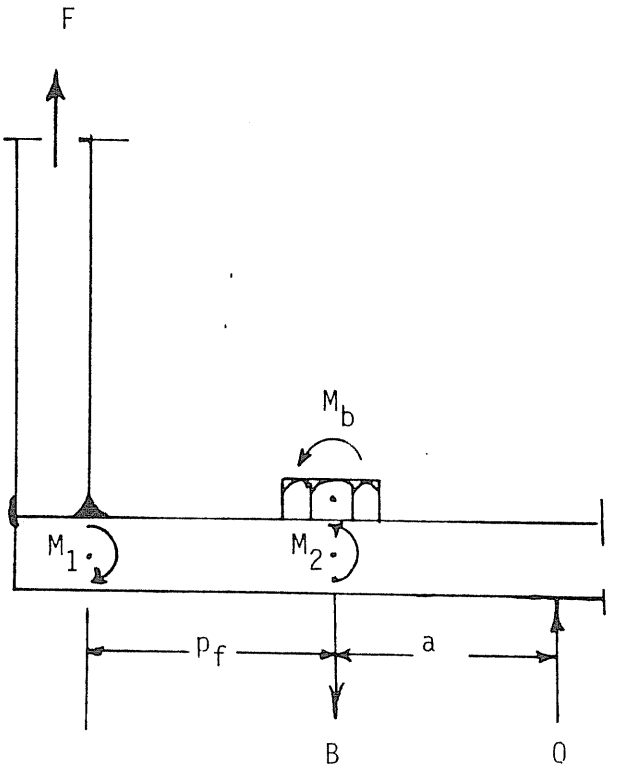

Figure 2.7 Modefied Kennedy Model for Two-Bolt Flush End-Plate

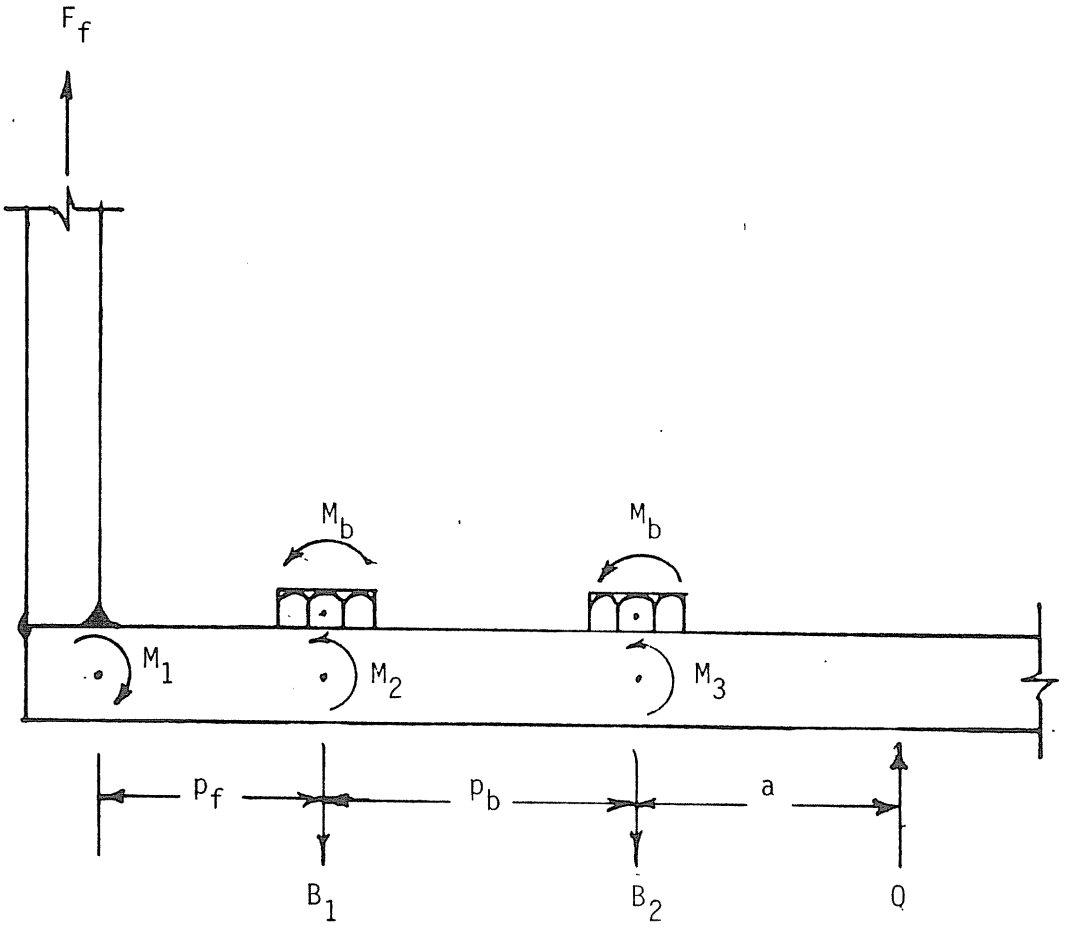

Figure 2.8 Modefied Kennedy Model for Four-Bolt Flush End-Plate

Then using the following exact iterative equation:

$$t_1 = \sqrt{\frac{2t_f\sigma_f p_f}{\sqrt{F_{py}^2 - 3\left(\frac{t_f\sigma_f}{2t_1}\right)^2}}} \qquad (2.28)$$

Once the thick plate limit is determined, the actual end-plate thickness, t_p, is compared to it. If $t_p > t_1$, then the prying force, Q, is taken as zero, otherwise $Q \neq 0$ and the next step is used.

3. Find the thin plate limit, t_{11}, using the following approximate equation:

$$t_{11} = \sqrt{\frac{2(b_f t_f \sigma_f p_f - (\pi/16)d_b^3 F_{yb})}{F_{py}(0.85b_f + 0.80\ w')}} \qquad (2.29)$$

where F_{yb} = yield stress of the bolt. Then using the iterative exact equation:

$$t_{11} = \left[\frac{2(b_f t_f \sigma_f p_f - (\pi/16)d_b^3 F_{yb}}{b_f\sqrt{F_{py}^2 - 3(\frac{t_f\sigma_f}{2t_{11}})^2} + w'\sqrt{F_{py}^2 - 3(\frac{b_f t_f\sigma_f}{2w't_{11}})^2}}\right]^{\frac{1}{2}} \qquad (2.30)$$

Again the end-plate thickness is compared to t_{11}. If $t_p > t_{11}$, then the plate is intermediate and one of two equations for prying action is used. Equation 2.31 is used to determine the prying force for one-row flush end-plates and for extended end-plates:

$$Q = \frac{Fp_f}{a} - \frac{b_f t_p^2}{4a}\sqrt{F_{py}^2 - 3\left(\frac{F}{b_f t_p}\right)^2} - \frac{\pi}{32a} d_b^3 F_{yb} \qquad (2.31)$$

where $a = t_p$ if $t_p/d_b < 2/3$ and $a = 2t_p$ otherwise, F = flange force per bolt. Equation 2.32 is used for the two-row flush end-plates.

$$Q = F_2\frac{(p_f+0.1)}{(a+p_b)} - \frac{b_f t_p^2}{4(a+p_b)}\sqrt{F_{py}^2-3\left(\frac{F_2}{b_f t_p}\right)^2} - \frac{\pi d_b^3 F_{yb}}{16(a+p_b)} \qquad (2.32)$$

where $F_2 = F_f/2$.

The bolt force, B, in one-row flush end-plates and extended end-plates is equal to

$$B = F + Q \qquad (2.33)$$

but B must be greater than the pretension force. The bolt force in the two-row flush end-plates is given by

$$B_1 = \frac{F_2}{1.25} + Q \qquad (2.34)$$

where B_1 = the outer row bolt force. Again, B_1 must be greater than the pretension force.

4. If $t_p < t_{11}$ the end-plate is said to be thin and the prying force is at its maximum.

$$Q_{max} = \frac{w' t_p^2}{4a}\sqrt{F_{py}^2-3\left(\frac{F'}{w' t_p}\right)^2} \qquad (2.35)$$

where F' is the lesser of the following:

$$F_{limit} = \frac{t_p^2 F_{py}(0.85b_f+0.80w') + (\pi/16)d_b^3 F_{yb}}{4p_f} \qquad (2.36)$$

or $F_{max} = (F_f)_{max}/2$

The bolt force for the one-row flush end-plates or the extended end-plate is then given by

$$B = F + Q_{max} \tag{2.37}$$

For the two-row flush end-plates, the bolt force is then given by

$$B_1 = \frac{F_2}{1.5} + Q_{max} \tag{2.38}$$

Bolt forces that are calculated using the above procedure are compared to experimentally obtained forces in Chapter III.

2.3 Finite Element Analysis

The finite element method (FEM) is basically an extension of matrix methods used in the solution of frame structures. The continuum is assumed to be divided into "finite" number of elements or substructures connected at discrete points (called nodes). For a typical element, its physical properties, such as stiffness coefficients, are developed using the principle of minimum potential energy. Then the discrete set of equations governing the continuum are formulated by assembling the element equations together such as to satisfy compatibility of displacements and equilibrium of forces. The FEM is basically formulated for linear elastic materials, but nonlinearity can be incorporated. The accuracy of results obtained from the FEM analyses depends on the fineness of the mesh and the kind of element chosen, however, a trade off does exist between accuracy of results desired as limited by cost or core memory capacity of the computer being used.

Finite element analyses of the two-bolt flush end-plate connection are being conducted by Abolmaali[17]. His study utilizes the FEM

program "Non-linear End-Plate Analysis Program" (NONPAP) developed by a research team at Fears Structural Engineering Laboratory, University of Oklahoma. The analyses are performed using both two dimensional plane stress models and partial three dimensional models (referred to as hybrid 2D-3D models). The 2-D model is formulated with all elements parallel to the plane of the web and with the flange, web, plate, and bolt shank of different widths normal to the vertical plane of symmetry being treated as in-plane components with different thicknesses. In the 2-D study, the effects of welds are not incorporated. Figure 2.9 shows a typical 2-D mesh.

The primary objective of the 2D-3D analysis was to improve the prediction of the plate behavior. The 3-D elements were used where most accuracy is needed: the end-plate, bolt heads, bolt shank, and for welds connecting beam flanges and web to the end-plate. Two dimensional elements are used for beam flanges, beam web, and welds connecting beam flanges to beam web. The configuration of the model used in most analyses is shown in Figure 2.10 with all the geometric variables shown for both the actual beam and the FEM model.

Applied moment versus plate separation FEM predictions are compared in chapter III with the results of the testing program of the one-row flush end-plate connections. Predicted and measured stress distributions at beam cross-sections are also compared. Bolt forces were also predicted by the program and they are compared to the actual forces obtained.

The FEM analysis was conducted exclusively for the one-row

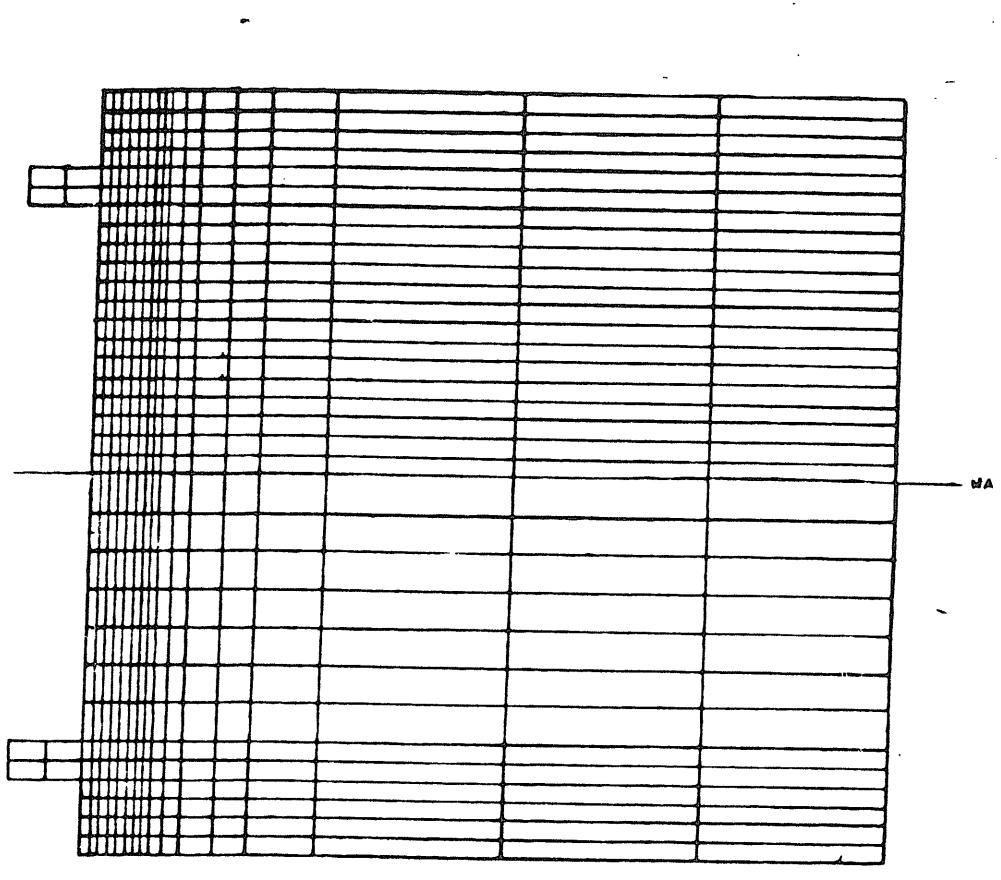

a) Elevation

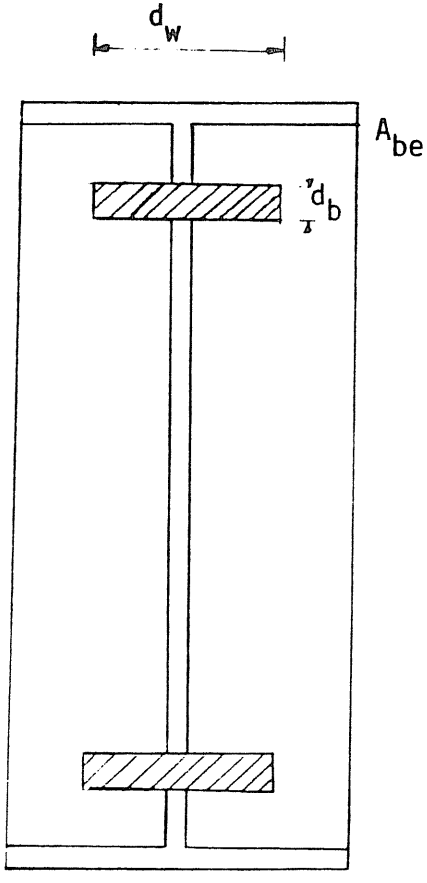

b) Section

626 NODES

560 ELEMENTS

Figure 2.9 2-D Mesh Configuration

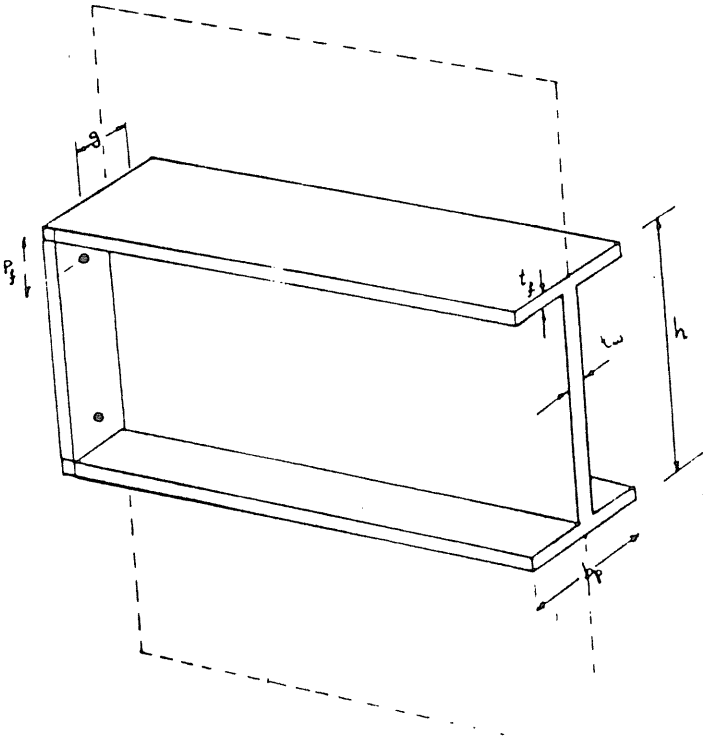

a) Section at End-Plate

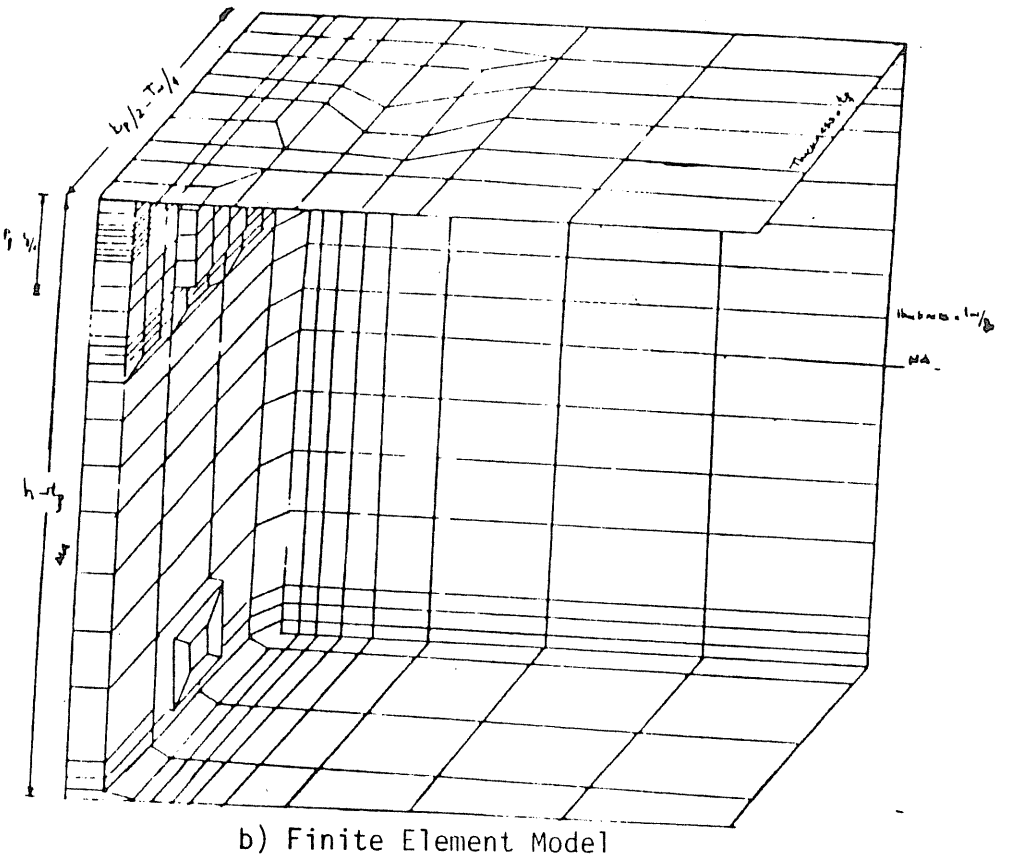

b) Finite Element Model

Figure 2.10 2D-3D Mesh Configuration

flush end-plate connections. A model based only on geometric considerations was developed to predict the plate separation for the two-row flush end-plate connections that were tested. The basic assumption in this model is that the vertical deflection at the end-plate results in a proportional plate separation, governed by the following relationship.

$$\frac{\delta_p}{P_t} = \frac{\Delta_c \ \alpha_s}{L/2} \tag{2.43}$$

where δ_p = Plate separation, Δ_c = vertical deflection at the end-plate, L = length of the test beam, α_s = correction factor experimentally obtained. A detailed description of this method will be given in the next chapter.

CHAPTER III

COMPARISON OF ANALYTICAL AND EXPERIMENTAL RESULTS

3.1 Testing Program for Flush End-Plate Connections

3.1.1 Test Set-up and Procedure

To verify the analytical procedures described for the flush end-plate connections in Chapter II, two sets of tests were conducted. The first set consisted of eight one-row flush end-plate specimens, grouped into three series. The second set consisted of six two-row flush end-plate specimens, grouped into two series. The test set-up was as shown in Figures 3.1, 3.2 and 3.3. The end-plates were welded to two beams and tested as splice connections under pure moment. All beam and end-plate material was A572 Gr50 steel and bolts were A325. Tables 3.1 and 3.2 list the nominal geometry of the one-row and two-row flush end-plate specimens tested, respectively. The tables also list the measured yield stress obtained using coupons cut from identical material. The test designations shown in the two Tables are to be interpreted as follows: F1-3/4-1/2-16 designates a flush end-plate test with one row of 3/4 in. diameter bolts at the tension flange. The end-plate thickness is 1/2 in. and the beam depth is 16 in. In the first set, tests were conducted using 10 in., 16 in.,

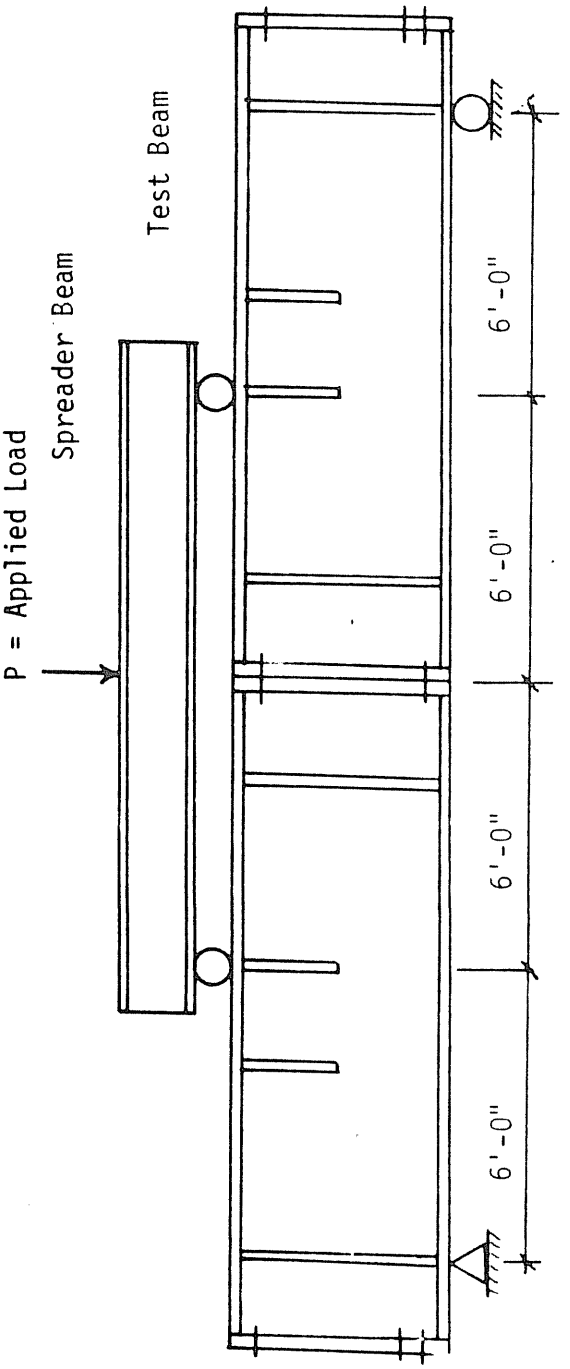

Figure 3.1 Elevation of Test Set-up

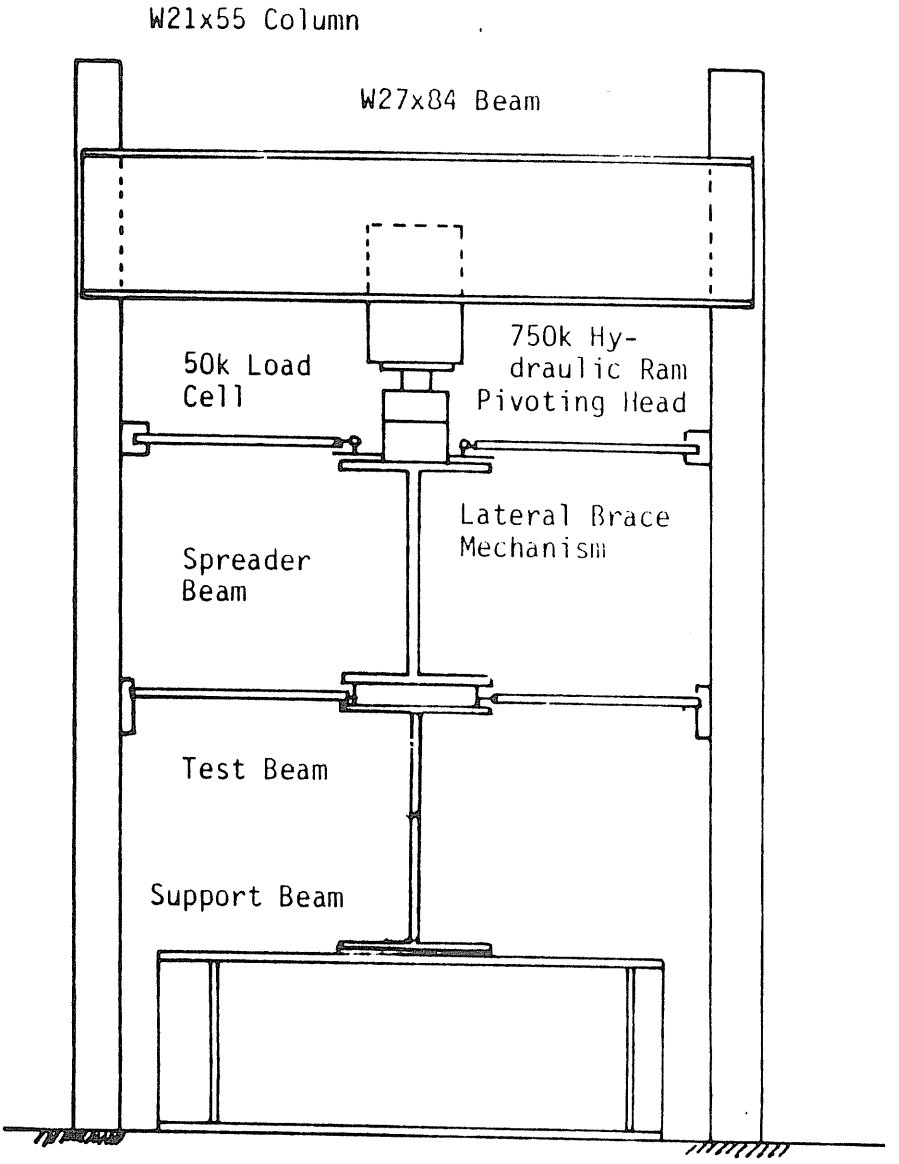

Figure 3.2 Cross-Section of Test Set-up

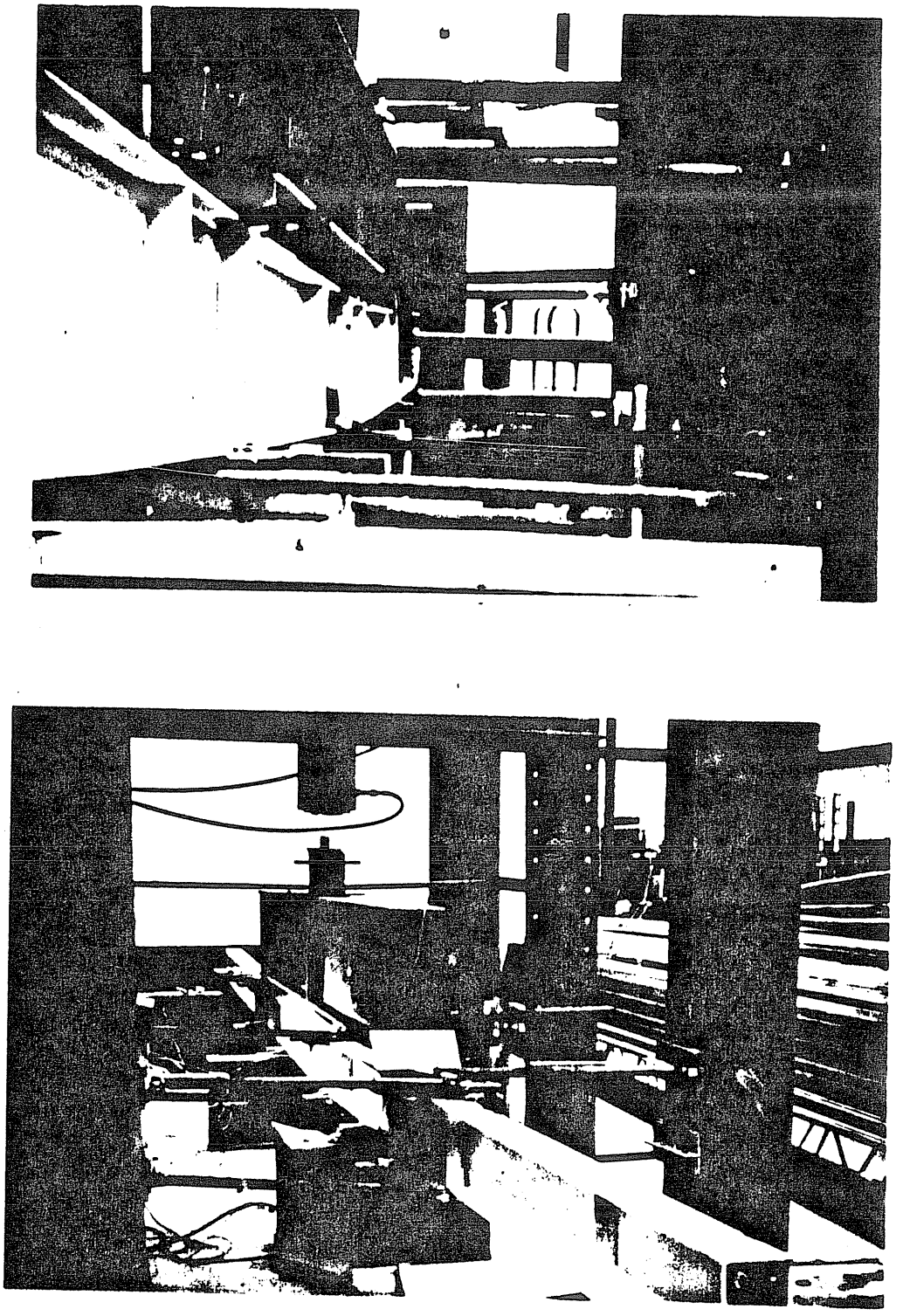

Figure 3.3 Photographs of Test Set-up

Table 3.1
Two-Bolt Flush End-Plate Parameters

Test No.	Test Designation	Bolt Diameter d_b (in)	End-Plate Thickness t_p (in)	Beam Depth h (in)	Flange Width b_f (in)	Pitch p_f (in)	Gage g (in)	Yield Stress (ksi)
1	F1-3/4-1/2-16	3/4	1/2(.505)	16	6	1 1/2	3 1/2	55.48
2	F1-3/4-3/8-16	3/4	3/4(.383)	16	6	1 1/2	3 1/2	59.45
3	F1-5/8-1/2-16	5/8	1/2(.508)	16	6	1 7/8	3 3/4	53.98
4	F1-5/8-3/8-16	5/8	3/8(.385)	16	6	1 3/8	2 3/4	56.95
5	F1-5/8-3/8-10	5/8	3/8(.384)	10	5	1 1/4	2 1/4	51.90
6	F1-5/8-1/2-10	5/8	1/2(.506)	10	5	1 1/2	3	55.80
7	F1-3/4-1/2-24A	3/4	1/2(.504)	24	6	1 3/4	3 1/4	57.53
8	F1-3/4-1/2-24B	3/4	1/2(.502)	24	6	1 3/8	2 3/4	57.53

Notes: Flange and web thicknesses for all tests were 1/4 in.
(.xxx) indicates measured thickness.

Table 3.2
Four-Bolt Flush End-Plate Parameters

Test No.	Test Designation	Bolt Diameter d_b (in)	End-Plate Thickness t_p (in)	Beam Depth h (in)	Flange Width b_f (in)	Pitch p_f (in)	Gage g (in)	Yield Stress (ksi)
1	F2-5/8-1/2-16	5/8	1/2	16	6	1 7/8	3 3/4	58.6
2	F2-5/8-3/8-16	5/8	3/8	16	6	1 3/8	2 3/4	60.5
3	F2-3/4-1/2-24	3/4	1/2	24	6	1 3/4	3 1/4	54.0
4	F2-3/4-3/8-24	3/4	3/8	24	6	1 3/8	2 3/4	64.1
5	F2-3/4-1/2-16	3/4	1/2	16	6	1 1/2	3 1/2	54.8
6	F2-3/4-3/8-16	3/4	3/8	16	6	1 1/2	3 1/2	59.7

and 24 in. deep beams. In the second set the tests were conducted with 16 in. and 24 in. deep beams. Bolt pitch, gage and diameter were varied within the limits shown in Table 3.3

In the test set-up, the load for the first set of tests and the first two tests in the second set was applied using a hydraulic ram powered by an electric pump. The load was monitored using a load cell and standard strain indicator. For the last tests a closed-loop hydraulic testing (MTS system) was used. The test beams were laterally supported at three locations using lateral brace mechanisms. The spreader beam was also laterally supported at the centerline (see Figure 3.1, 3.2 and 3.3).

3.1.2 Instrumentation

Instrumentation consisted of wire displacement transducers, calipers, strain gages and instrumented bolts. For all the tests a HP3497A data acquisition/control unit was used with an HP 85 desktop computer to collect and record the data. One wire displacement transducer was placed at the end-plate to measure the vertical deflection, two more were placed on the top and bottom flange of the test beam to measure the lateral displacement close to the end-plate. Calipers were used to measure the plate separation at different locations on the end-plate. One of the calipers was placed on the centerline of the plate while the others were attached to the edges.

Strain gages were used to measure web and flange strains. In the first set of tests, strain gages were placed at two locations, 2 in. and 16 in. from the face of the end-plate. In the second set

Table 3.3
Limits of Geometric Parameters

Parameter	Low	Intermediate	High
g	2 1/4	2 3/4	3 1/2
d_b	5/8	3/4	1.00
p_f	1 1/8	1 3/4	2 1/2
b_p	5	7	10
t_p	5/16	1/2	3/4
t_f	.18	.375	.50
t_w	.10	.1875	.25

the strain gages were placed only at 2 in. from the end-plate. Figure 3.4 shows the typical location of the strain gages; the number of gages on the web at the 2 in. section varied with the depth of the beam. The instrumented bolts were used in the tension side to monitor the bolt strains resulting from the applied loads. The bolts were pretensioned after the spreader beam was placed on top of the test beams. Measured strains were converted to stress assuming a modulus of elasticity of 29,000 ksi, but not to exceed the yield stress of the material.

3.1.3 Loading procedures

At the beginning of each test the specimen was loaded to approximately 20% of the expected maximum load to check the test setup and instrumentation. Load-deflection and Load-plate

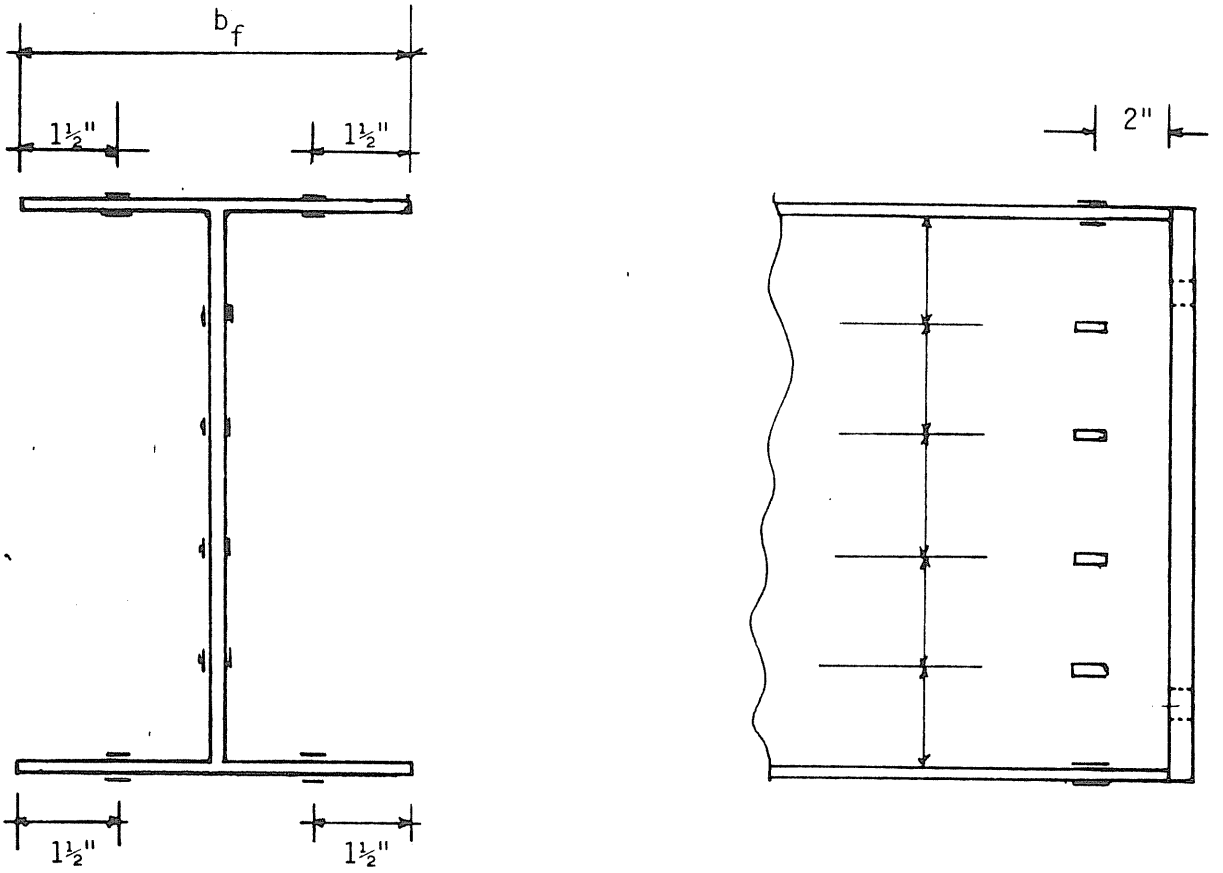

Figure 3.4 Typical Strain Gage Locations

separation curves were plotted simultaneously using an HP 7470A graphics plotter. The specimen was then unloaded and initial readings recorded at zero load.

The first two tests conducted (F1-3/4-1/2-16 and F1-3/4-3/8-16) were loaded continuously in approximately 2 kip increments to the failure load and then unloaded. Data was recorded at every load level using the data acquisition system. For all the other tests that were loaded using the hydraulic ram, the specimens were loaded to approximetely 2/3 of the expected failure load at varying increments depending on the expected failure load of each test. The specimens were then unloaded at increments of 5 kips or more to a load of 2 or 5 kips, taking readings at every step while unloading. The load was then increased to the previous load, and then increased 5 to 10%. The process was repeated with resulting load versus deflection curves as shown for a typical test in Figure 3.5. For the tests where the closed-loop hydraulic testing system was used, the test beams were displaced to preselected vertical deflection instead of a certain load. The load required to impose the deflection was obtained by the internal load cell of the system. The vertical deflection was controlled by the actuator of the closed-loop hydraulic testing system. The same cyclic pattern of loading was used and the data was recorded using the same data acquisition system. Figure 3.6 shows photographs of the MTS test setup.

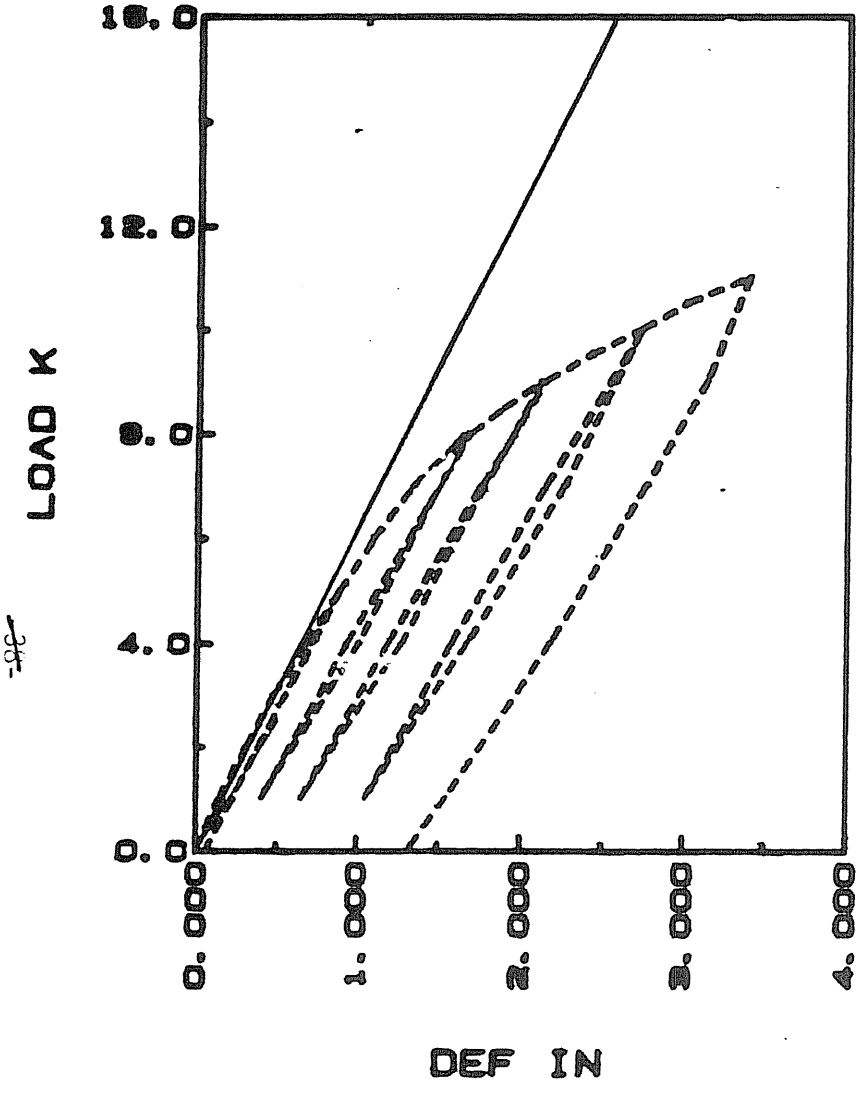

a) Load vs. Vertical Deflection

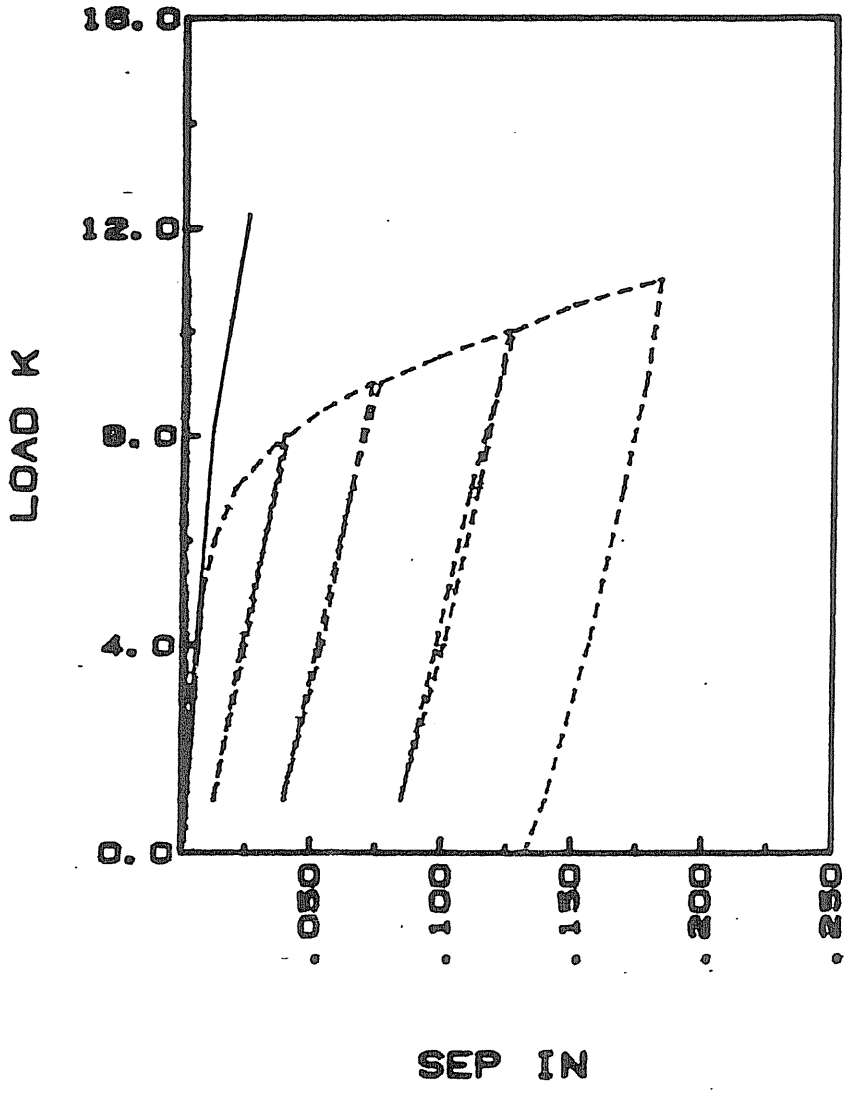

b) Load versus Plate Separation

Figure 3.5 Typical Loading versus Deflection Curves

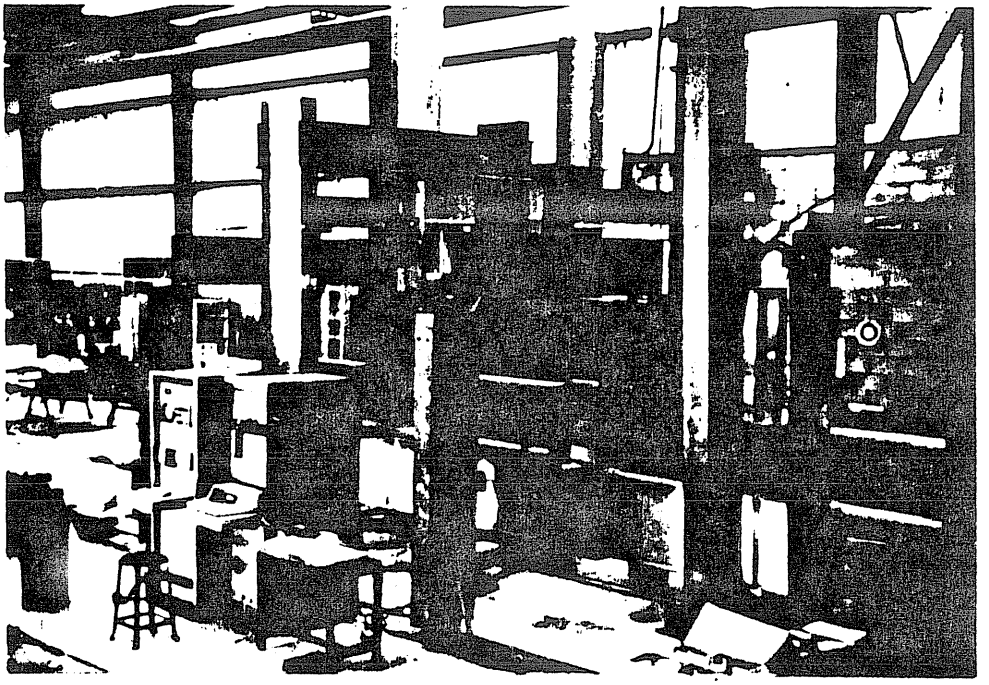

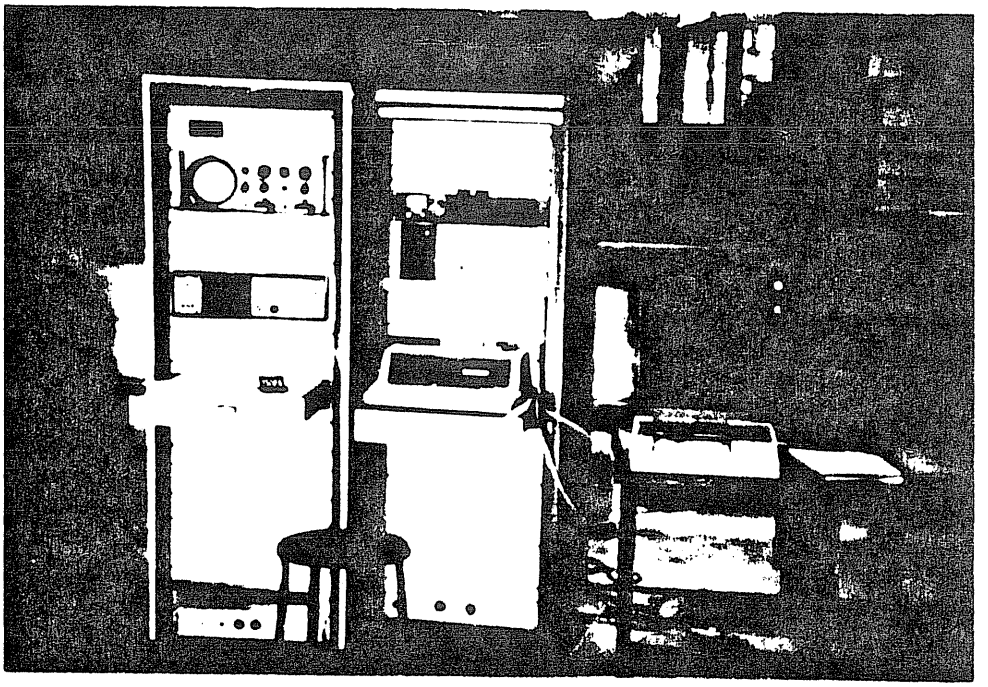

Figure 3.6 Photographs of the MTS Test Set-Up

3.2 Comparisons with Test Results

3.2.1 Results of Two-Bolt Flush End-Plate Tests

As mentioned previously, eight specimens were tested in this series. Four of these tests were conducted using a 16 in. deep beam, two tests were conducted using a 10 in. deep beam, and two others using a 24 in. deep beam. The test results consist of load versus vertical deflection, load versus plate separation, load versus bolt forces, and stress distribution at the instrumented cross-sections. Failure moment and the failure mode were also noted and recorded during the tests.

Table 3.4 summarizes the strength data. The ratio of maximum applied moment to predicted failure moment using the straight yield-line mechanism varied from 0.94 to 1.08, excluding Test F1-3/4-1/2-24A where the test was stopped before a yield plateau was reached. For the curved yield-line mechanism, the maximum applied to predicted failure moment varied from 1.03 to 1.16, excluding test F1-3/4-1/2-24A, which was not conducted to failure.

Failure modes varied between tests. The web-to-end-plate fillet weld cracked near the tension bolts in Tests F1-3/4-1/2-16 and F1-5/8-3/8-16, Figure 3.7, and the bolt fractured in Test F1-5/8-1/2-10, Figure 3.8. Test F1-3/4-1/2-24A was stopped due to rapidly increasing bolt strains. For all other tests, the loading was increased until a yield plateau was reached in either the moment versus vertical deflection or moment versus plate separation curve. Figure 3.9 shows a typical end-plate yielding in the vicinity of the tension bolts after

Table 3.4
Summary of Strength Data for Two-Bolt Flush End-Plate Tests

Test Number	Maximum Applied Moment (ft.-k)	Straight Yield-lines			Curved Yield-lines			Comment on Failure
		Predicted Failure Moment (ft.-k)	$\frac{M_{max}}{M_{pred.}}$	Difference	Predicted Failure Moment (ft.-k)	$\frac{M_{max}}{M_{pred.}}$	Difference	
F1-3/4-1/2-16	92.5	90.12	1.03	3%	80.4	1.15	15%	See 1 below
F1-3/4-3/8-16	53.96	54.33	0.99	-1%	48.46	1.11	10%	" 2 "
F1-5/8-1/2-16	77.08	80.04	0.96	-3.8%	71.06	1.08	7.8%	" 2 "
F1-5/8-3/8-16	64.75	62.02	1.04	4.2%	57.17	1.13	11.7%	" 1 "
F1-5/8-1/2-10	39.47	38.36	1.03	2.9%	34.82	1.13	13.4%	" 3 "
F1-5/8-3/8-10	33.92	31.3	1.08	8.3%	29.18	1.16	16.1%	" 4 "
F1-3/4-1/2-24A	120.2	145.2	0.83	17%	129.13	0.93	7%	" 5 "
F1-3/4-1/2-24B	154.2	164.5	0.94	6%	150.22	1.03	3%	" 4 "

1. Crack of weld
2. Excessive bolt forces, deflection, and yielding
3. Bolt fracture
4. Yielding of end-plate
5. Not tested to failure, rapidly increasing bolt strains

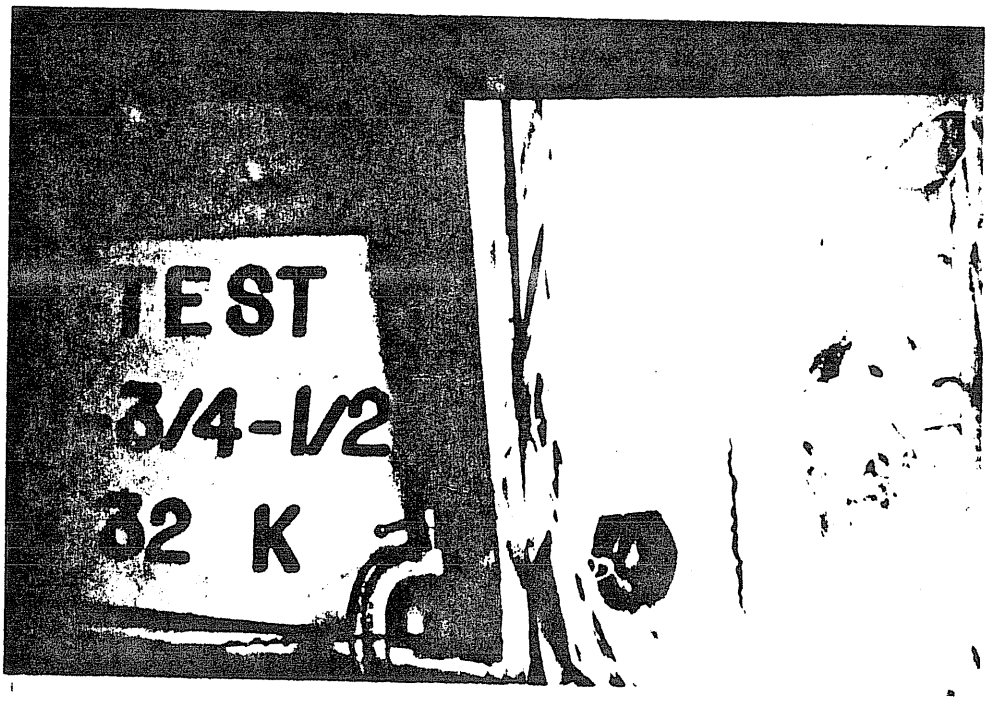

Figure 3.7 Photograph of Weld Crack

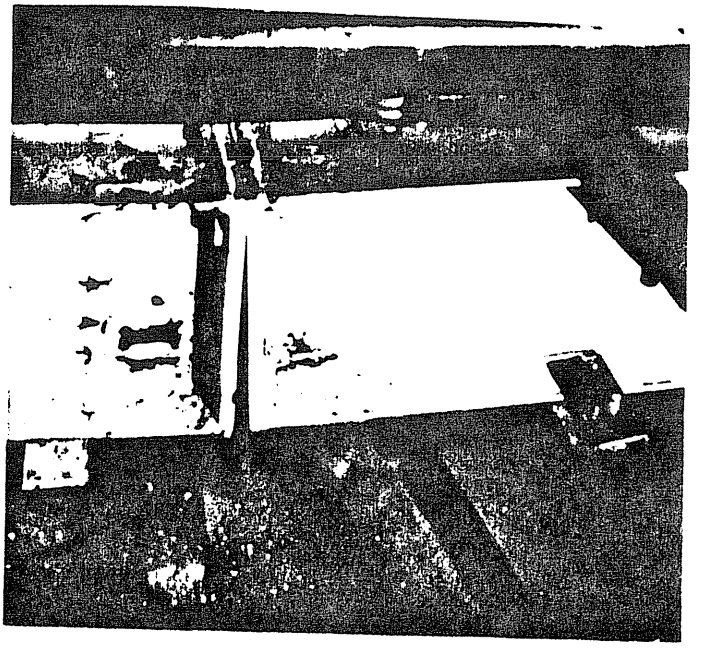

Figure 3.8 Photograph of Bolt Fracture

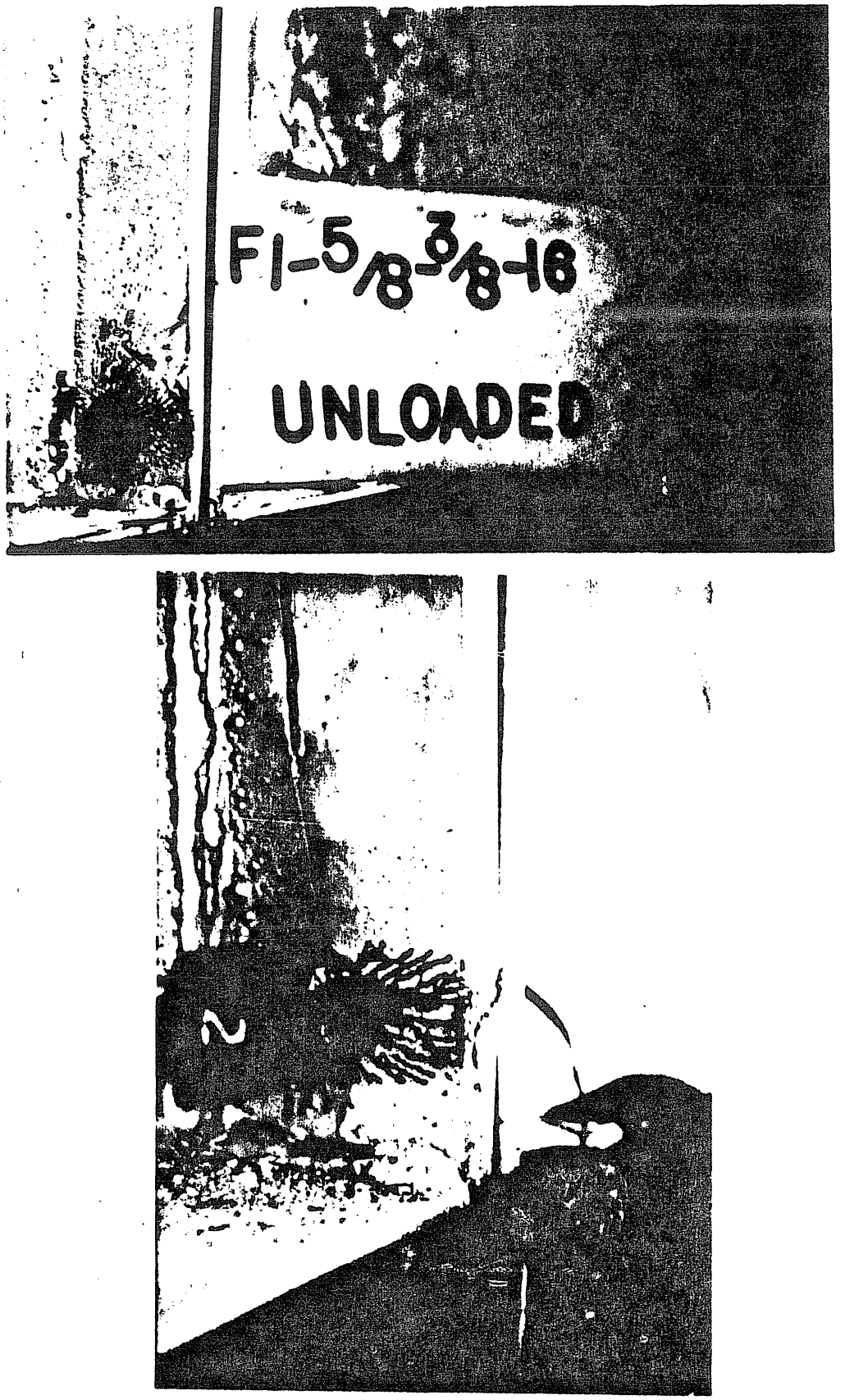

Figure 3.9 Photographs Showing End-Plate Yielding

unloading.

The end-plate moment versus vertical deflection data includes a theoretical line using the following

$$\delta_{max} = Pa\ (3L^2 - 4a^2)/24EI \qquad (3.1)$$

where a is the distance from the beam support to the point of load application. The predicted strength using the previously described straight line yield-line mechanism for the measured yield stress is also indicated on these plots. Moment versus plate separation plots include predictions from both the 2D and hybrid 2D - 3D finite element analyses. Bolt force versus moment plots include predictions using the modified Kennedy et al. procedures described in Section 2.2 and results from 2D finite element analyses. The cross-section stress distribution plots include 2D finite element analyses results.

Figure 3.10 shows the moment versus vertical displacement relationships for all eight tests. From these plots it is noted that the test beams always deflected as predicted to a certain moment, whereupon the curve softened. The moment at this load level is defined here as M_{yv} and is taken at the level when the measured deflection exceeded the theoretical deflection by 10%. The predicted failure moments from the straight yield-line mechanisms are also shown in the plots.

Moment versus plate separation relationships are shown in Figure 3.11. Good agreement exists between the measured and 2D finite element model predictions to 40 - 50% of the maximum applied moment. At this level, the experimental curves soften and yield plateau forms.

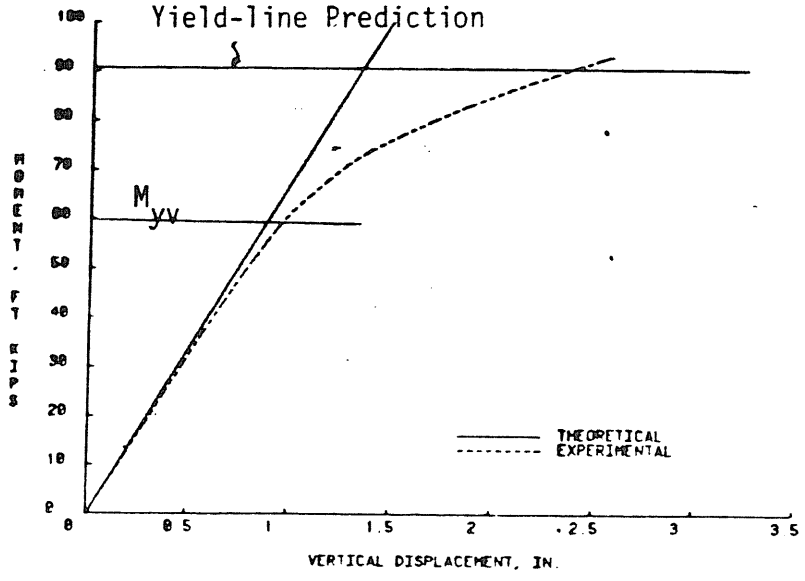

a) Moment vs. Vert. Displacement, F1-3/4-1/2-16

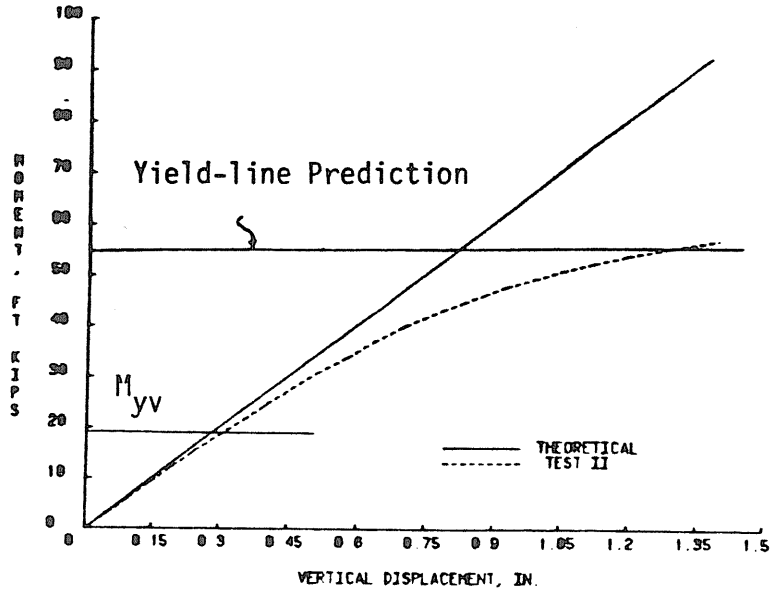

b) Moment vs. Vert. Displacement, F1-3/4-3/8-16

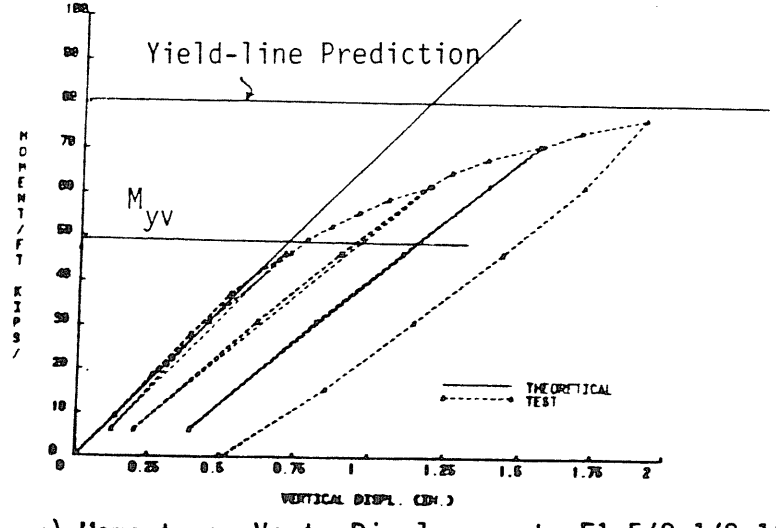

c) Moment vs. Vert. Displacement, F1-5/8-1/2-16

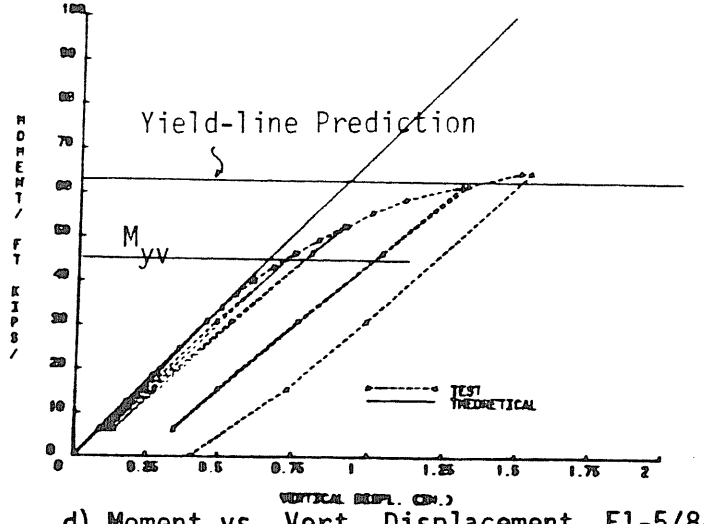

d) Moment vs. Vert. Displacement, F1-5/8-3/8-16

Figure 3.10 Moment vs. Vertical Displacement Relationship for Two-Bolt Flush End-Plates

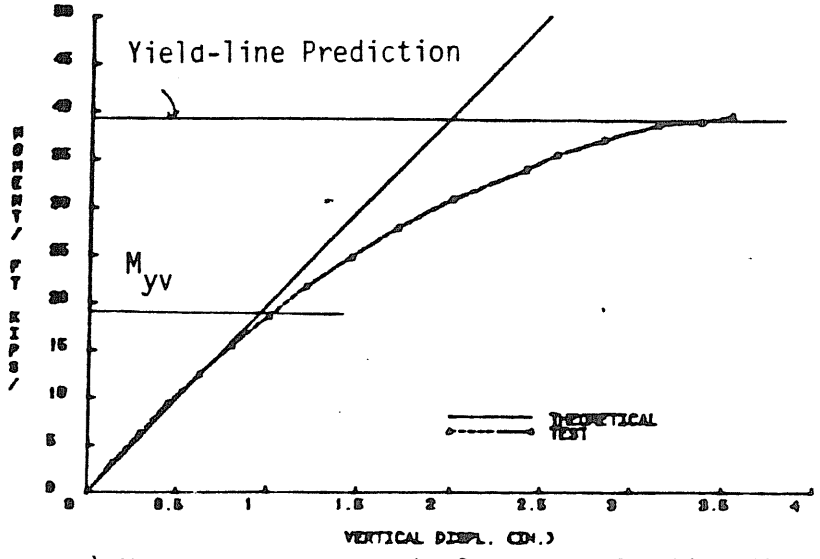

e) Moment vs. Vert. Displacement, F1-5/8-1/2-10

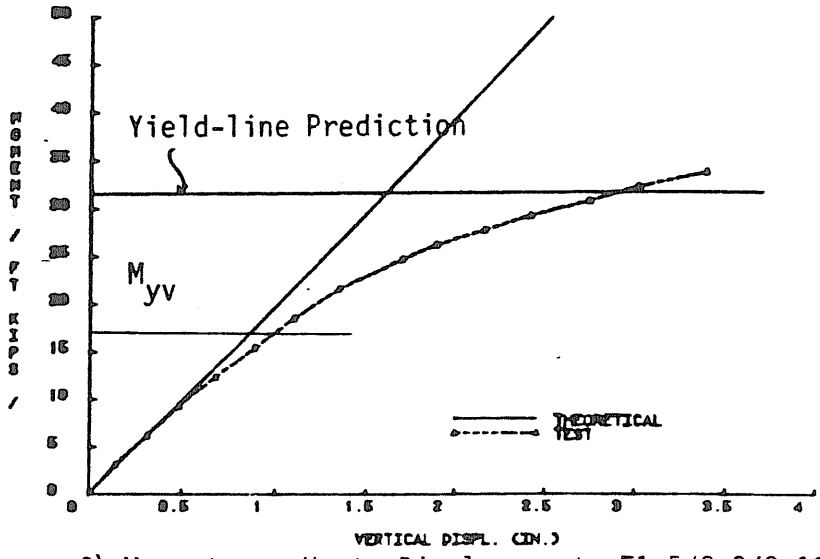

f) Moment vs. Vert. Displacement, F1-5/8-3/8-10

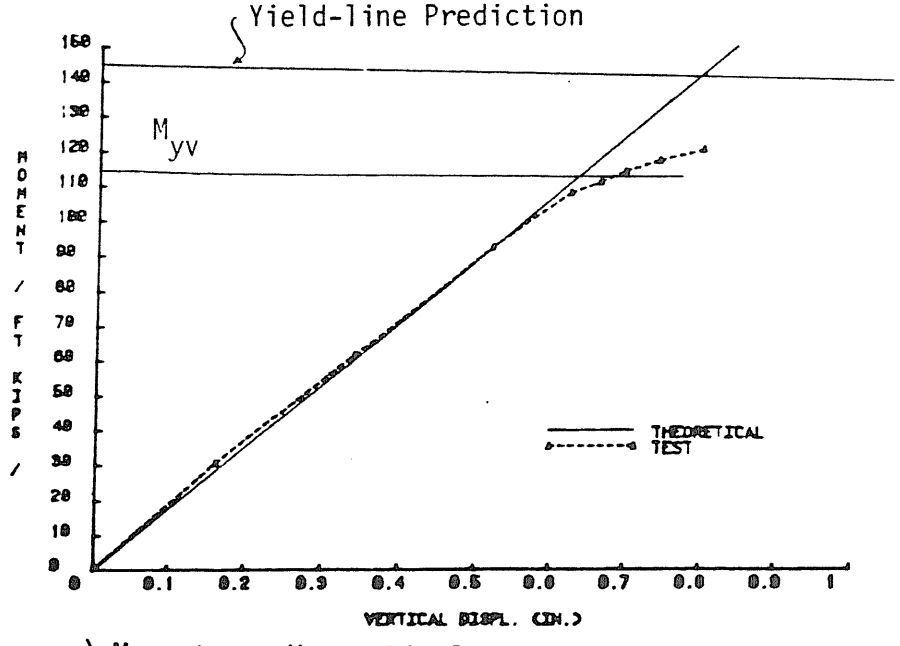

g) Moment vs. Vert. Displacement, F1-3/4-1/2-24A

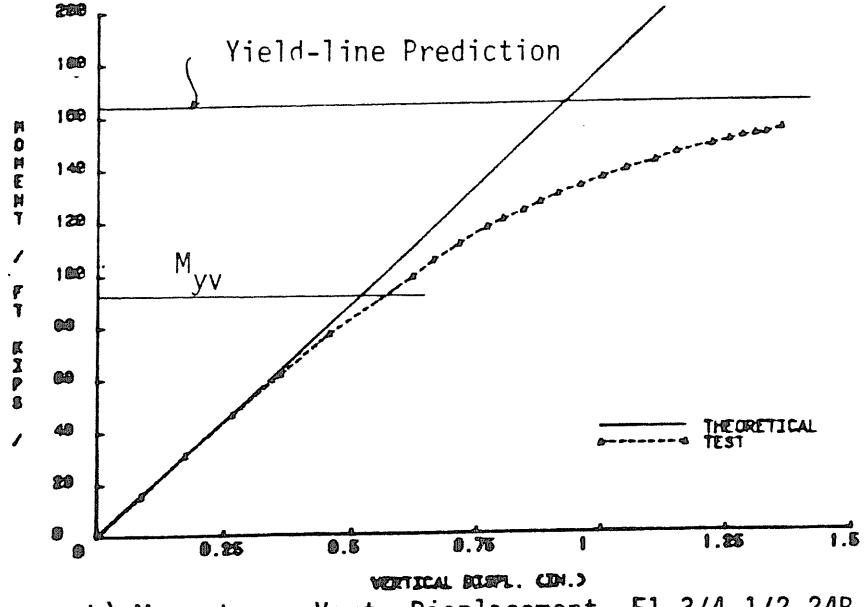

h) Moment vs. Vert. Displacement, F1-3/4-1/2-24B

Figure 3.10 Moment vs. Vertical Displacement Relationship for Two-Bolt Flush End-Plates

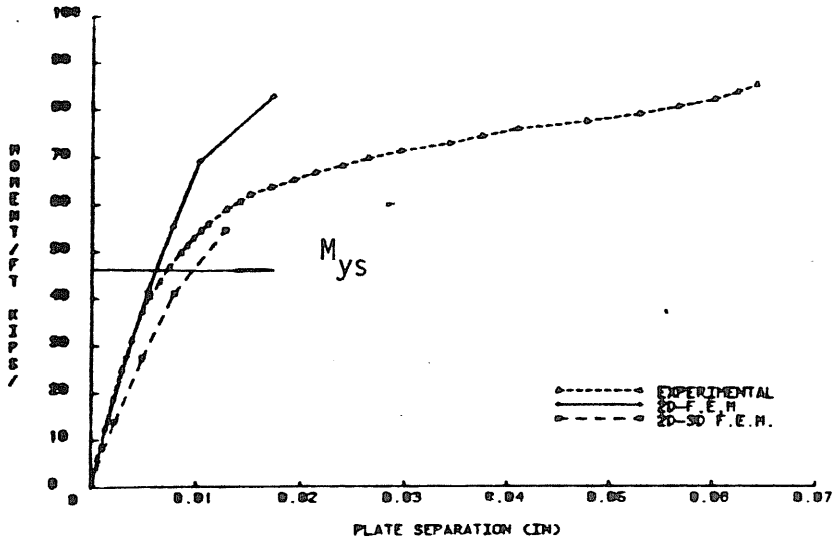

a) Moment vs. Plate Separation, Test F1-3/4-1/2-16

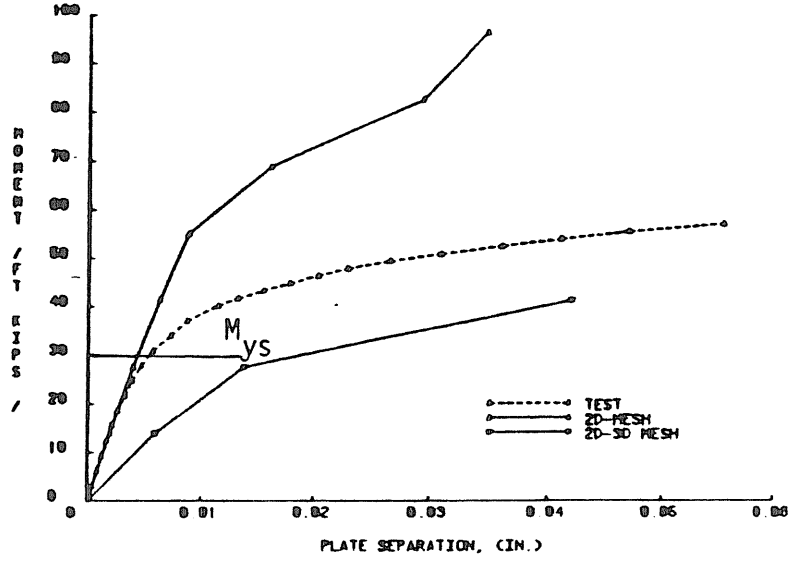

b) Moment vs. Plate Separation, Test F1-3/4-3/8-16

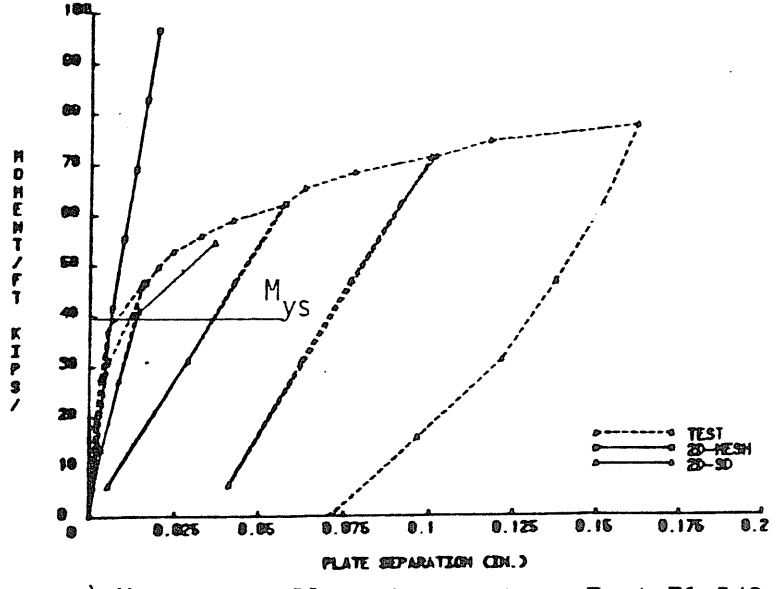

c) Moment vs. Plate Separation, Test F1-5/8-1/2-16

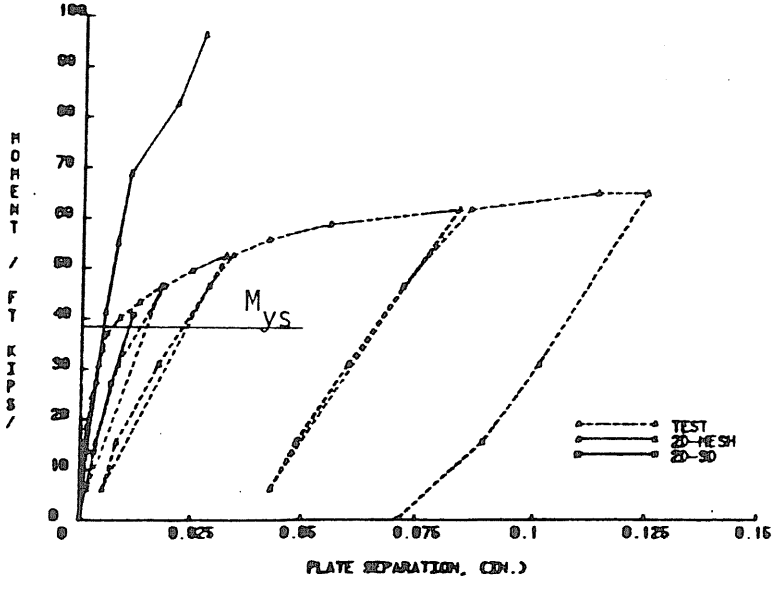

d) Moment vs. Plate Separation, Test F1-5/8-3/8-16

Figure 3.11 Moment vs. Plate Separation Relationship for Two-Bolt Flush End-Plate

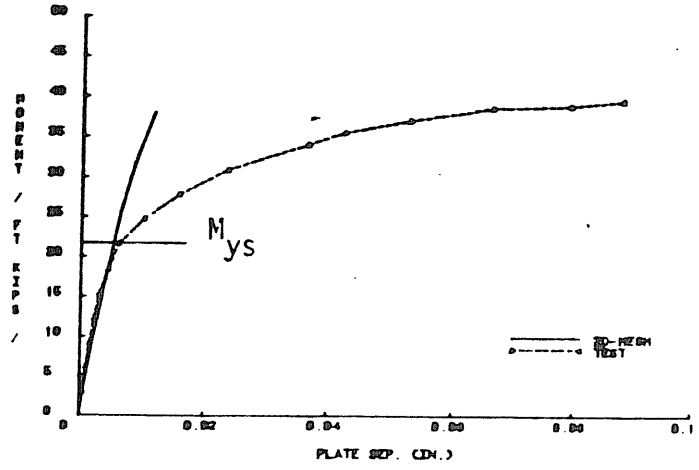

e) Moment vs. Plate Separation, Test F1-5/8-1/2-10

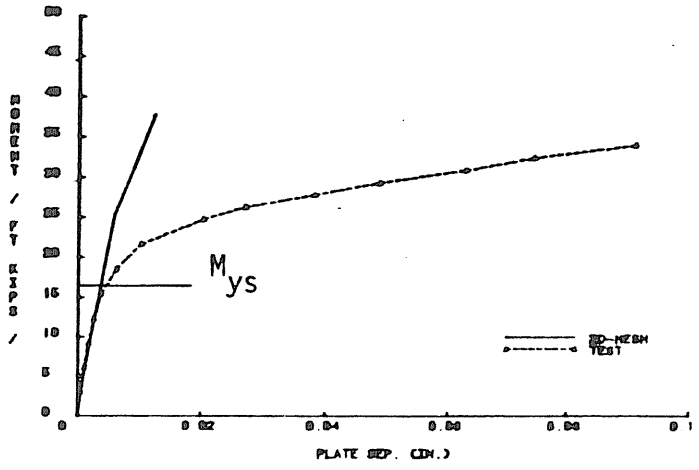

f) Moment vs. Plate Separation, Test F1-5/8-3/8-10

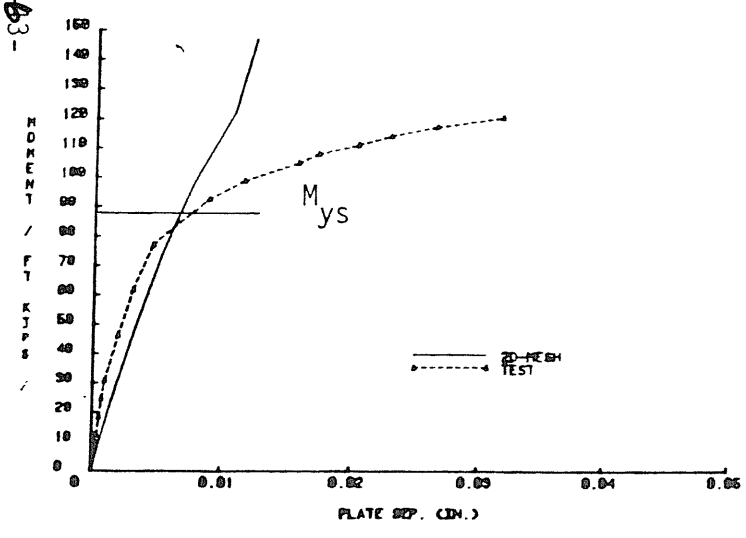

g) Moment vs. Plate Separation, Test F1-3/4-1/2-24A

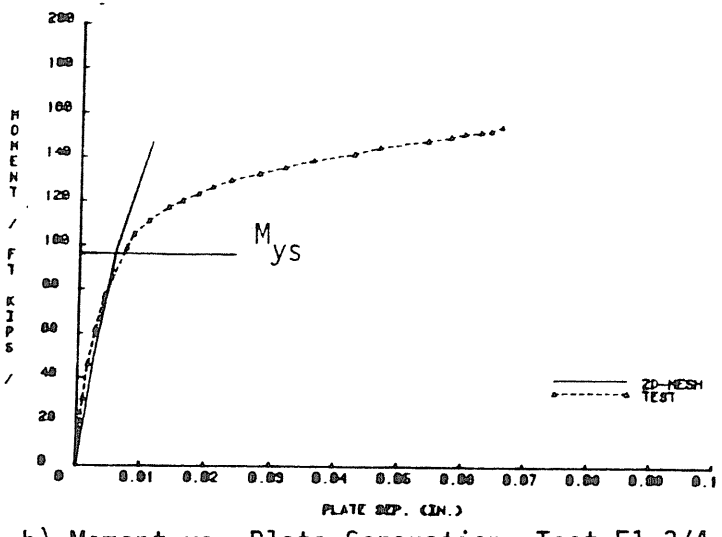

h) Moment vs. Plate Separation, Test F1-3/4-1/2-24B

Figure 3.11 Moment vs. Plate Separation Relationship for Two-Bolt Flush End-Plate

The moment when the measured plate separation exceeds the predicted value by 10% is defined here as M_{ys}.

Figure 3.12 shows bolt force versus moment relationships for the eight tests. Predicted bolt forces using the 2D finite element and the Kennedy et al. method are also shown in the figures. The measured bolt forces were calculated from strain data assuming elastic material properties and a modulus of elasticity of 29,000 ksi. The actual material stress strain curve was not considered in calculating the bolt forces shown in Figure 3.12. The measured bolt forces were close to the predicted values to near the bolt proof load, which is twice the allowable tension capacity given in the AISC Manual[10]. The corresponding moment is designated as M_{yb}.

Table 3.5 presents ratios of vertical yield moment, M_{yv}; plate separation yield moment, M_{ys}; and bolt proof load moment, M_{yb} to the maximum applied moment for all tests except F1-3/4-1/2-24A where the straight yield-line mechanism failure moment was used. The moment governed by the bolt proof load exceeds in all cases the yield moments defined by vertical deflection and plate separation. The ratio of the vertical deflection yield moment to the maximum moment varied from 0.33 to 0.69 and that for the plate separation yield moment from 0.41 to 0.64, excluding Test F1-3/4-1/2-24A.

For Test F1-3/4-1/2-24B, stress distributions calculated from measured strains at cross-sections 2 in. and 16 in. from the end-plate and at two applied load levels together with predictions from 2D finite element analyses are shown in Figure 3.13. In this figure,

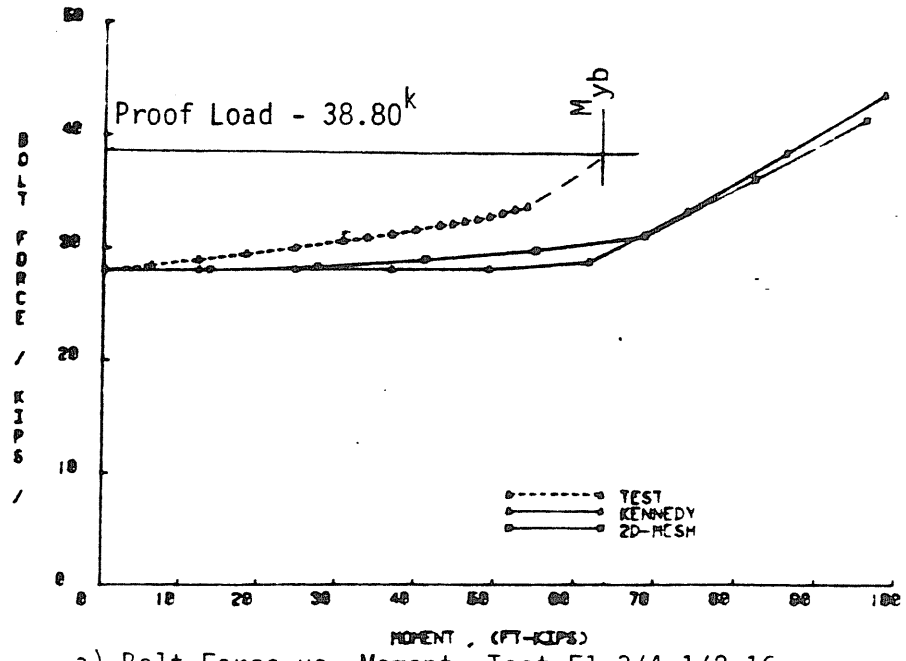

a) Bolt Force vs. Moment, Test F1-3/4-1/2-16

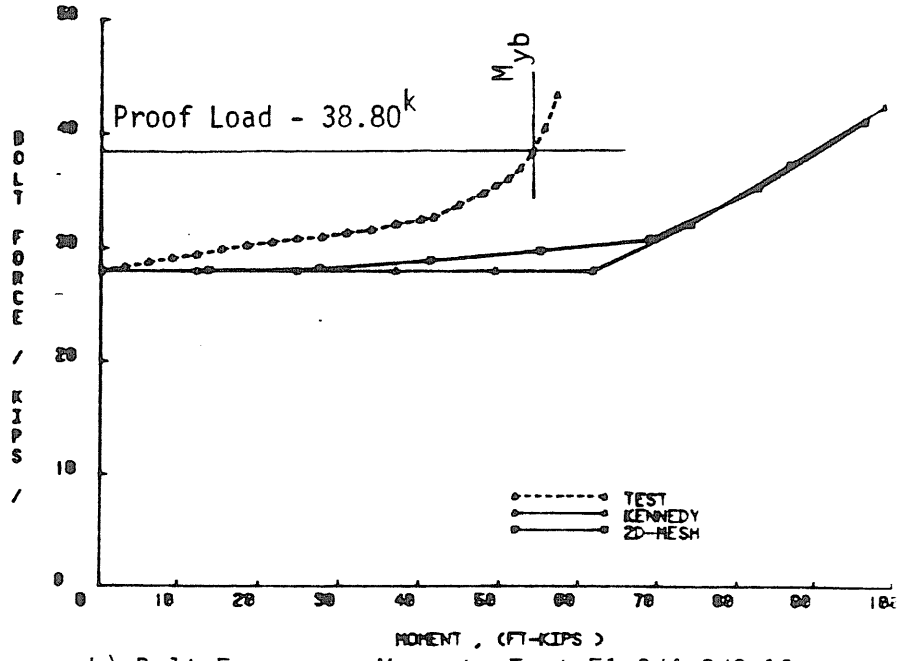

b) Bolt Force vs. Moment, Test F1-3/4-3/8-16

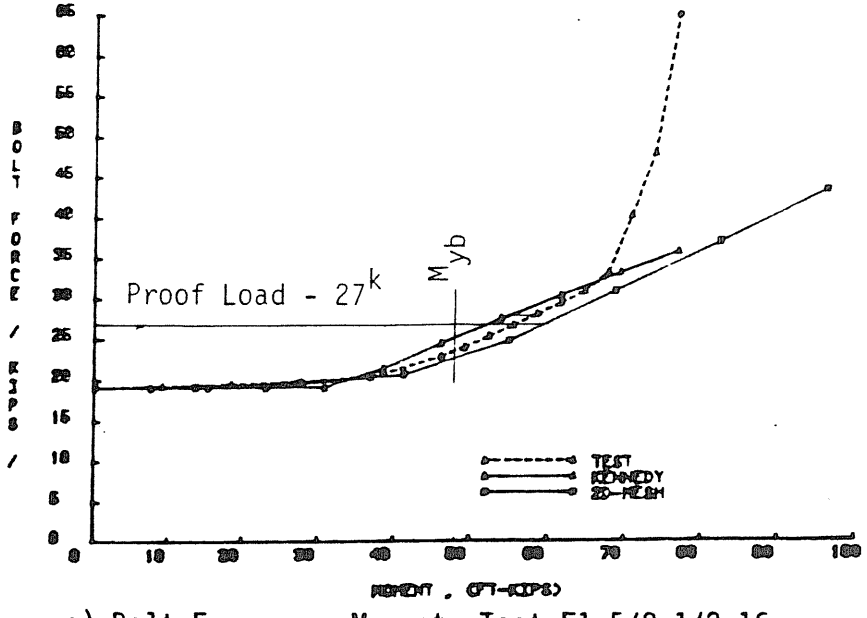

c) Bolt Force vs. Moment, Test F1-5/8-1/2-16

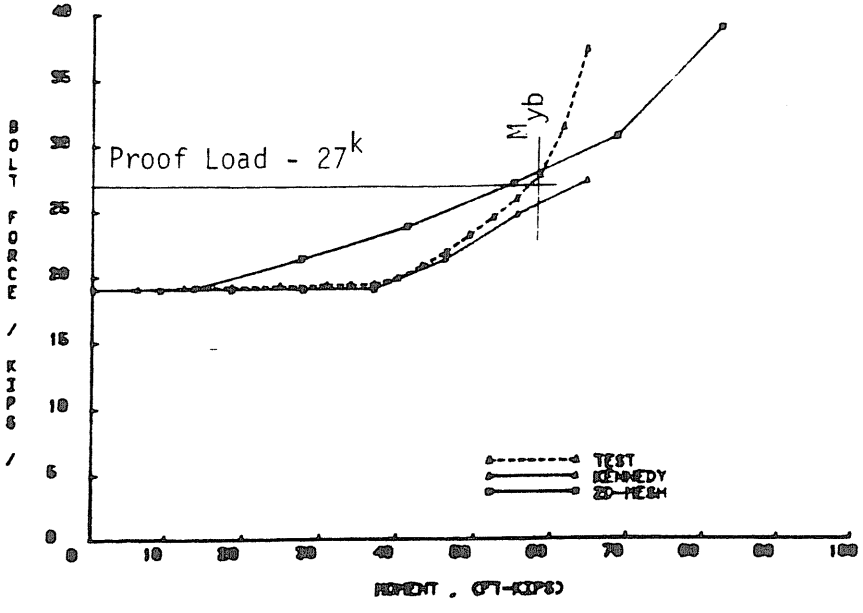

d) Bolt Force vs. Moment, Test F1-5/8-3/8-16

Figure 3.12 Bolt Force vs. Moment Relationship for Two-Bolt Flush End-Plates

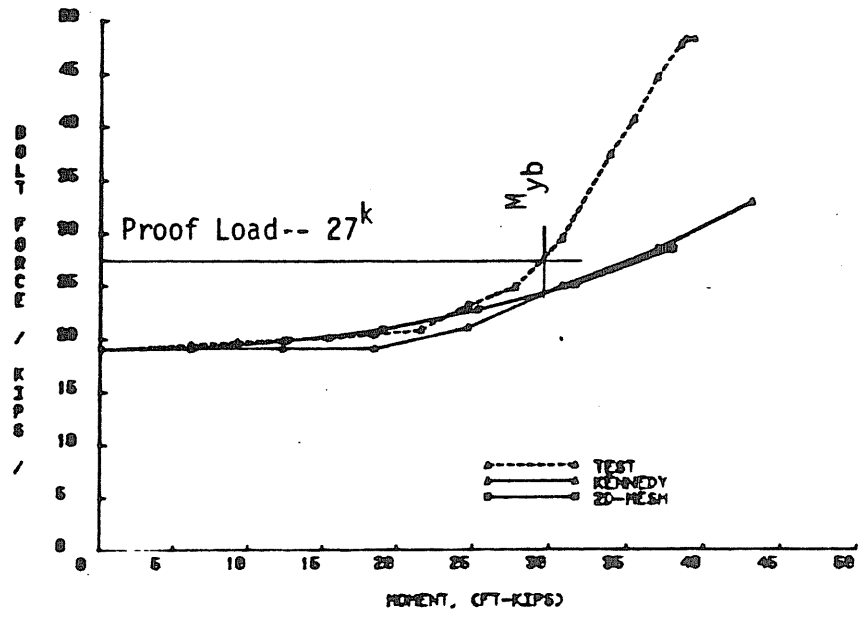

e) Bolt Force vs. Moment, Test F1-5/8-1/2-10

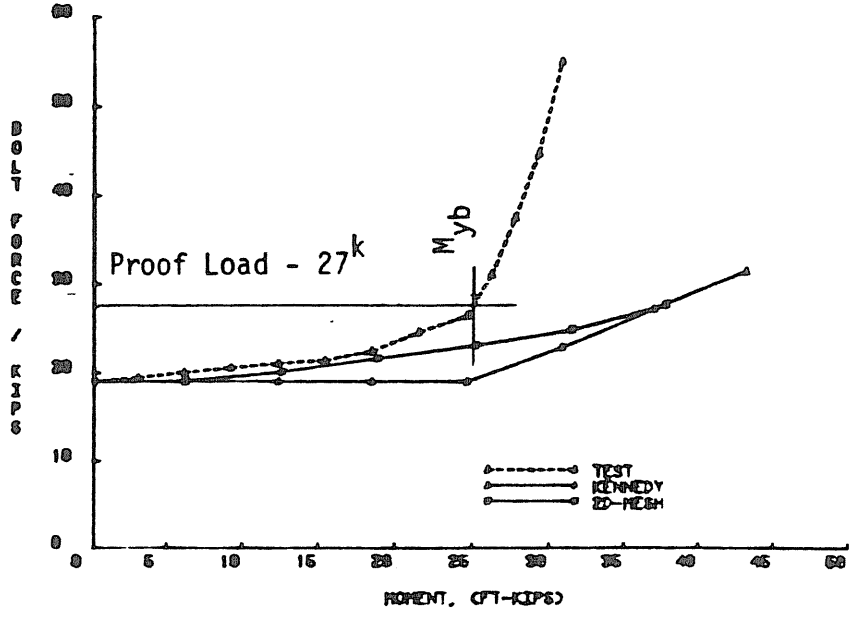

f) Bolt Force vs. Moment, Test F1-5/8-3/8-10

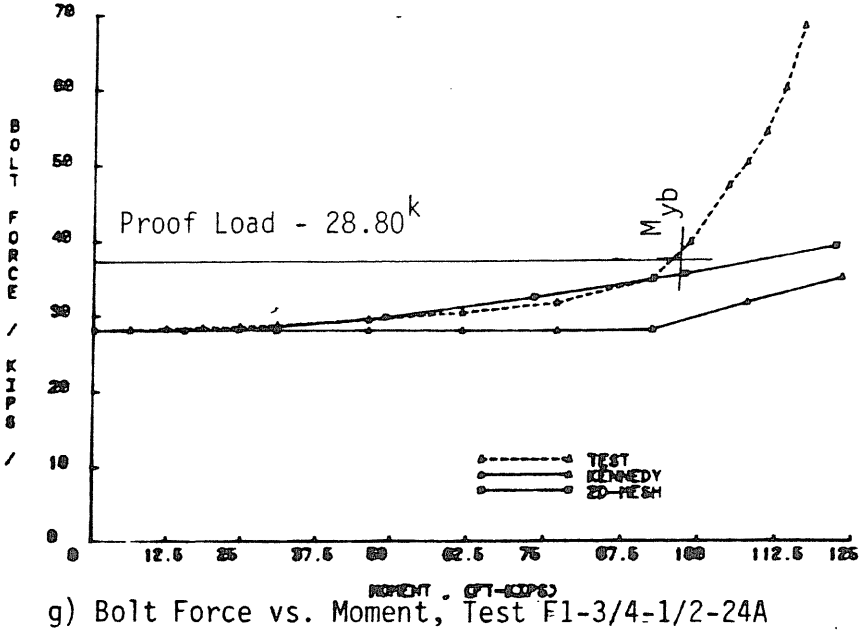

g) Bolt Force vs. Moment, Test F1-3/4-1/2-24A

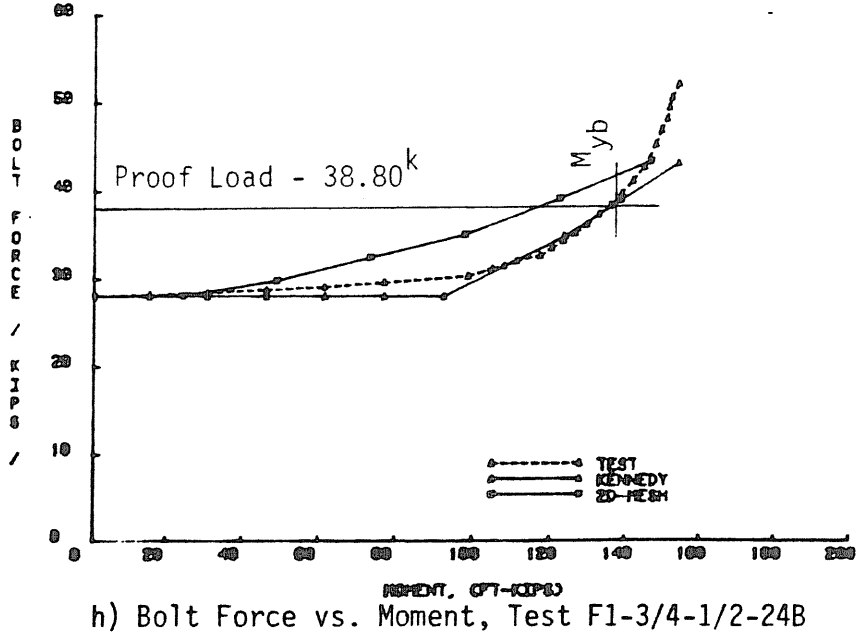

h) Bolt Force vs. Moment, Test F1-3/4-1/2-24B

Figure 3.12 Bolt Force vs. Moment Relationship for Two-Bolt Flush End-Plates

Table 3.5
Yield Moment Comparisions for Two-Bolt Flush End-Plate Tests

Test	Maximum Applied Moment (ft.-k)	Yield Moments			Ratios		
		Strength M_{yv} (ft-k)	Separation M_{ys} (ft-k)	Bolt M_{yb} (ft-k)	$\frac{M_{yv}}{M_{max}}$	$\frac{M_{ys}}{M_{max}}$	$\frac{M_{yb}}{M_{max}}$
F1-3/4-1/2-16	92.50	60.0	46.2	64*	0.65	0.50	0.69
F1-3/4-3/8-16	53.96	18.0	30.0	53.5	0.33	0.56	0.99
F1-5/8-1/2-16	77.08	49.6	39.8	48.0	0.64	0.52	0.62
F1-5/8-3/8-16	64.75	45.0	38.1	58.0	0.69	0.59	0.90
F1-5/8-3/8-10	33.92	16.7	16.3	25.0	0.42	0.41	0.63
F1-5/8-1/2-10	39.47	18.8	21.7	29.3	0.55	0.64	0.86
F1-3/4-1/2-24A	120.2	115.0	87.5	96.3	0.96	0.73	0.80
F1-3/4-1/2-24B	154.2	92.3	95.4	137.0	0.60	0.62	0.89

*Extrapolated

M_{yv} = moment at which the experimental vertical deflection exceeds the predicted deflection by 10%.

M_{ys} = moment at which the experimental plate separation exceeds the predicted separation by 10%.

M_{yb} = moment at which the experimental bolt force is at the proof load (twice the allowable) of the bolt.

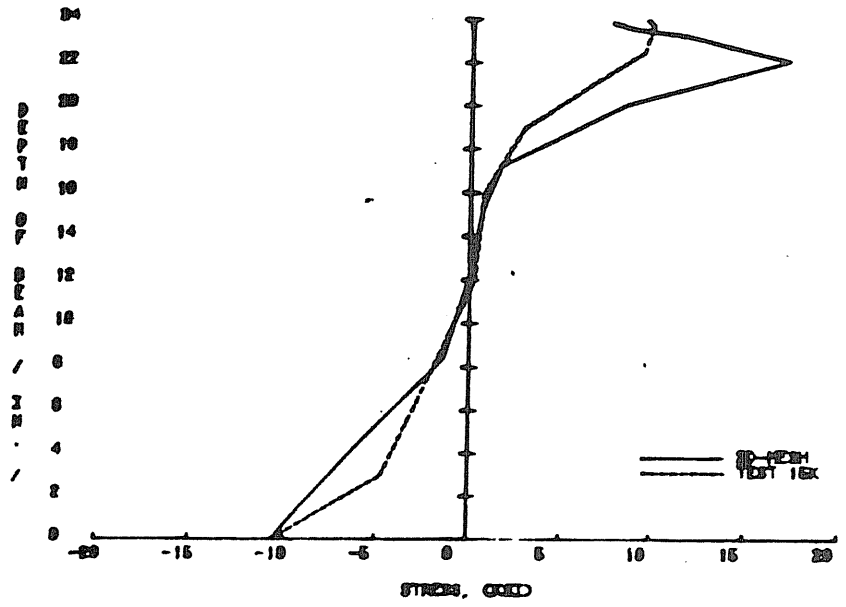

a) Stress Distribution 2 in. from End-Plate at 30% of Maximum Moment

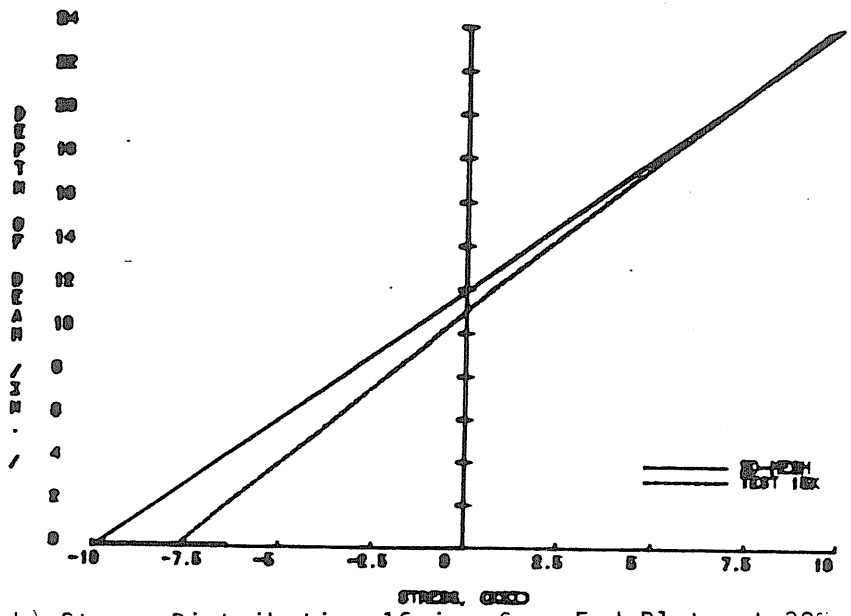

b) Stress Distribution 16 in. from End-Plate at 30% of Maximum Moment

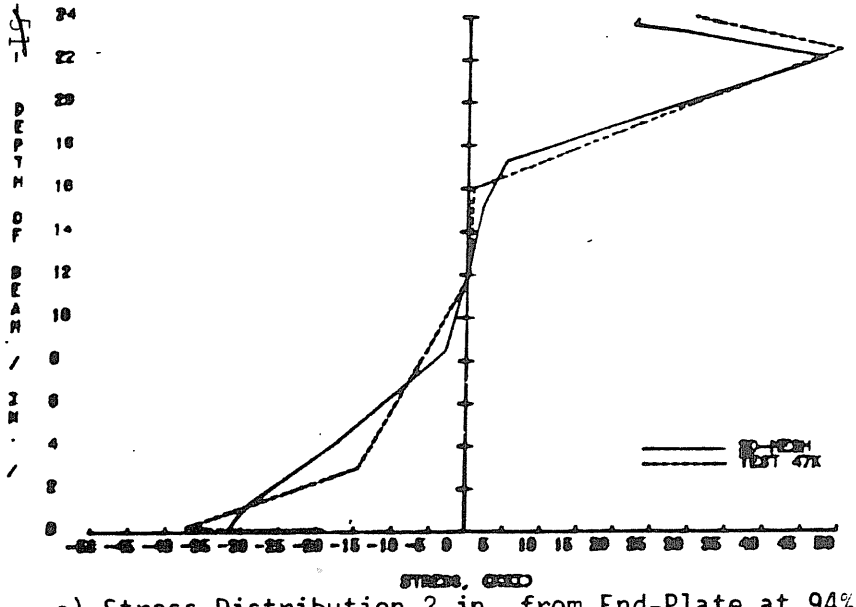

c) Stress Distribution 2 in. from End-Plate at 94% of Maximum Load

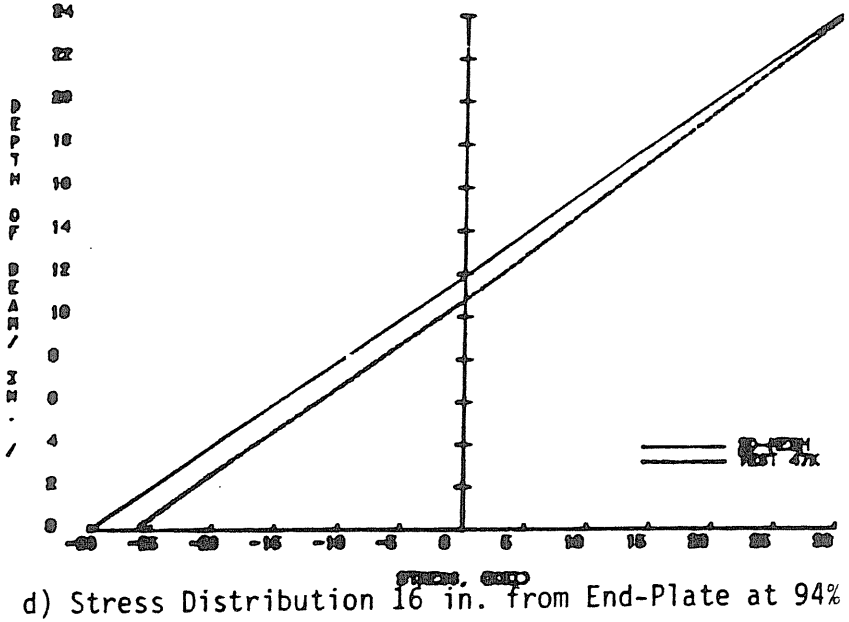

d) Stress Distribution 16 in. from End-Plate at 94% of Maximum Load

Figure 3.13 Stress Distribution for Two-Bolt Flush End-Plate

the tension flange of the beam is at the top. This comparison was made for all the tests and similar results were observed. The 2D finite element model over-estimates the web stresses in the vicinity of the tension bolts at low load levels, Figure 3.13(a). Excellent agreement was found at higher load levels, Figure 3.13(c). At 16 in. from the end-plate, the predicted and measured tension flange stresses were in aggreement at both load levels, but the measured compression flange stresses were 20% to 35% less than the predicted stresses.

3.2.2 Results of Four-Bolt Flush End-Plate Tests

Six specimens were tested in this series. Four of these specimens were tested using a 16 in. deep beam and two were tested using a 24 in. deep beam. The test results consist of the same data as the two-bolt flush end-plate; load versus vertical deflection, load versus plate separation, load versus bolt forces, and stress distribution at the cross-sections. Again failure moment and the failure mode were noted during the tests.

Table 3.6 summarizes the strength data for the four bolt flush end-plate connection tests. The ratio of maximum applied moment to predicted failure moment using the yield-line mechanism varied from 0.97 to 1.06; the resulting errors are less than 6% for all the tests.

To predict the vertical deflection of the test beam, Equation 3.1 was used. The predicted failure load, obtained using the yield-line analysis, is indicated on these plots, in the same manner as it was for the two-bolt flush end-plate tests.

Table 3.6
Summary of Strength Data for Four-Bolt Flush End-Plate Tests

Test Number	Actual Failure Moment (ft-k)	Straight Yield Lines		
		Predicted Failure Moment (ft-k)	$\frac{M_{act}}{M_{pred}}$	Error
F2-5/8-1/2-16	108	109.1	0.99	1%
F2-5/8-3/8-16	85.5	81.6	1.05	5%
F2-3/4-1/2-24	171.8	177.3	0.97	3%
F2-3/4-3/8-24	144.7	136.4	1.06	6%
F2-3/4-1/2-16	115.5	112.2	1.03	3%
F2-3/4-3/8-16	73.2	68.8	1.06	6%

For the load versus plate separation plots, the prediction equation included a factor that was determined experimentally. The correction factor for Equation 2.43 was found to be a function of the end-plate thickness and is given by

$$\alpha_s = (0.375/t_p)^2 \qquad (3.2)$$

This factor indicates that an end-plate more than 3/8 in. thick should experience less plate separation than a 3/8 in. end-plate. Similarly, an end-plate that is less than 3/8 in. thick should experience a higher plate separation. The correction factor is equal to one when the end-plate is 3/8 in. thick. This was determined from the observation that the experimental plate separation for the tests with a 3/8 in. end-plate followed the line given by Equation 2.43 without any correction required, while the 1/2 in. end-plate tests experienced a lower plate-separation than the prediction line of Equation 2.43 without a corection factor. However, with the correction factor applied, the prediction line is closer to the experimental values.

Bolt force versus load plots include predictions obtained by the modified Kennedy et. al. method. The cross-section stress distribution plots included the flexure formula line (σ = My/I) for comparison purposes.

Figure 3.14 shows the moment versus vertical displacement relationship for all six tests. From these plots it is noted that the vertical deflection of the beams always followed the prediction line upto a certain moment at which the curve softened. This behavior is similar to that observed in the two-bolt flush end-plate tests.

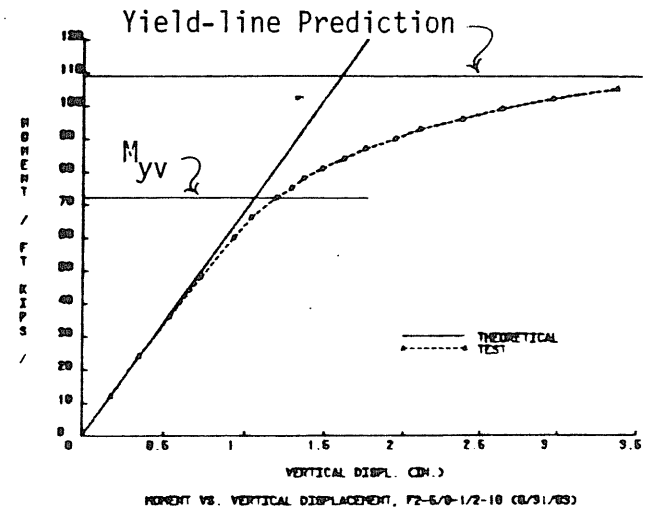

a) Moment vs. Vert. Displ., F2-5/8-1/2-16

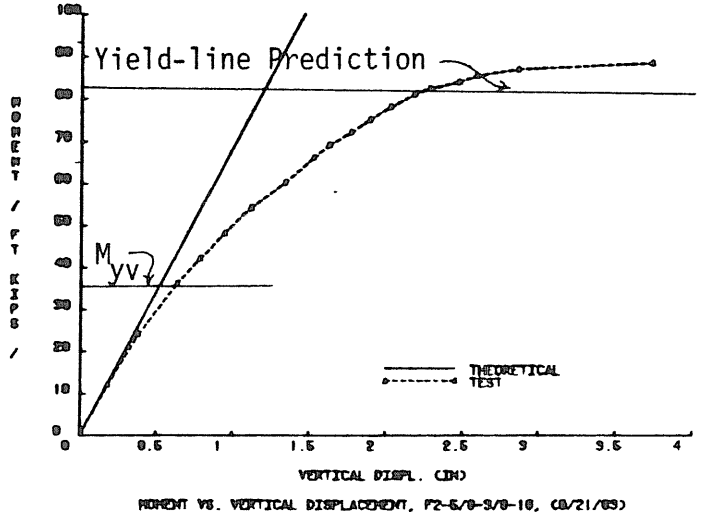

b) Moment vs. Vert. Displ., F2-5/8-3/8-16

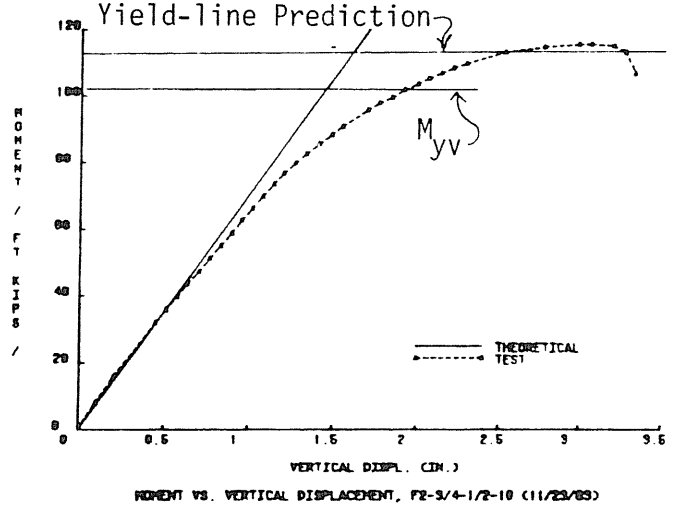

c) Moment vs. Vert. Displ., F2-3/4-1/2-16

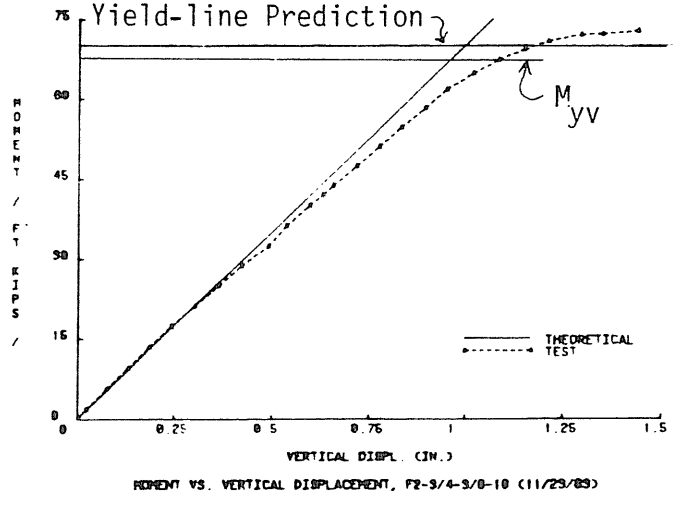

d) Moment vs. Vert. Displ., F2-3/4-3/8-16

Figure 3.14 Moment vs. Vertical Displacement Relationship for Four-Bolt Flush End-Plates

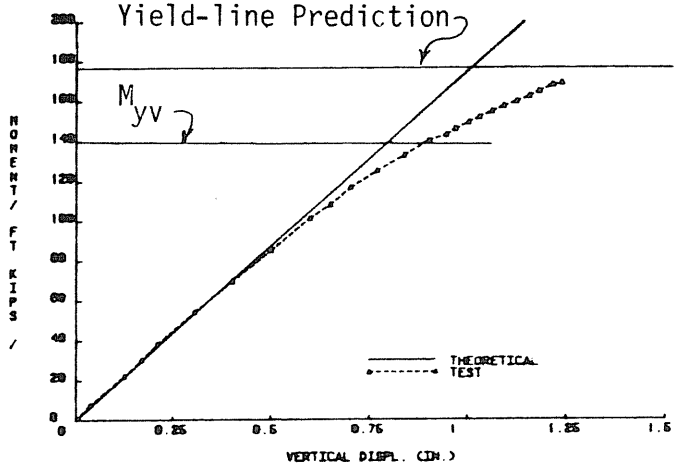

a) Moment vs. Vert. Displ., F2-3/4-1/2-24

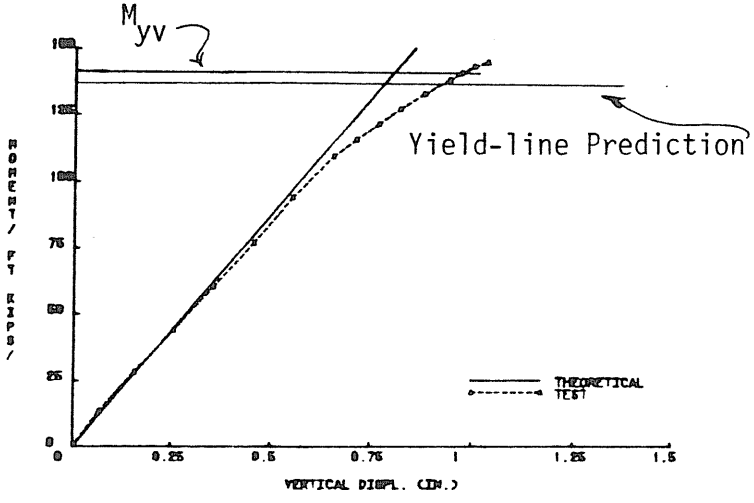

b) Moment vs. Vert. Displ., F2-3/4-3/8-24

Figure 3.14 Moment vs. Vertical Displacement Relationship for Four-Bolt Flush End-Plates

Moment versus plate separation plots for the tests are shown in Figure 3.15. The theoretical line is made up of two straight lines, the line obtained using Equation 2.43 and the yield-line failure line. Good agreement exists between the measured and theoretical lines to 60-90% of the maximum applied moment, except for F2-5/8-3/8-16, the experimental curves soften and a yield plateau forms. The plate separation yield moment, M_{ys}, is noted on the plots in Figure 3.15.

Comparisons between the experimental bolt forces and the predicted values using the modified Kennedy et al. method are shown in Figure 3.16. The bolt strains were measured for both the inner and the outer row and the bolt forces calculated from these strains are shown on the plots. Although in some tests, at the early stages of loading, the inner bolt forces were slightly higher than the outer bolt forces, the outer bolt forces increased rapidly as the applied moment was increased. The measured bolt forces for the outer row were close to the predicted values to near the bolt proof load. The moment at which the bolt proof load is attained is designated as M_{yb}. The ratio of M_{yb} to the maximum applied moment varied from 0.46 to more than 1.0.

Stress distribution, calculated from measured strains, at the beam cross section 2 in. from the end-plate at two applied load levels with the flexure formula prediction line are shown in Figure 3.17. This particular stress distribution is for test F2-5/8-1/2-16 which failed by fracture of the two outer bolts. As for the two bolt tests, the stress distribution plots are such that the tension flange of the beam is at the top. Figure 3.17(a) shows the stress distribution at a

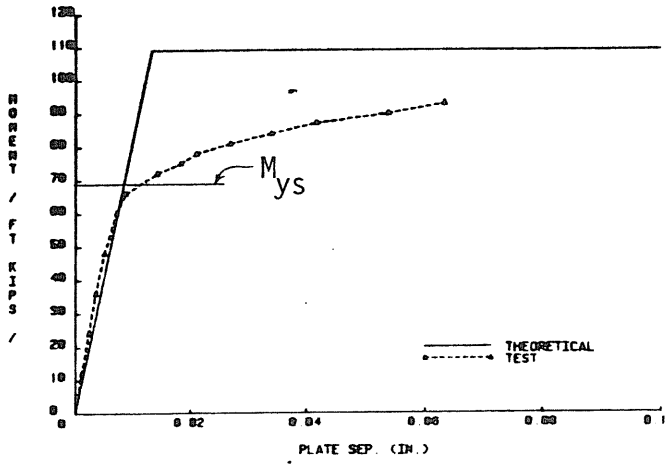

a) Moment vs. Plate Sep., F2-5/8-1/2-16

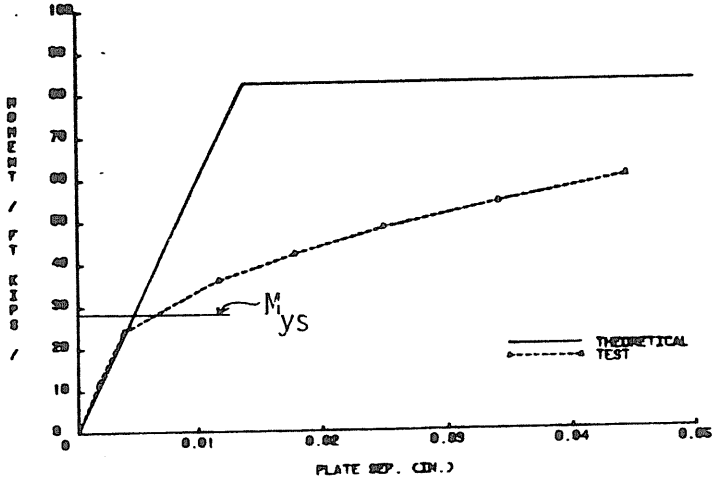

b) Moment vs. Plate Sep., F2-5/8-3/8-16

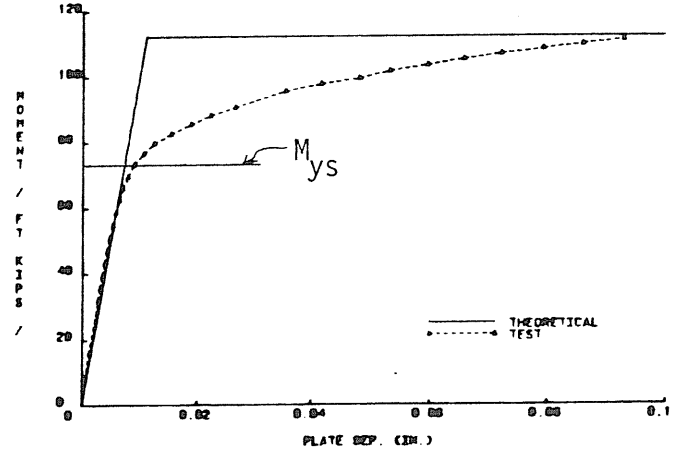

c) Moment vs. Plate Sep., F2-3/4-1/2-16

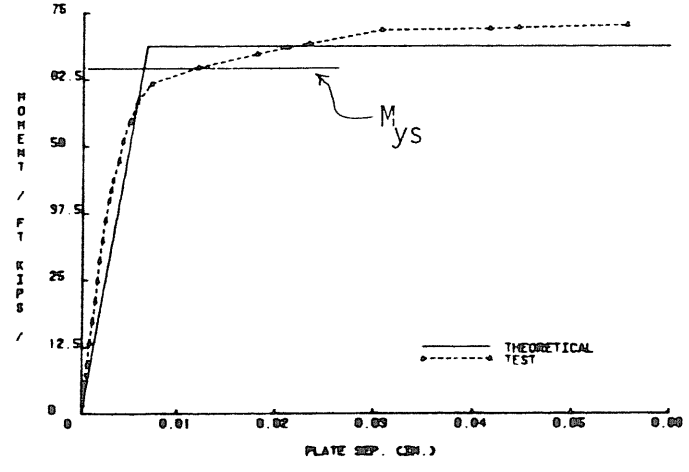

d) Moment vs. Plate Sep., F2-3/4-3/8-16

Figure 3.15 Moment vs. Plate Separation Relationship for Four-Bolt Flush End-Plates

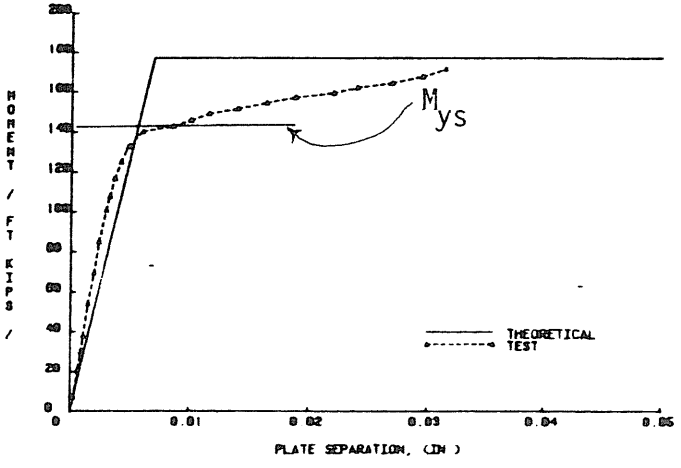

a) Moment vs. Plate Sep., F2-3/4-1/2-24

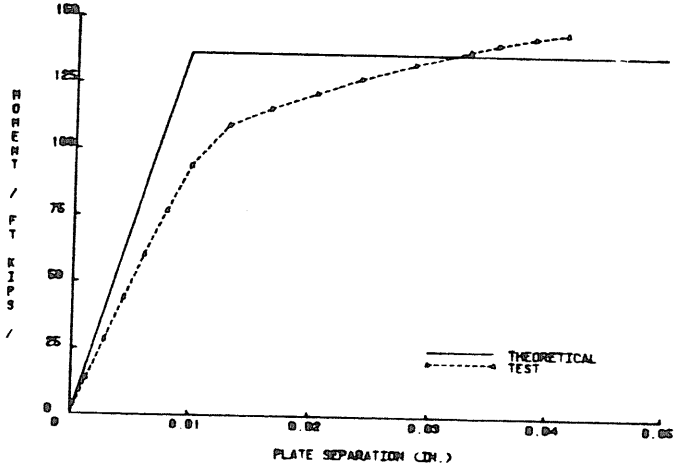

b) Moment vs. Plate Sep., F2-3/4-3/8-24

Figure 3.15 Moment vs. Plate Separation Relationship for Four-Bolt Flush End-Plates

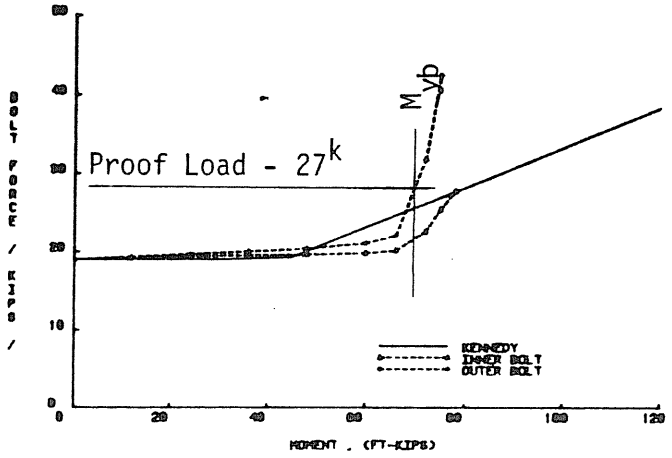

a) Bolt Force vs. Moment, F2-5/8-1/2-16

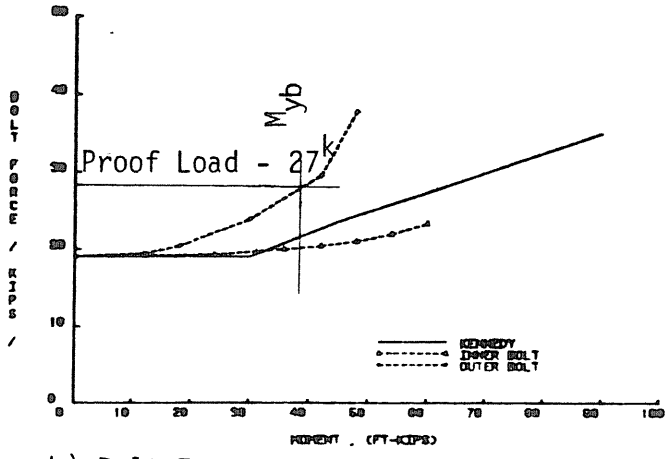

b) Bolt Force vs. Moment, F2-5/8-3/8-16

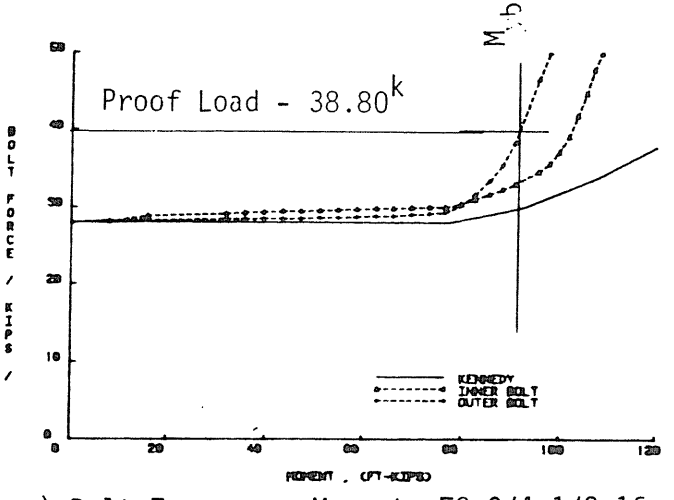

c) Bolt Force vs. Moment, F2-3/4-1/2-16

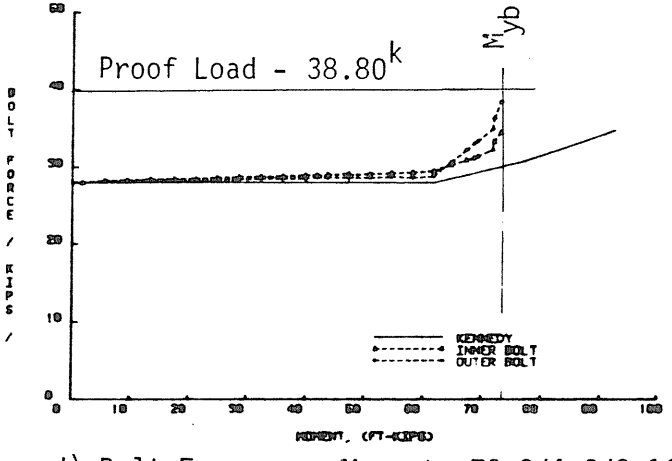

d) Bolt Force vs. Moment, F2-3/4-3/8-16

Figure 3.16 Bolt Force vs. Moment Relationship for Four-Bolt Flush End-Plates

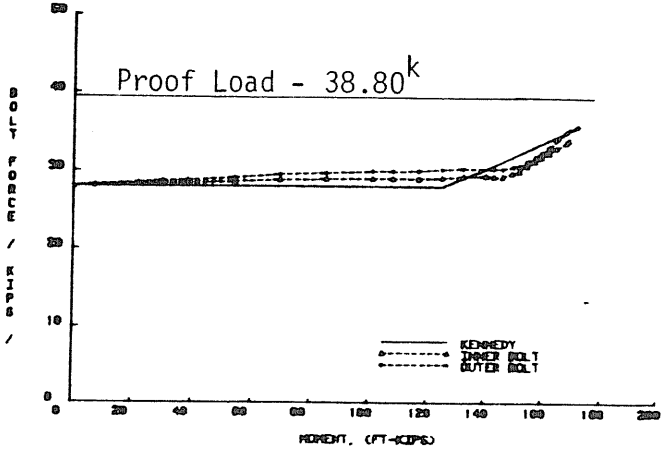

a) Bolt Force vs. Moment, F2-3/4-1/2-24

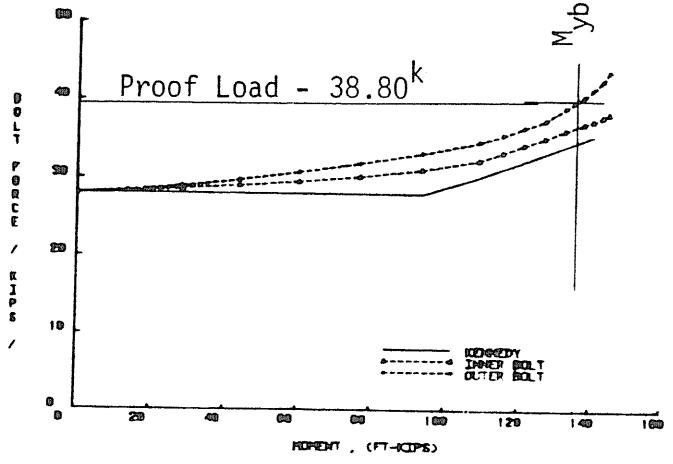

b) Bolt Force vs. Moment, F2-3/4-3/8-24

Figure 3.16 Bolt Force vs. Moment Relationship for Four-Bolt Flush End-Plates

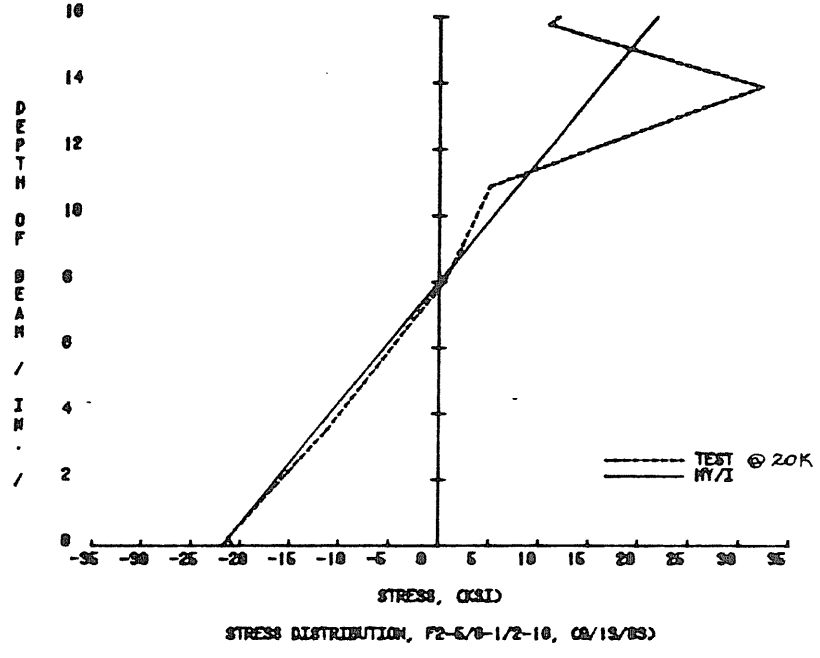

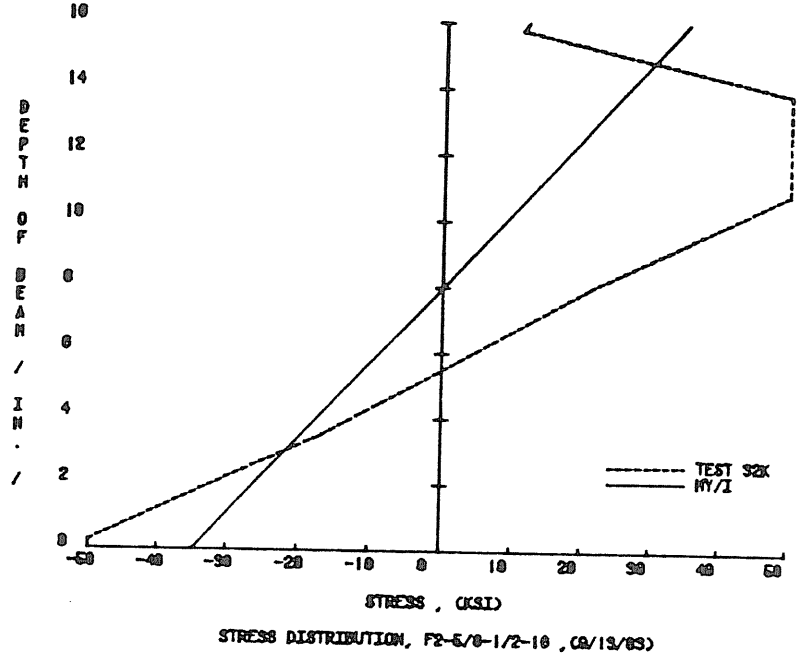

Figure 3.17 Stress Distribution for Four-Bolt FLush End-Plate

load of 20 kips. It is seen that the experimental stresses are very close to the flexure formula in the compression region. However, in the tension region it is seen that the stress is higher than predicted expecially at the line of action of the outer bolts. Figure 3.17(b) shows the stress distribution at a load level of 32 kips. From this plot it is evident that the web in the tension side has yielded at the line of action of both the outer and inner bolts. Further, the expermental stresses are not close to the values obtained by the flexure formula.

Table 3.7 presents ratios of vertical yield moment, M_{yv}; plate separation yield moment, M_{ys}; and bolt proof load moment, M_{yb} to the maximum applied moment for all six tests.

The failure modes in these tests were varied. Bolt fracture occured in test F2-5/8-1/2-16. Test F2-5/8-3/8-16 was stopped due to high bolt forces and a yielding of the end-plate. In tests F2-3/4-3/8-24, F2-3/4-1/2-24 and F2-3/4-3/8-16 yield plateau was reached in the plate separation curve. In F2-3/4-1/2-16 the beam could not handle any more load as evidenced by the moment versus vertical displacement curve.

3.2.3 Comparison of Two-Bolt and Four-Bolt Flush End-Plate Tests

Figure 3.18 shows comparisons between results from Tests F1-3/4-3/8-16 and F2-3/4-3/8-16. These two tests are geometrically identical, except for the number of bolts involved. From the moment versus vertical displacement curves shown in Figure 3.18, it can be seen that the four-bolt flush end-plate provides a stiffer connection

Table 3.7
Yield Moment Comparisons for Four-Bolt Flush End-Plate Tests

Tests	Maximum Applied Moment (ft-k)	Yield Moments			Ratios		
		Strength M_{yv} (ft-k)	Separation M_{ys} (ft-k)	Bolt M_{yb} (ft-k)	$\frac{M_{yv}}{M_{max}}$	$\frac{M_{ys}}{M_{max}}$	$\frac{M_{yb}}{M_{max}}$
F2-5/8-1/2-16	108	72	68	68	0.67	0.63	0.63
F2-5/8-3/8-16	85.5	36	27	39	0.42	0.32	0.46
F2-3/4-1/2-24	171.8	140	142	$>M_{max}$	0.81	0.83	>1.0
F2-3/4-3/8-24	144.7	142.5	—	136	0.98	—	0.94
F2-3/4-1/2-16	115.5	104	74	92	0.90	0.64	0.80
F2-3/4-3/8-16	73.2	73	65	73	1.00	0.89	1.0

M_{yv} = moment at which the experimental vertical deflection exceeds the predicted deflection by 10%.
M_{ys} = moment at which the experimental plate separation exceeds the predicted separation by 10%.
M_{yb} = moment at which the experimental bolt force is at the proof load (twice the allowable) of the bolt.

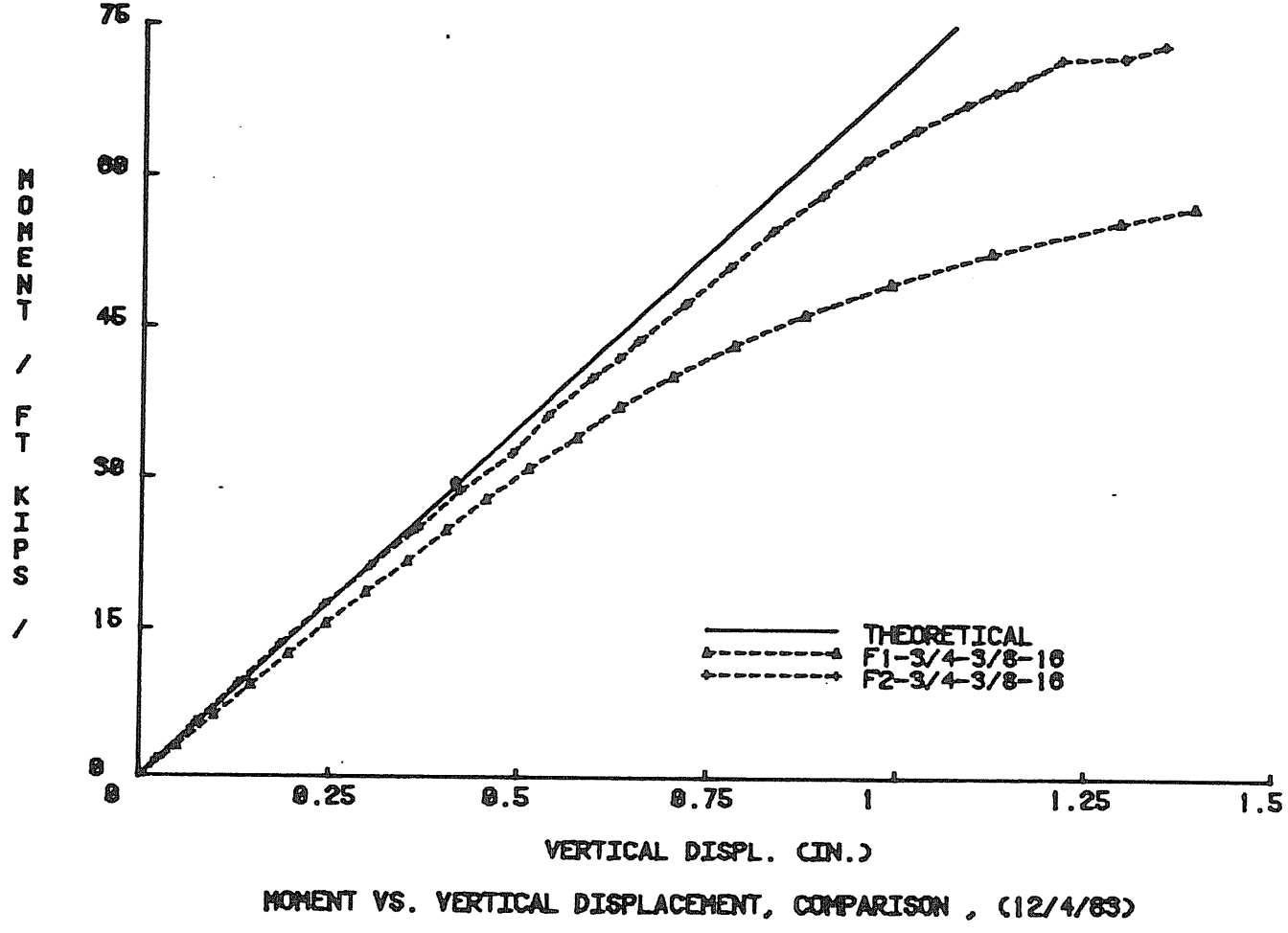

Figure 3.18 Comparison of Four-Bolt and Two-Bolt Flush End-Plate Load vs. Vertical Displacement Relationship

than a two-bolt flush end-plate, especially at higher loads. A similar conclusion is reached from the moment versus plate separation curves shown in Figure 3.19. From the bolt force comparison, Figure 3.20, it is evident that the addition of two bolts at the tension flange reduces the force that is carried by the bolts nearer the tension flange.

A complete comparison of the data from both tests is presented in Tables 3.8 and 3.9. Only five tests are compared in these tables. This is due to the fact that of the six tests performed using the four-bolt flush configuration only five had a geometrically identical counterpart in the two-bolt tests. The sixth test in the four-bolt flush end-plate series, F2-3/4-3/8-24, was with a thinner end-plate than its two-bolt flush end-plate counterpart, F2-3/4-1/2-24B.

Table 3.8 presents strength and comparison data for the two series of tests. The strength data includes the maximum applied moment, the predicted failure moment, and their ratios. The comparisons includes the ratios of the maximum applied moments for the four-bolt flush end-plates to the maximum applied moments to the two-bolt flush end-plates, the ratios of the predicted failure moment, and the ratios of the maximum to predicted failure moment ratios.

The maximum moment ratios ranged from 1.25 to 1.43, which indicates that the four-bolt flush end-plates are 25% to 43% stronger than the two-bolt flush end-plates. The predicted failure moment ratios ranged from 1.22 to 1.37, showing that the predicted increase in strength is 22% to 37%. The ratio of the ratios varied from 1.00

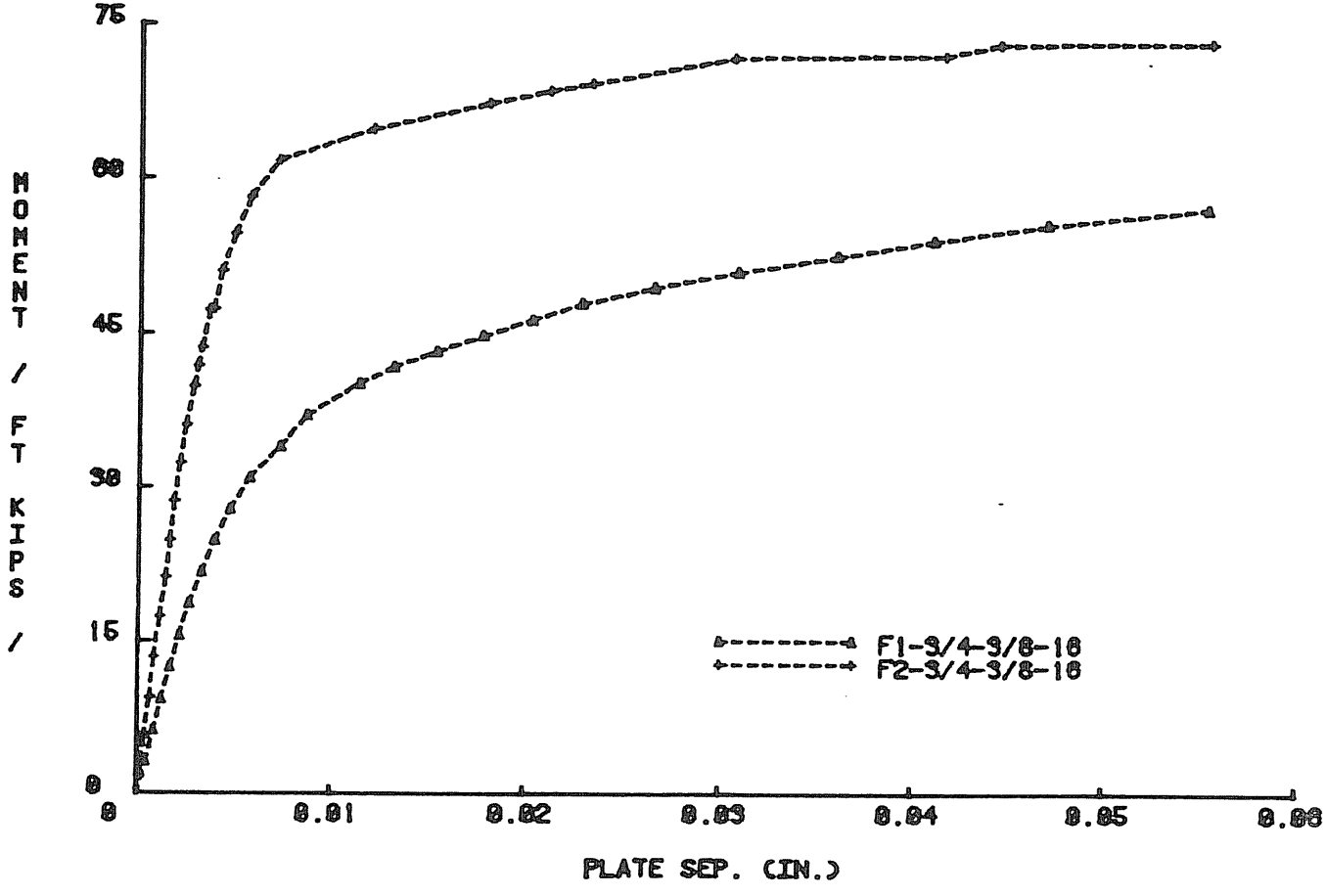

Figure 3.19 Comparison of Four-Bolt and Two-Bolt Flush End-Plate Load vs. Plate Separation Relationship

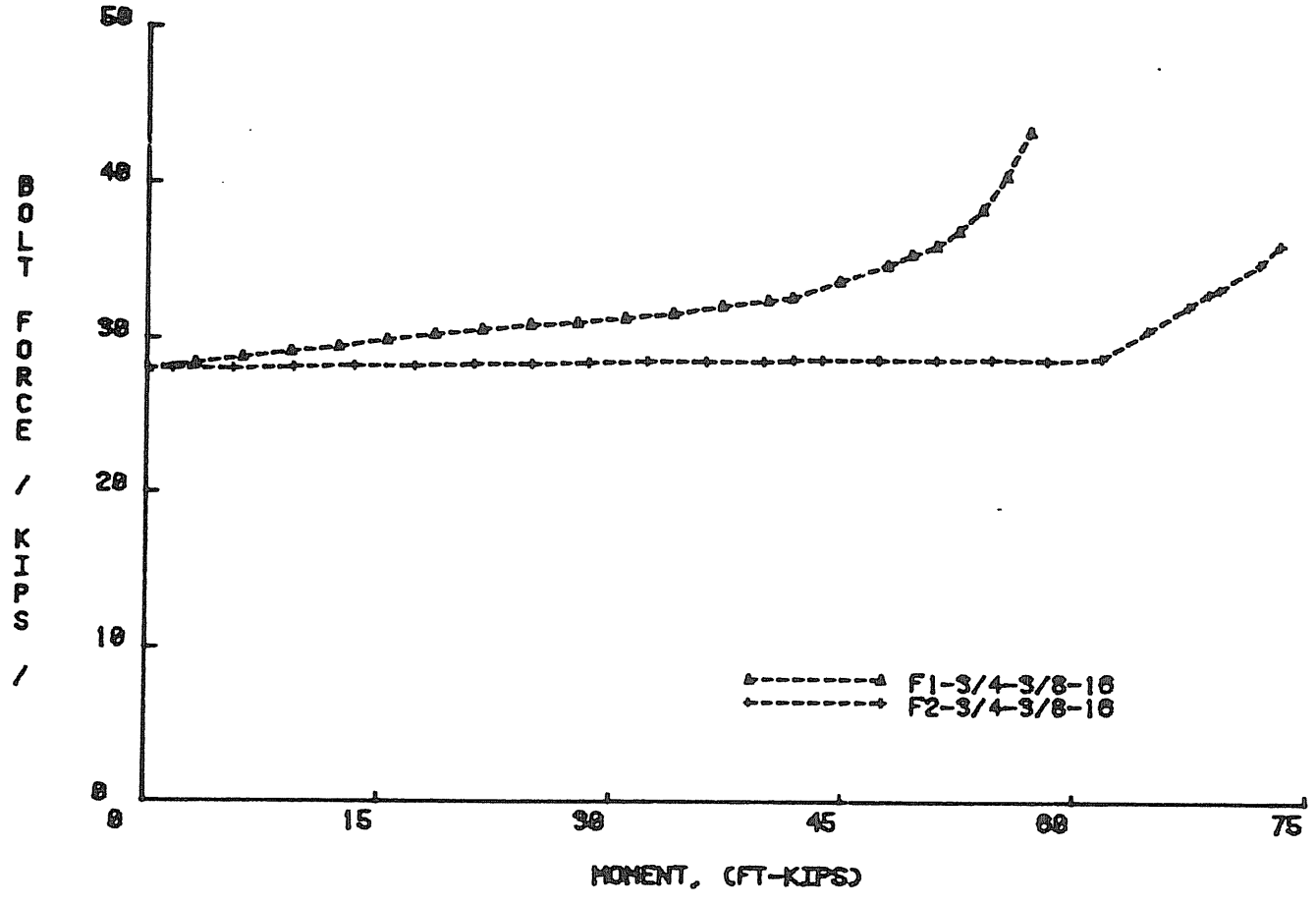

Figure 3.20 Comparison of Four-Bolt and Two-Bolt Flush End-Plate Bolt Force vs. Moment Relationship

Table 3.8 Comparisons of Two-Bolt and Four-Bolt Flush End-Plate Strength Data

Two Bolt-Flush End-Plates				Four-Bolt Flush End-Plates				Comparison		
Test No.	Maximum Applied Moment (ft-k)	Predicted Failure Moment (ft-k)	$\frac{M_{max}}{M_{pred}}$	Test No.	Maximum Applied Moment (ft-k)	Predicted Failure Moment (ft-k)	$\frac{M_{max}}{M_{pred}}$	$\frac{(M_{max})_4}{(M_{max})_2}$	$\frac{(M_{pred})_4}{(M_{pred})_2}$	$\frac{(Ratio)}{(Ratio)_2}$
F1-5/8-1/2-16	77.1	80.0	0.96	F2-5/8-1/2-16	108	109.1	0.99	1.41	1.37	1.03
F1-5/8-3/8-16	64.8	62.0	1.04	F2-5/8-3/8-16	85.5	81.6	1.05	1.32	1.37	1.01
F1-3/4-1/2-24A	120.2	145.2	0.83	F2-3/4-1/2-24	171.8	177.3	0.97	1.43	1.22	1.16
F1-3/4-1/2-16	92.5	90.1	1.03	F2-3/4-1/2-16	115.5	112.2	1.03	1.25	1.25	1.00
F1-3/4-3/8-16	54.0	54.3	0.99	F2-3/4-3/8-16	73.2	68.8	1.06	1.25	1.27	1.08

Table 3.9 Comparisons of Two-Bolt and Four-Bolt Flush End-Plate Yield Moments Data

Two-Bolt Test No.	Four-Bolt Test No.	$\frac{(M_{yv})_4}{(M_{yv})_2}$	$\frac{(M_{ys})_4}{(M_{ys})_2}$	$\frac{(M_{yb})_4}{(M_{yb})_2}$	$\frac{(M_{yv}/M_{max})_4}{(M_{yv}/M_{max})_2}$	$\frac{(M_{ys}/M_{max})_4}{(M_{ys}/M_{max})_2}$	$\frac{(M_{yb}/M_{max})_4}{(M_{yb}/M_{max})}$
F1-5/8-1/2-16	F2-5/8-1/2-16	1.45	1.71	1.42	1.05	1.21	1.02
F1-5/8-3/8-16	F2-5/8-3/8-16	0.80	0.71	0.67	0.61	0.54	0.51
F1-3/4-1/2-24A	F2-3/4-1/2-24	1.22	1.62	>1.79	0.84	1.14	>1.25
F1-3/4-1/2-16	F2-3/4-1/2-16	1.73	1.60	1.44	1.38	1.28	1.16
F1-3/4-3/8-16	F2-3/4-3/8-16	4.06	2.17	1.36	3.03	1.59	1.01

to 1.16 and show that the prediction equations are consistent in accuracy between the two configurations.

Table 3.9 presents comparisons of the yield moments, M_{yv}, M_{ys}, and M_{yb}, for the two configurations. Again, five pairs of tests are compared. In all but one test of the four-bolt flush end-plate connections, F2-5/8-3/8-16, the ratios showed an increase in stiffness and a decrease in the bolt force. For the vertical displacement yield moment ratios, $(M_{vs})_4/(M_{vs})_2$, four out of the five tests showed increases of 22% to 400% in stiffness. Similar results are obtained from the plate separation yield moment ratios, $(M_{ys})_4/(M_{ys})_2$. The increase in stiffness is shown to be 60% to over 100%. The ratios of the bolt proof load moments, $(M_{yb})_4/(M_{yb})_2$, show that the proof load is reached at 36% to over 79% higher moment for the four-bolt flush end-plate configurations. The ratios of the ratios, shown in the last three columns of Table 3.9, show that the four-bolt flush end-plates, in four out of five tests, reached the three yield moments at moments closer to the failure moment than the two-bolt flush end-plates.

The results of test F2-5/8-3/8-16 exhibited low values for the vertical displacement yield moment, M_{yv}, and the plate separation yield moment, M_{ys}. The reasons for this behavior are unknown. However, as a result of the low yield moment values, the ratios obtained for this test in Table 3.9 are not consistent with the other tests.

3.3 Comparison with Existing Data for Extended End-Plates

The experimental portion of the present study was limited to flush end-plates. However, experimental results for four bolt, extended

end-plates are available in the literature. Krishnamurthy[11,12] has reported two series of tests on unstiffened extended end-plates. The first series was an experimental validation for the unstiffened extended end-plate design procedure suggested by Krishnamurthy and later adopted by the AISC[10]. The second series was an experimental investigation of thin splice-plate connections that were designed using the AISC equation. The purpose of this series was to determine the behavior of extended end-plate connections when very thin plates are used.

The first series consisted of nine tests with dimensions given in Table 3.10. The end-plates were selected to develop the beam plastic moment. The failure mode for test 1 was lateral-torsional buckling of the beam. Additional lateral restraint was provided for the rest of the tests, however, torsional movement still occurred between load points in these tests. The failure modes of the other specimens were due to compression flange local buckling at load points or near the end-plate.

The strength results of this series of tests are shown in Table 3.11 along with the yield-line predicted failure moments obtained from Equation 2.35. Comparing the maximum applied moments with the predicted failure moments, it is evident that the specimens failed at a moment close to or less than the predicted value. The failures in all the tests were due to torsion or local buckling in the beam elements, with no signs of distress in the end-plates. Thus in some cases the ultimate moment capacity of the end-plate was not reached, however, the yield-line equation predicts the ultimate moment of the end-plate.

In the second series ten specimens were tested. The dimensions

Table 3.10

Dimension of Test Specimens for First Series of Krishnamurthy Tests

Test No.	h (in.)	b_f (in.)	p_f (in.)	t_f (in.)	t_p (in.)
1	15.65	5.50	1.3125	0.345	0.625
2	11.96	6.50	1.4375	0.40	0.750
3	16.00	7.00	1.50	0.503	0.760
4	13.00	6.00	1.344	0.500	0.622
5	15.65	5.50	1.0625	0.345	0.500
6	9.00	6.00	1.3125	0.500	0.6875
7	16.00	7.00	1.5625	0.503	0.75
8	24.75	6.00	1.25	0.375	0.50
9	24.75	6.00	1.75	0.375	0.75

Table 3.11

Test Results of First Series of Krishnamurthy Tests

Test No.	M_p (ksi)	M_{max} (ksi)	M_{pred} (ksi)	$\frac{M_{max}}{M_p}$	$\frac{M_{max}}{M_{pred}}$	Failure* Mode
1	162.8	97.7	167.5	0.60	0.58	TF
2	124.3	125.6	167.5	1.01	0.75	TB
3	226.6	228.9	221.5	1.01	1.03	FB
4	182.9	181.1	178.2	0.99	1.02	FB
5	168.7	185.6	146.4	1.10	0.82	FB
6	116.0	120.7	121.1	1.04	1.00	TF
7	263.7	266.3	270.3	1.01	0.99	FB
8	420.6	336.5	318.1	0.80	1.06	WFB
9	338.1	280.6	402.5	0.83	0.70	WFB

* TF- Torsional failure
TB- Torsional buckling
FB- Compression flange buckling
WFB- Compression web and flange buckling
T- Torsional twisting

of the soecimens are given in Table 3.12. These tests are separated into five sets of two each. Each test in a set was conducted using the same beam and end-plate geometry, except the plate thickness, to determine the effect of the thickness on the behavior of the connection. Strength results from this series of tests, along with the predicted yield-line moments, are given in Table 3.13. Comparing the maximum moments applied within each set, it is seen that the thinner end-plate in every set reached a higher moment. This seems to indicate some discrepancy in either the testing or the reporting of the results. The yield-line predicted values are close to the maximum applied moments for the thicker end-plates in every set. For the thinner end-plate of each set, the predicted values are much lower than reported maximum moments.

In summary, the predicted moments from the yield-line solutions developed here, agree well with Krishnamurthy's test results except for the B,-tests in the second series and the tests in the first series which failed due to torsion.

As mentioned earlier, no test results for stiffened, extended end-plate tests were found in the literature. Thus, the prediction equation developed herein cannot be verified.

Table 3.12

Dimensions of Test Specimens for Second Series of Krishnamurthy Tests

Test No.	h (in.)	b_f (in.)	p_f (in.)	g (in.)	t_f (in.)	t_p (in.)
4A	13.00	6.0	1.3125	3.0	0.5	0.50
4B	13.00	6.0	1.3125	3.0	0.5	0.375
6A	9.00	6.0	1.3125	3.0	0.5	0.50
6B	9.00	6.0	1.3125	3.0	0.5	0.375
8A	24.75	6.0	1.3125	3.0	0.375	0.4375
8B	24.75	6.0	1.3125	3.0	0.375	0.375
9A	24.74	6.0	1.75	3.0	0.375	0.5625
9B	24.75	6.0	1.75	3.0	0.375	0.375
10A	36.00	8.0	1.5	5.0	0.375	0.5
10B	36.00	8.0	1.5	5.0	0.375	0.375

Table 3.13

Test Results for Second Series of Krishnamurthy Tests

Test No.	M_p (ksi)	M_{max} (ksi)	M_{pred} (ksi)	$\frac{M_{max}}{M_p}$	$\frac{M_{max}}{M_{pred}}$	Failure Mode *
4A	151.2	152.8	150.2	1.01	1.02	T
4B	168.8	154.4	84.5	0.91	1.83	FB
6A	94.4	91.0	100.9	0.96	0.90	T
6B	106.3	92.6	56.8	0.87	1.63	H
8A	271.6	250.3	265.0	0.92	0.94	WFB
8B	289.0	266.5	154.8	0.92	1.72	WFB
9A	271.6	243.8	299.8	0.90	0.81	WFB
9B	289.0	253.5	168.6	0.87	1.50	WB
10A	736	500.5	505.5	0.68	0,99	WFB
10B	689.8	448.4	226.2	0.65	1.98	X

CHAPTER IV

SUMMARY, CONCLUSIONS AND RECOMMENDATIONS

4.1 Summary

The investigation of four types of end-plates; two-bolt flush end-plates, four-bolt flush end-plates, stiffened extended end-plates, and unstiffened extended end-plate; has been described in the preceding chapters. The investigation included yield-line analyses of the four types of end-plates, finite element analyses of the two-bolt flush end-plate, and procedures to estimate bolt forces, along with expermental testing of the two-bolt flush end-plates and the four-bolt flush end-plates to verify the analytical models. Comparisons with existing test data for the unstiffened extended end-plates are also conducted to verify the analytical model for that particular end-plate configuration.

Eight two-bolt flush end-plates and six four-bolt flush end-plates were tested and the data obtained was compared to the analytical predictions. The test results in both sets were very similar and compared well with the predictions.

4.2 Conclusions

The major conclusions drawn from this study are:

1. The straight yield-line mechanism adequately predicts the

strength of the two- and four-bolt flush end-plate connections. In the seven tests of the two-bolt flush end-plate where yielding of the end-plate governed the maximum applied moment, the ratio of applied to predicted moment varied from 0.94 to 1.08 (Table 3.4). In the eighth test, the maximum moment was governed by rapidly increasing bolt force. In all six tests of the four-bolt flush end-plate, the yielding of the end-plate governed the maximum applied moment. The ratio of applied moment to the straight yield-line prediction moment varied from 0.97 to 1.06 (Table 3.6).

2. The straight yield-line analysis of the unstiffened extended end-plates adequately predicted the failure moments of most of the Krishnamurthy tests. However, some discrepancy existed with the thin plate results in the second series of tests.

3. Results from the curved yield-line mechanism used for the two-bolt flush end-plates are conservative. For the seven tests mentioned above, the ratio of maximum applied to predicted moment varied from 1.03 to 1.15 (Table 3.4).

4. If the moment due to the dead load of the beam and various test fixtures (approximately 3 ft - kips) is added to the maximum applied moments the ratios are increased by 2 - 10%.

5. The modified Kennedy et. al. procedure adequately predicts bolt forces to the proof load. (See Figures 3.12 and 3.16)

6. The 2D finite element model accurately predicts plate separation and, hence, curvature for the two-bolt flush end-plates until excessive end-plate yielding occurs (Figure 3.11).

7. The moment versus vertical displacement curves for the two-bolt flush end-plates tested were linear to 50% - 60% of the total strength (See Figure 3.10). The curves for the four-bolt flush end-plates were linear to 70% - 100% of the total strength (Figure 3.14).

8. The applied moment corresponding to the bolt proof load was always equal to or greater than the "yield moment" based on the plate separation or the vertical displacement. This was true for both the two-bolt and the four-bolt flush end-plate connections.

9. The useful strength of the two-bolt flush end-plate connection studied here may be limited to 50% - 60% of the strength predicted by the straight yield-line mechanism because of excessive deformation due to end-plate yielding unless the connection is located at an assumed plastic hinge. Similarly, the useful strength of the four-bolt flush end-plate connection may be limited to 70% - 100% of the strength predicted by the yield-line mechanism.

10. The strength of the connection can be governed by the web-to-end-plate weld strength.

11. Stresses in the beam web of the two-bolt flush end-plate can adequately be predicted using the 2-D finite element model. The stresses near the tension bolts are the highest, but did not exceed the nominal yield stress of the web material.

12. Stresses in the beam web of the four-bolt flush end-plate was not predicted well by the flexture formula, and in some tests the nominal yield stress was exceeded.

4.3 Recommendations

For the two-bolt flush end-plates, with the range of geometries used in this research, it is recommended that Equation 2.16 be used to determine end-plate thickness for a given ultimate design moment. For stiffness requirements, the following design moments are recommended:

- Type III Construction (Semi Rigid Framing)

$$M_w = 0.6\ M_u$$

- Type I Construction (Rigid or Continuous Framing)

$$M_w = 0.75\ M_y = 0.75\ (0.5\ M_u)$$

$$M_w = 0.375\ M_u$$

The required bolt size can then be determined using Equations 2.27 to 2.38 and

$$d_b = \sqrt{2B/\pi F_a} \qquad (4.1)$$

where F_a = the allowable stress of the bolt material. In the AISC specification [18], the allowable tensile stress for A325 bolt material is 44 ksi with a factor of safety against yielding of 2.0. Equation 4.1 reflects this factor of safety. The recommended procedure is demonstrated in the following design example.

Design Example (1). Determine end-plate thickness, for both Type III and Type I Construction, and bolt size for build-up beam with dimensions below and a working moment of 30 ft-kips - A572 Gr50 steel and A325 bolts. (using two-bolt flush end-plate).

$h = 16$ in. $\quad b_f = 6$ in. $\quad p_f = 1\ 3/8$ in.

$t_w = 1/4$ in. $\quad t_f = 1/4$ in. $\quad g = 2\ 3/4$ in.

a). For Type III Construction

Step 1. Determine Mu and end-plate thickness (Equations 2.6 and 2.16)

$$M_u = 30/0.6 = 50 \text{ ft. - Kips}$$

$$s = \tfrac{1}{2}\sqrt{6 \times 2.75} = 2.03 \text{ in.}$$

$$P_t = 1.375 + 0.25 = 1.625 \text{ in.}$$

$$t_p = \left[\frac{50 \times 12/50}{\{ \frac{6}{2} (\frac{1}{1.375} + \frac{1}{2.03}) + (1.375 + 2.03)(\frac{2}{2.75}) \} (16 - 1.625)} \right]^{\frac{1}{2}}$$

$t_p = 0.369$ in. Try PL 6 x 3/8

Step 2. Compute flange force and flange stress.

$$F_f = (50 \times 12)/(16 - 0.25) = 38.1 \text{ Kips}$$

$$\sigma_f = 38.1/(6 \times 0.25) = 25.4 \text{ Ksi}$$

Step 3. Find the thick plate limit, t_1, (Equation 2.27 and 2.28). Approximate thickness (Equation 2.27).

$$t_1 = \sqrt{(2.11)(1.375)(0.25)(25.4)/50}$$

$$= 0.607 >> t_p = 0.375 \text{ in.}$$

Therefore $Q \neq 0$

Step 4. Determine the thin plate limit, t_{11}, (Equation 2.29 and 2.30).

Assume $d_b = 5/8$ in.

$$w' = \frac{6}{2} - (5/8 + 1/16) = 2.313 \text{ in.}$$

F_{yb} = 120 Ksi for A325 material

Approximate thickness (Equation 2.29).

$$t_{11} = \sqrt{\frac{2\{(6.0x0.25x25.4x1.375) - \pi(0.625)^3(120)/16\}}{50(0.85x6 + 0.3x2.313)}}$$

$$= 0.518 \text{ in.}$$

Using the exact equation (Equation 2.30).

$$t_{11} = \sqrt{\frac{2(6.0x0.25x25.4x1.375 - \pi(0.625)^3(120)/16)}{6.0\sqrt{50^2-3\left(\frac{0.25x25.4}{2x0.518}\right)^2} + 2.313\sqrt{50^2-3\left(\frac{6.0x0.25x25.4}{2x2.313x0.518}\right)^2}}}$$

$$= 0.489 \text{ in.} \simeq 0.518 \text{ in.}$$

Since $t_{11} > t_p = 0.375$ in., $Q = Q_{max}$.

Step 5. Determine prying force, Q, (Equations 2.31, 2.32 or 2.35).

F_{limit} from Equation 2.36

$$F_{limit} = \frac{0.375^2 \times 50\ (0.85 \times 6.0 + 0.3 \times 2.313) + \pi\ (0.625)^3\ 120/16}{4 \times 1.375}$$

$$= 9.93 \text{ Kips}$$

$(F_f)_{max}/2 = 6.0 \times 0.25 \times 50/2 = 37.5$ Kips

Thus, F' = 9.93 Kips and a = 0.75 in.

$$Q_{max} = \frac{(2.313)(0.375)^2}{4 \times 0.75}\sqrt{50^2 - 3\left(\frac{9.93}{2.313 \times 0.375}\right)^2}$$

Q_{max} = 4.98 Kips

Step 6. Select bolt diameter

From Equation 2.33

$B = 19.05 + 4.98 = 24.03$ Kips

$d_b = \sqrt{2X\ 24.03/(\pi X44.0)} = 0.590$ in. < 0.625 in.

Use PL 6x 3/8 A572 Gr50, 2- 5/8 in. diameter A325 bolts.

Connection Strength = 51.7 ft.-Kips (Equation 2.15)

b). For Type I Construction

Step 1. Determine M_u and end-plate thickness (Equation 2.6 and 2.16)

$M_u = 30/0.375 = 80$ ft.-Kips

$s = \frac{1}{2}\sqrt{6.0x2.75} = 2.03$ in.

$$t_p = \left[\frac{80x12/50}{\left[\frac{6}{2}\left(\frac{1}{1.375}+\frac{1}{2.03}\right)+(2.03+1.375)\left(\frac{2}{2.75}\right)\right](16-1.625)}\right]^{\frac{1}{2}}$$

$= 0.47$ in. Try PL 6 x 1/2

Step 2. Compute flange force and flange stress

$F_f = 80x12/(16-0.25) = 60.95$ Kips

$\sigma_f = 60.95/(6.0x0.25) = 40.6$ Ksi

Step 3. Find the thick plate limit, t_1.

Approximate thickness (Equation 2.27)

$t_1 = \sqrt{2.11x1.375x0.25x40.6/50} = 0.767$ in.

Exact thickness (Equation 2.28)

$$t_1 = \sqrt{\frac{2x0.25x40.6x1.375}{\sqrt{50^2-3\left(\frac{0.25x40.6}{2x0.767}\right)^2}}} = 0.757 \text{ in.}$$

$t_1 > t_p = 0.50$ in.

Therefore $Q \neq 0$

Step 4. Determine the thin plate limit, t_{11}.

Assume $d_b = 3/4$ in.

$w' = \frac{6}{2} - (3/4 + 1/16) = 2.188$ in.

Approximate thickness (Equation 2.29)

$$t_{11} = \sqrt{\frac{2(6.0x0.25x40.6x1.375-(\pi/16)0.75^3x120)}{50(0.85x6.0+0.80x2.188)}}$$

$= 0.656$ in. $>> 0.5$ in.

Therefore $Q = Q_{max}$

Step 5. Determine prying force, Q.

From Equation 2.36

$$F_{1limit} = \frac{0.5^2x50(0.85x6.0+0.80x2.188) + (\pi/16)0.75^3x120}{4x1.375}$$

$= 17.38$ Kips

$(F_f)max/2 = 37.5$ Kips

Thus $F' = 17.38$ Kips and $a = 2x\ 0.5 = 1.0$ in.

$$Q_{max} = \frac{(2.188)(0.5)^2}{4x1.0}\sqrt{50^2-3(\frac{17.38}{2.188x0.5})^2}$$

$= 5.71$ Kips

Step 6. Select bolt diameter

$B = 30.48 + 5.71 = 36.19$ Kips

$$d_b = \sqrt{2x36.19/(\pi x44.0)}$$

$= 0.724$ in. < 0.75 in.

Use PL 6 x 1/2 A572 Gr50, 2- 3/4 in. diameter A325 bolts

Connection strength = 91.9 ft.-Kips (Equation 2.15)

For the four-bolt flush end-plate, with the range of geometries used, it is recommended that Equation 2.20 be used to determine the thickness for a given ultimate design moment. For stiffness requirements, the following design moments are recommended:

- Type III Construction (Semi-Rigid Framing)

$$M_w = 0.6M_u$$

- Type Construction (Rigid or Continuous Framing)

$$M_w = 0.75\ M_y = 0.75(0.7M_u)$$
$$= 0.525\ M_u$$

The required bolt size is determined using Equation 2.27 to 2.38 and 4.1. The same design example is repeated for the design of a four-bolt flush end-plate .

Design Example (2). For the working moment and geometry given in example (1), determine the thickness for a four-bolt flush end-plate and the bolt size. P_b = 3.0 in.

a). For Type III Construction:

Step 1. Determine M_u and end-plate thickness (Equations 2.10 and 2.20)

$$M_u = 30/0.6 = 50 \text{ ft. - kips}$$

$$P_{t2} = 4.625 \text{ in.}$$

$$u = \frac{1}{2}\ 6.0 \times 2.75 \times (16 - 4.625)/(16 - 1.625)$$
$$= 1.807 \text{ in.}$$

$$t_p = \left[\frac{50x12/50}{\frac{6}{2}\ (\frac{16-1.625}{1.375} + \frac{16-4.625}{1.807}) + 2(1.375+3.0+1.807)\ (\frac{16-1.625}{2.75})}\right]^{\frac{1}{2}}$$

$$= 0.323 \text{ in.} \qquad \text{Try } 6 \times 3/8$$

Step 2. Compute flange force and flange stress

$$F_f = (50 \times 12)/(16 - 0.25) = 38.1 \text{ kips}$$

σ_f = 38,1/6 x 0,25 = 25,4 ksi

Step 3. Find the thick plate limit, t_1.

same as example (1-a), t_1 = 0.607 >> t_p = 0.375 in.

Therefore, Q ≠ 0

Step 4. Determine the thin plate limit, t_{11}.

Same as example (1-a), assume d_b = 5/8 in.

$Q = Q_{max}$.

Step 5. Determine prying force, Q.

$Q = Q_{max}$ = 4.98 kips

Step 6. Select bolt diameter.

From Equation 2.38

$$B_1 = \frac{19.05}{1.5} + 4.98 = 17.68 \text{ kips} < P_T = 19.0 \text{ kips}$$

$$B_2 = F_f/6 = 6.35 \text{ kips}$$

select all bolts for B_1.

$$d_b = \sqrt{2x19.0/\pi x44.0}$$

$$= 0.524 \text{ in.} < 0.625 \text{ in.}$$

Use PL 6 x 3/8 A572 Gr50, 4- 5/8 in. diameter A325 bolts.

Connection strength = 67.3 ft.-Kips (Equation 2.19)

b). For Type I Construction

Step 1. Determine M_u and end-plate thickness.

M_u = 30/0.525 = 57.1 ft.-kips

u = 1.807 in.

From Equation 2.20.

$$t_p = \left[\frac{57.1 \times 12/50}{\frac{6}{2}\left(\frac{16-1.625}{1.375} + \frac{16-4.625}{1.807}\right) + 2(1.375+3.0+1.807)\left(\frac{16-1.625}{2.75}\right)} \right]^{\frac{1}{2}}$$

t_p = 0.345 in. Try PL 6x3/8

Step 2. Determine flange force and flange stress.

$F_f = 57.1 \times 12/(16-0.25) = 43.5$ Kips.

$\sigma_f = 43.5/(6 \times 0.25) = 29.0$ Ksi.

step 3. Find the thick plate limit, t_1, Equation 2.27.

$t_1 = \sqrt{2.11 \times 1.375 \times 0.25 \times 29.0/50}$

$= 0.649$ in. >> $t_p = 0.375$ in.

Therefore, $Q \neq 0$

Step 4. Determine the thin plate limit, t_{11}.

Approximate thickness from Equation 2.29

Assume d_b = 5/8 in.

$$t_{11} = \sqrt{\frac{2(6.0 \times 0.25 \times 29.0 \times 1.375 - (\pi/16) \times 0.625^3 \times 120)}{50(0.85 \times 6.0 + 0.80 \times 2.313)}}$$

$= 0.558$ in. > $t_p = 0.375$ in.

Exact thickness from Equation 2.30

$$t_{11} = \sqrt{\frac{2(6.0 \times 0.25 \times 29.0 \times 1.375 - (\pi/16) 0.625^3 \times 120)}{6.0\sqrt{50^2 - 3\left(\frac{0.25 \times 29.0}{2 \times 0.558}\right)^2} + 2.313\sqrt{50^2 - 3\left(\frac{6.0 \times 0.25 \times 29.0}{2 \times 2.313 \times 0.558}\right)^2}}}$$

$= 0.524$ in. > $t_p = 0.375$ in.

Therefore $Q = Q_{max}$

Step 5. Determine prying force, Q

From Example (1-a), Q_{max}= 4.98 Kips

Step 6. Select bolt diameter.

From Equation 2.38

$$B_1 = \frac{21.75}{1.5} + 4.98 = 19.48 \text{ Kips}$$

$$d_b = \sqrt{2x\ 19.48/(\pi x 44.0)}$$

$$= 0.531 \text{ in.} < 0.625 \text{ in.}$$

Use PL 6 x 3/8 A572 Gr50, 4- 5/8 in. diameter A325 bolts

Connection strength = 67.3 ft.-kips.

For comaprison, the results of the previous examples are summarized in Table 4.1.

Table 4.1

Summary of Flush End-Plate Design Examples

	Type	Bolt Diameter (in.)	Plate Thickness (in.)	Connection Strength (ft.-kips)
Two-Bolt	I	5/8	3/8	51.7
	III	3/4	1/2	91.9
Four-Bolt	I	5/8	3/8	67.3
	III	5/8	3/8	67.3

It is noted that the required moment capacity for the four-bolt flush end-plate in Example 2 increased from 50 ft.-kips, for Type III construction, to 57.1 ft-kips, for Type I construction. This increase did not result in an increase in the required end-plate thickness, as can be seen from Table 4.1.

For the unstiffened extended end-plates it is recommended that Equation 2.22 be used to determine end-plate thickness for a given design moment. The design procedure suggested here is based on strength requirements only. The required bolt size is determined using the same method as described earlier. The following design example is identical to that given in the AISC Manual of Steel Construction[10] (p. 4-114).

Design Example (3). Determine the required end-plate thickness and bolt diameter for a connection with a working moment of 120 ft.-kips, F_y = 36ksi, and the following geometry. Use unstiffened extended end-plate.

d = 16.01 in. b_f = 6.995 in., t_f = 0.505 in.

Assume P_f = 1.5 in. g = 2.75

Step 1. Determine M_u and end-plate thickness (Equation 2.22)

M_u = 120/0.6 = 200 ft.-kips.

$s = \frac{1}{2}\sqrt{6.995 \times 2.75} = 2.193$ in.

$$t_p = \left[\frac{200 \times 12/36}{(16.01-2.005)\left[\frac{6.995}{2}\left(\frac{1}{1.5}+\frac{1}{2.193}\right)+(1.5+2.193)\left(\frac{2}{2.75}\right)\right]+\frac{6.995}{2}\left(0.5+\frac{16.01}{1.5}\right)} \right]^{\frac{1}{2}}$$

t_p = 0.712 in. Try PL 7x3/4

(An 8 in. wide end-plate was chosen in the AISC Manual example.)

Step 2. Compute flange force and flange stress.

F_f = (200x12)/(16-0.505) = 154.79 kips

σ_f = 154.79/(6.995x0.505) = 43.82 ksi

Step 3. Find the thick plate limit, t_1.

Approximate thickness (Equation 2.27).

$$t_1 = \sqrt{2.11 \times 1.5 \times 0.505 \times 43.82/36}$$

$$= 1.395 \text{ in.} >> t_p = 0.75 \text{ in.}$$

Therefore $Q \neq 0$

Step 4. Determine the thin plate limit, t_{11}.

Assure $d_b = 7/8$ in.

$$w' = \frac{6.995}{2} - (7/8+1/16) = 2.56 \text{ in.}$$

Approximate thickness (Equation 2.29)

$$t_{11} = \sqrt{\frac{2(6.995 \times 0.505 \times 43.82 \times 1.5 - \pi(.875)^3 (120)/16)}{36(0.85 \times 6.995 + 0.80 \times 2.56)}}$$

$$= 1.226 \text{ in.} >> t_p = 0.75 \text{ in.}$$

Therefore, $Q = Q_{max}$

Step 5. Determine prying force, Q.

$$F_{limit} = \frac{0.75^2(36)(0.85 \times 6.995 + 0.80 \times 2.56) + \pi(.875)^3(120)/16}{4 \times 1.5}$$

$$= 29.61 \text{ kips}$$

$$F_{max} = 6.995 \times 0.505 \times 36/2 = 63.58 \text{ kips.}$$

By Equation 2.35.

$$Q_{max} = \frac{2.56 \times 0.75^2}{4 \times 1.5} \sqrt{36^2 - 3\left(\frac{29.61}{2.56 \times 0.75}\right)^2}$$

$$= 5.79 \text{ kips}$$

Step 6. Select bolt diameter

$$B = \frac{154.79}{4} + 5.79 = 44.49 \text{ kips}$$

$$d_b = \sqrt{44.49 \times 2/\pi(44.0)}$$

$$0.802 \text{ in} < 0.875 \text{ in.}$$

Use PL 7x3/4 A36 and 4- 7/8 in. diameter A325 bolts. This result is exactly the same as that arrived at in the AISC Manual, except for end-plate width.

For the stiffened extended end-plates, it is recommended that Equations 2.24 or 2.26 be used to determine the end-plate thickness for a given moment. Again the design is based on strength requirements only. The above design example is repeated here to demonstrate the recommended design procedure.

Design Example (4). Determine the required plate thickness for the connection given in example (3) if a stiffened extended end-plate is to be used.

Step 1. Determine M_u and end-plate thickness.

$$M_u = 120/0.6 = 200 \text{ ft.-Kips}$$

Assume $d_e < s = \frac{1}{2}\sqrt{6.995 \times 2.75} = 2.193$ in.

$$t_p = \left[\frac{200 \times 12/36}{\{\frac{6.995}{2}(\frac{1}{1.5}+\frac{1}{2.193})+(1.5+2.193)(\frac{2}{2.75})\}\{(16.01-2.005)+(16.01+1.05)\}}\right]^{\frac{1}{2}}$$

$$= 0.566 \text{ in.} \qquad \text{Try PL 7x5/8}$$

Step 2. Compute flange force and flange stress

$$F_f = (200 \times 12)/(16.01-0.505) = 154.79 \text{ kips}$$

$$\sigma_f = 154.79/(6.995 \times 0.505) = 43.82 \text{ ksi}$$

Setp 3. Find the thick plate limit, t_1

Approximate thickness (Equation 2.27)

$$t_1 = \sqrt{2.11 \times 1.5 \times 0.505 \times 43.82/36}$$

$$= 1.395 \text{ in.} >> t_p = 0.625$$

Therefore, $Q \neq 0$

Step 4. Determine thin plate limit, t_{11}.

Assume $d_b = 7/8$ in.

$w' = 2.56$ in.

Approximate thickness, from Example (3):

$$t_{11} = 1.226 \text{ in.} >> t_p = 0.625$$

Therefore, $Q = Q_{max}$

Step 5. Determine prying force, Q

$$F_{limit} = \frac{0.625^2(36)(0.85 \times 6.995 + 0.80 \times 2.56) + \pi(0.875)^3(120)/16}{4(1.5)}$$

$$= 21.37 \text{ kips}$$

$$F_{max} = 63.58 \text{ kips}$$

From Equation (2.35)

$$Q_{max} = \frac{2.56 \times (0.625)^2}{4 \times 1.25} \sqrt{36^2 - 3\left(\frac{21.37}{2.56 \times 0.625}\right)^2}$$

$$= 5.25 \text{ kips}$$

Step 6. Select bolt diameter.

$$B = \frac{154.79}{4} + 5.52 = 44.22 \text{ kips}$$

$$d_b = \sqrt{44.22 \times 2/\pi(44.0)}$$

$$= 0.799 \text{ in.} < 0.875 \text{ in.}$$

Use PL 7x5/8 A36 and 4- 7/8 in. diameter A325 bolts.

The addition of the end-plate to tension flange stiffener resulted in a reduction in required end-plate thickness of 0.146 in. (0.712 in. versus 0.566 in.). The required bolt diameter remained the same for both designs. It is believed that the stiffness of the connection increases with the use of stiffeners, but experimental data is not available to substantiate this contention.

As a final comparison, the end-plate thicknesses determined in the previous examples are listed in Table 4.2 along with required thicknesses obtained using the various methods discussed in Chapter I. The first two columns in Table 4.2 give the thicknesses for the two-bolt and the four-bolt flush end-plates required for Type I Construction. Douty and McGuire[1] suggest a design procedure which is very conservative. The other suggested design procedures require that the tension bolt force be less than the bolt proof load. Hence, they satisfy both the strength and the stiffness requirements. Comparing the results given in Table 4.2, it is seen that the recommended design procedure for the flush end-plates results in a thinner end-plate than all the other design procedures, except Zoetermeijer's. The last two columns give the thicknesses required for the extended end-plates in Type III Construction. All the methods compared are based on the strength requirements only. The thicknesses obtained by the recommended design procedure are lower than or equal to the values obtained by the other methods.

The design procedures presented herein are based on specific

Table 4.2
Design Comparisons

Method	End-Plate Thickness, t_p (in.)			
	Flush End-Plates		Extended End-Plates	
	Ex. 1-(b)	Ex. 2-(b)	Ex. 3	Ex. 4
Recommended Procedure	0.47	0.35	0.75	0.625
Douty and McGuire	1.22	1.22		
Blockley		0.80		
German Specifications	0.95	0.95		
French Specifications	1.12	1.12		
Zoetermeijer	0.55			
Mann and Morris			0.72	0.72
Krishnamurthy			0.73	0.73
Kennedy et. al.	0.74		0.90	0.90

yield-line mechanisms. Significant changes in the geometric relationships can affect the mechanism configuration and thus the predicted capacity. For these reasons the following limitations apply to the four design procedures presented herein:

$$p_f \leq 2.0 \text{ in.} \qquad \frac{t_p}{d_b} \leq 1.0$$

$$g \leq 4.0 \text{ in.} \qquad \frac{b_f}{g} \leq 2.25$$

Specific recommendations for flange to end-plate and web to end-plate welds are not included in this study. Additional research is needed, particularly for the web weld, before design recommendations can be made. Finally, the design procedure developed for stiffened extended end-plates has not been substantiated with tests and it is recommended that tests be conducted before the procedure is used in routine design.

REFERENCES

1. Douty, R.T. and W. McGuire, "High Strength Bolted Moment Connections", Journal of the Structural Division, ASCE, Vol. 91, No. ST2, April 1965, pp. 101-128.

2. Blockley, D.I., "The Design of Single Story Pitched Roof Portal Frames", BCSA Brochure, 1970.

3. DSTV/DAST, Moment and Plate Connections with HSFG Bolts (in German), IHE 1, 1978.

4. Norme Francaise Enregistree, Metal Construction, Joining by means of Bolts Controlled Tightening, Structural Requirements and Checking of Jointing (in French), NF, 1979, pp. 22-460.

5. Zoetermeijer, P., "Semi-Rigid Bolted Beam-to-Beam Column Connections with Stiffened Column Flanges and Flush End-Plates", Joints in Structural Steelwork, Proceedings of the International Conference on Joints in Steelwork, held at Middlesbrough, Cleveland, John Wiley and Sons, New York - Toronto, 1981, pp. 2.99-2.118.

6. Packer, J.A. and L.J. Morris, "A Limit State Design Method for the Tension Region of Bolted Beam-Column Connections", The Structural Engineer, Vol.5, No. 10, October, 1977.

7. Phillips, J. and J.A. Parker, "The Effect of Plate Thickness on Flush End-Plate Connections", Joints in Structural Steelwork, Proceedings of the International Conference on Joints in Steelwork, held at Meddlesbrough, Cleveland, John Wiley and Sons, New York - Toronto, 1981, pp. 6.77-6.92.

8. Mann, A.P. and L.J. Morris, "Limit Design of Extended End-Plate Connections", Journal of the Structural Division, ASCE, Vol. 105, No. ST3, March 1979, pp. 511-526.

9. Krishnamurthy, N., "Fresh Look at Bolted End-Plate Behavior and Design", Engineering Journal, AISC Vol. 15, No. 2, Second Quarter, 1978, pp. 39-49.

10. Manual of Steel Construction, 8th ed., American Institute of Steel

Construction, Chicago, Illinois, 1980.

11. Krishnamurthy, N., "Experimental Validation of End-Plate Connection Design", Report Submitted to the American Institute of Steel Construction, April 1979.

12. Krishnamurthy, N., "Experimental Investigation of Thin Splice-Plate Connections", Report submitted to the Metal Building Manufacturing Association, May 1980.

13. Krishnamurthy, N., "Analytical Investigation of Bolted Stiffened Tee Stubs", Report submitted to the Metal Building Manufacturing Association, December 1978.

14. Krishnamurthy, N., "Experimental Investigation of Bolted Stiffened Tee Stubs", Report Submitted to the Metal Building Manufacturing Association, May 1979.

15. Kennedy, N.A., Vinnakota, S. and A.N. Sherbourne, "The Split-Tee Analogy in Bolted Splices and Beam-Column Connections", Joints in Structural Steelwork, Proceedings of the International Conference on Joints in Steelwork, held at Middlesbrough, Cleveland, John Wiley and Sons, New York - Toronto, 1981, pp. 2.138-2.157.

16. Mansfield, E.H., "Studies in Collapse Analysis of Rigid-Plastic Plates with a Square Yield Diagram", Proceedings of the Royal Society London, 241, Series A, August 1957, p. 311-338.

17. Abolmaali, Ali, "Elasto-Plastic Finite Element Modeling and Analysis of a Flush End-Plate Connection", A Thesis submitted to the Graduate Faculty in partial Fulfillment of the Requirements for the Degree of Master of Science, School of Civil Engineering and Environmental of Science, University of Oklahoma, Norman, Oklahoma, (in preparation).

18. "Specification for the Design, Fabrication and Erection of Structural Steel for Buildings", American Institute of Steel Construction, New York, 1978.

APPENDIX A

NOMENCLATURE

NOMENCLATURE

a = distance from edge of end-plate to the bolt line

a_1 = distance from bolt centerline to edge of web root fillet

a_5 = distance from top bolt row centerline to edge of flange root fillet

B = bolt force

B_1 = outer bolt force

B_2 = inner bolt force

b_f = beam flange width

$c = (b_f - g)/2$ = end-plate bolt edge distance

$c_1 = (p_f - 3/2t_f - t_p/2$ - diameter of washer/4)

d_b = bolt diameter

d_e = distance from bolt line above tension flange to edge of plate

d_h = bolt hole diameter

ds = elemental length of line n

ds_x = the x-component of the elemental length ds

ds_y = the y-component of the elemental length ds

E = Young's modulus of elasticity

F = flange force per bolt

F_a = allowable bolt stress

f_b = bending stress

F_{by} = yield stress of beam material

F_f = flange force = $Mu/(d-t_f)$

F_{limit} = flange force at which the end-plate becomes "thin"

F_{py} = yield stress of plate material

F_t = tensile strength of bolt material

F_{yb} = yield stress of bolt material

g = gage distance between bolts

h = beam depth

h_s = distance between bolt centerline and compression flange

I = moment of inertia

L = length of beam

Ln = length of yield line n

M_u = ultimate moment at end-plate

M_{yb} = moment at which the experimental bolt force is at the proof load (twice the allowable)

M_{ys} = moment at which the experimental plate separation exceeds the predicted separation by 10%

M_{yv} = moment at which the experimental vertical deflection exceeds the predicted deflection by 10%

m_p = plastic moment capacity of plate per unit length, equal to $F_{py}t_p^2/4$

m_{px} (m_{py}) = the x(y)-component of the normal moment capacity per unit length

m_{px} = the y-component of the normal moment capacity per unit length

N = number of yield lines in a mechanism

P_b = pitch between upper and lower rows of the tension bolts

P_f = pitch measured from bottom of flange to centerline of first bolt row

P_p = bolt proof load

P_T = Pretension force

P_t = pitch measured from top of flange to centerline of the first bolt row

Q = prying force

s = distance from bolt centerline to the lower yield line

s_t = stiffener thickness

t_f = flange thickness

t_p = end-plate thickness

t_1 = thick plate limit

t_{11} = thin plate limit

w_i = total internal energy stored

w = width of end-plate per bolt pair

w_{in} = internal work done in the nth yield line

w' = width of end-plate per bolt at bolt line minus bolt hole diameter

x = distance from the edge of the bolt head to the beam web

α_s = plate separation correction factor

σ = coefficient depending on bolt arrangement (Zoetermeijer)

β = angle between the edges

δ = normalized displacement at bolt line

Δ_c = vertical displacement

δ_{max} = maximum vertical deflection (at centerline of beam)

δ_p = plate separation

θ_n = relative normal rotation of yield line n

θ_{nx} = the x-component of the relative normal rotation of the yield line n

θ_{ny} = the y-component of the relative normal rotation of the yield line n

σ_f = stress in beam flange

σ_{yb} = yield stress of bolt material

APPENDIX B

YIELD-LINE PATTERNS

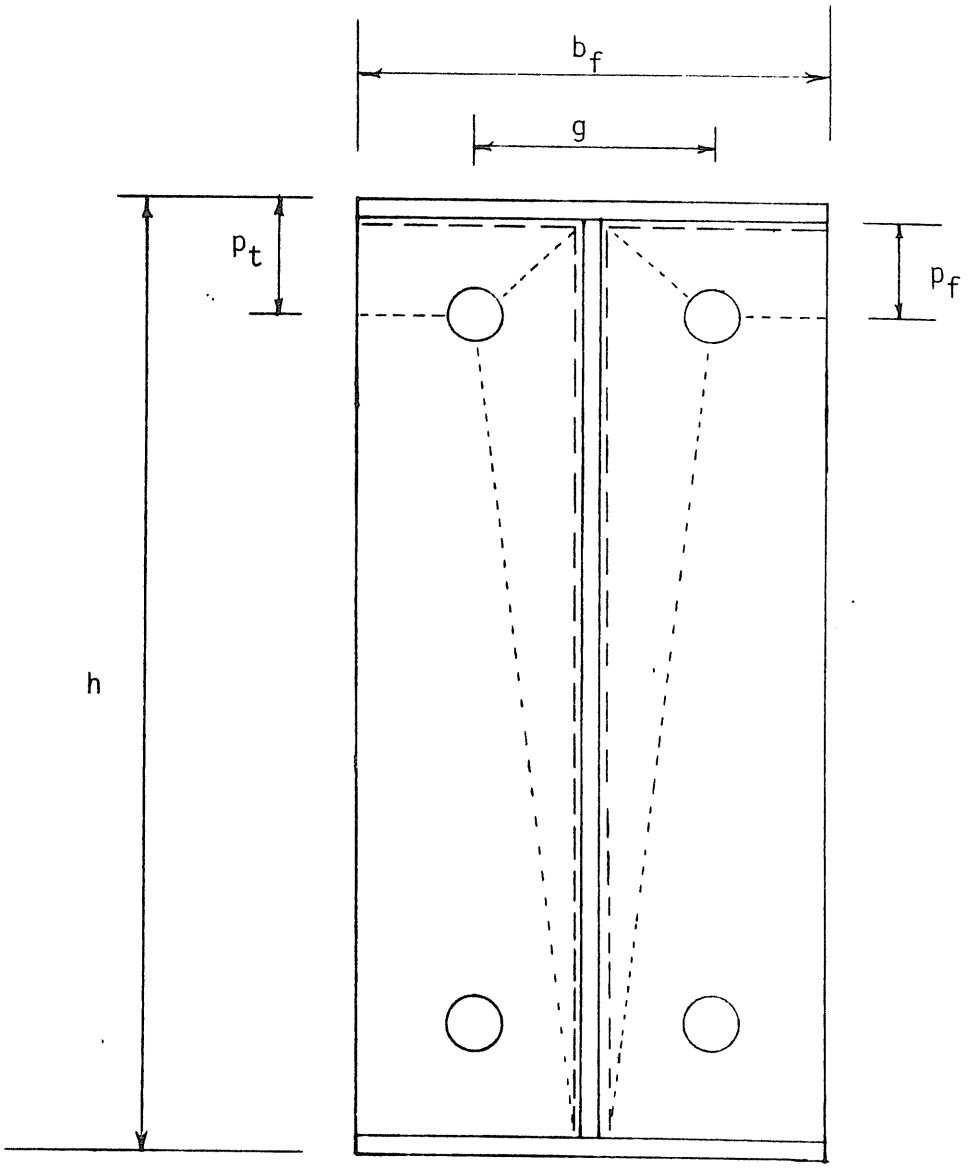

Figure B1 Mechanism F1-1

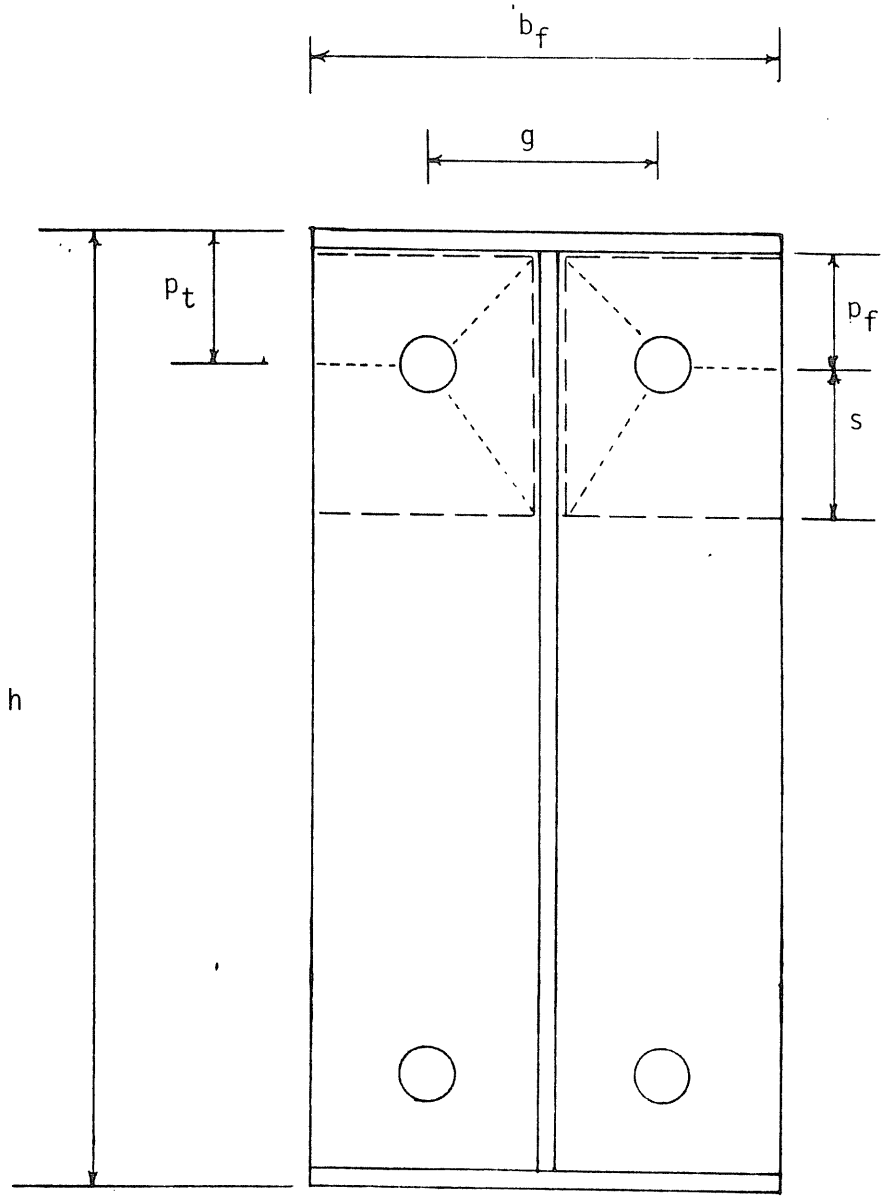

Figure B2 Mechansim F1-2

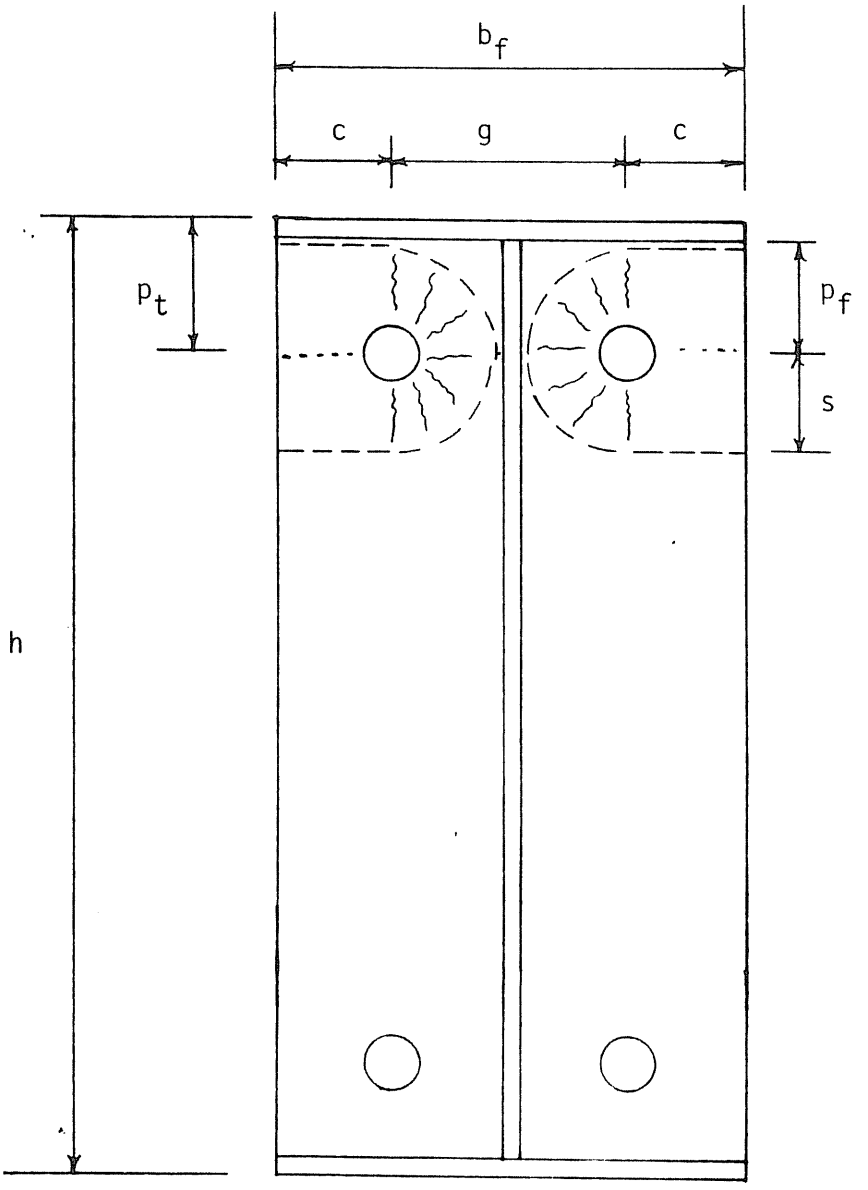

Figure B3 Mechanism F1-3

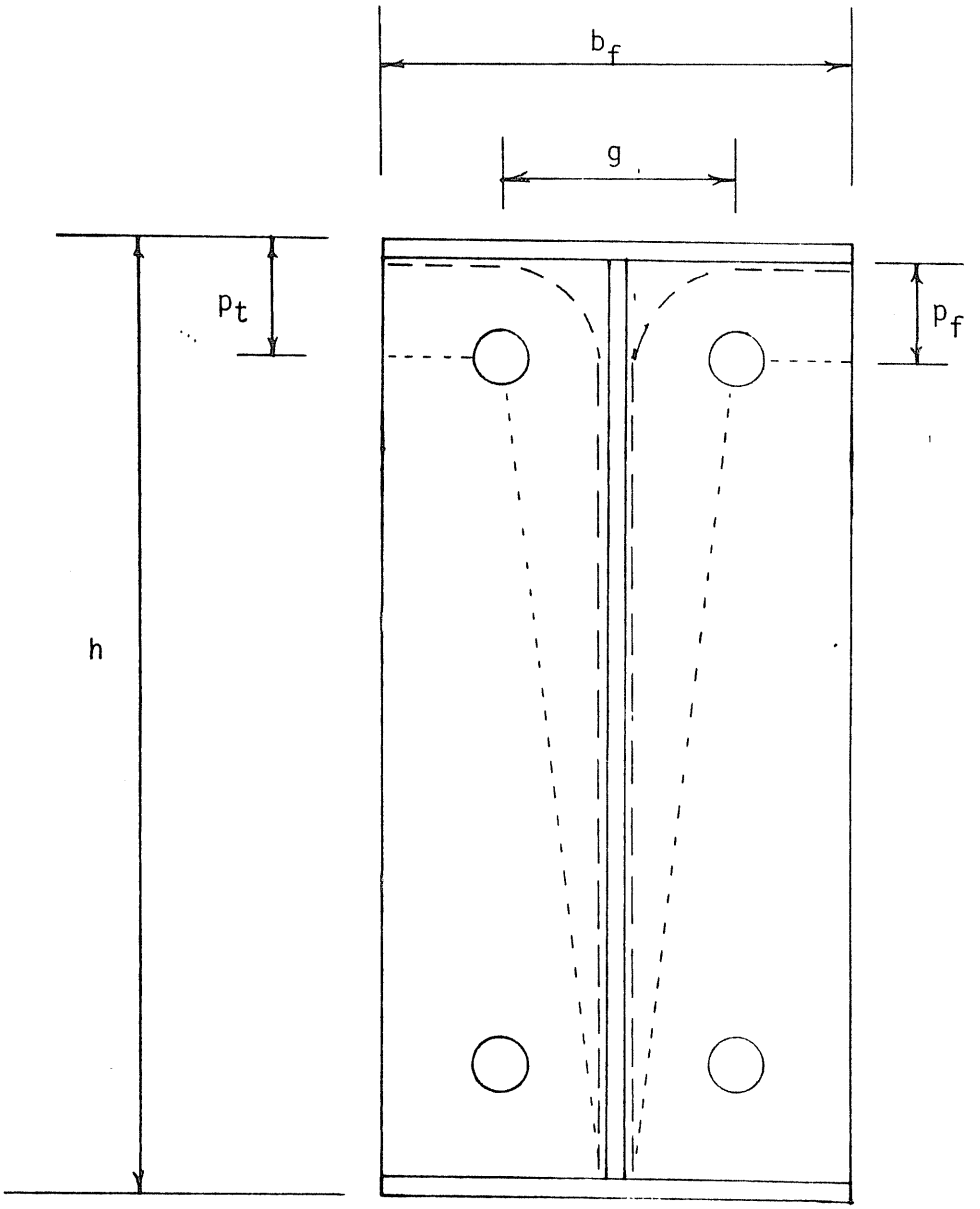

Figure B4 Mechanism F1-4

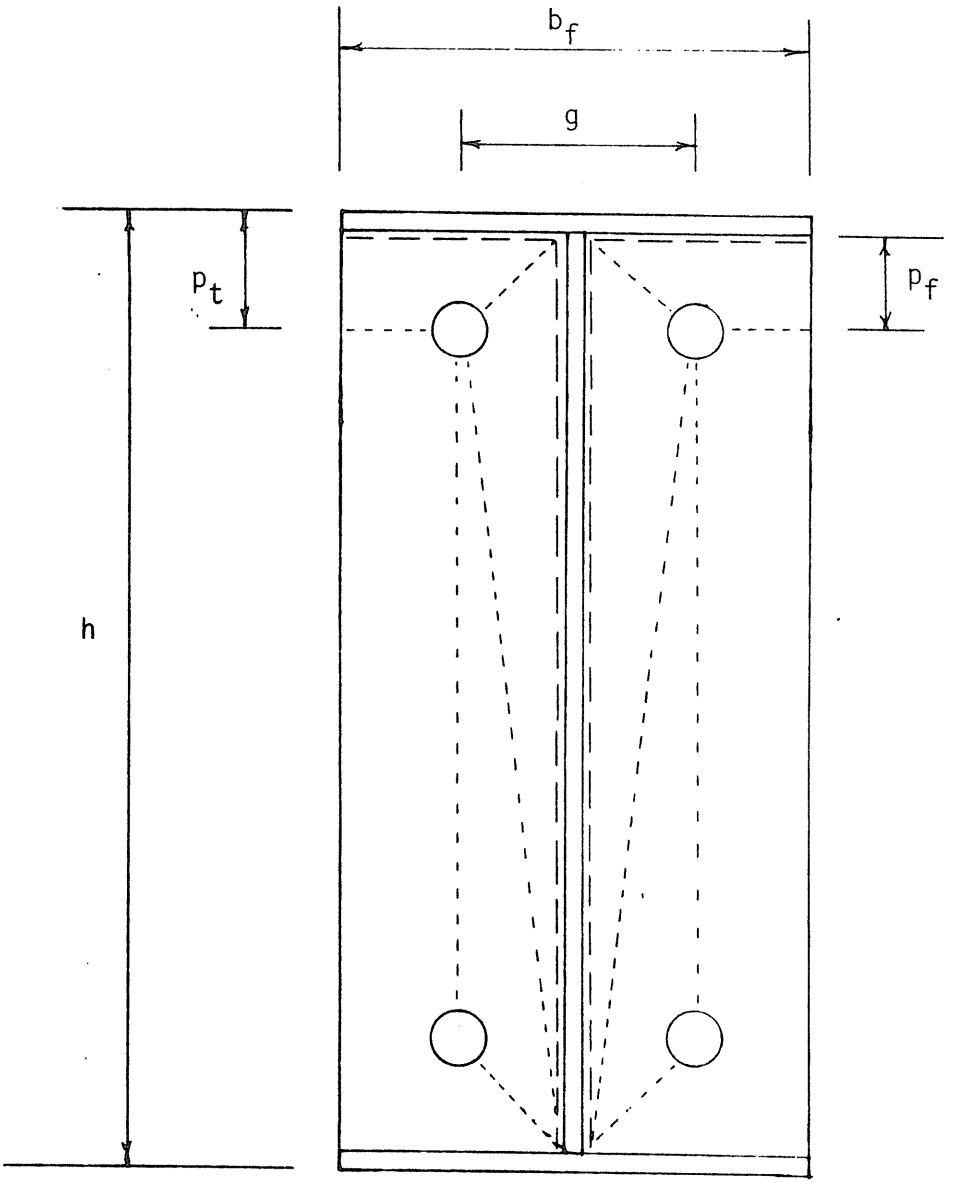

Figure B5 Mechanism F1-5

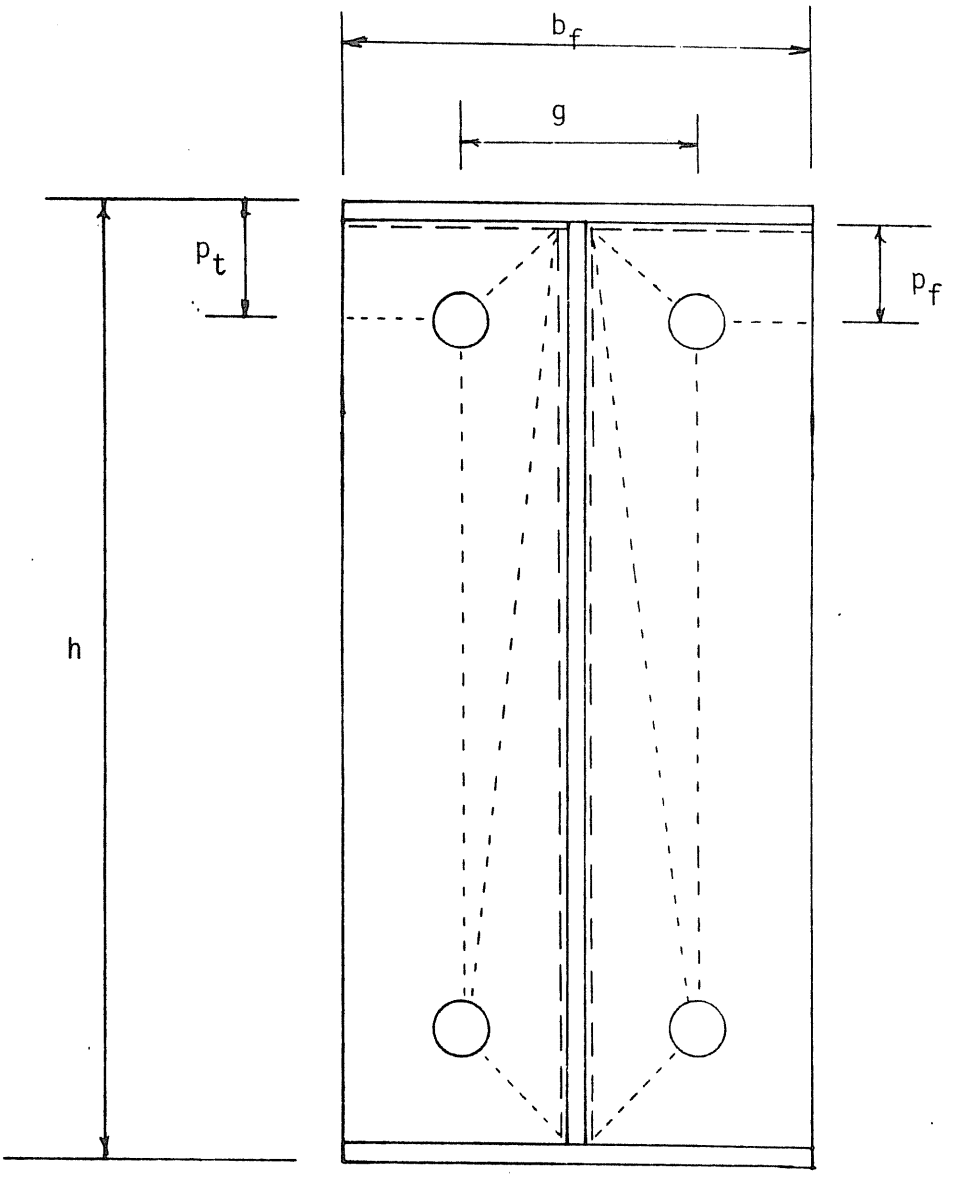

Figure B6 Mechanism F1-6

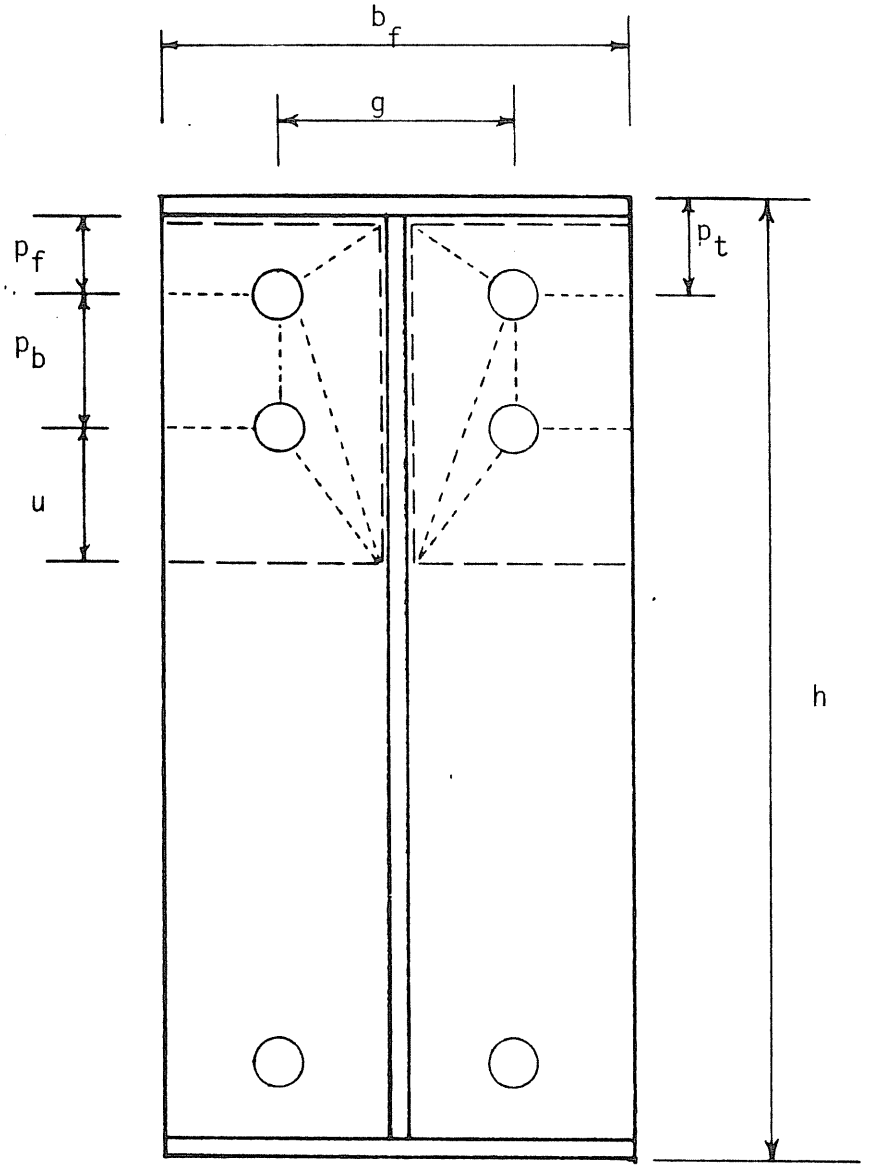

Figure B7 Mechanism F2-1

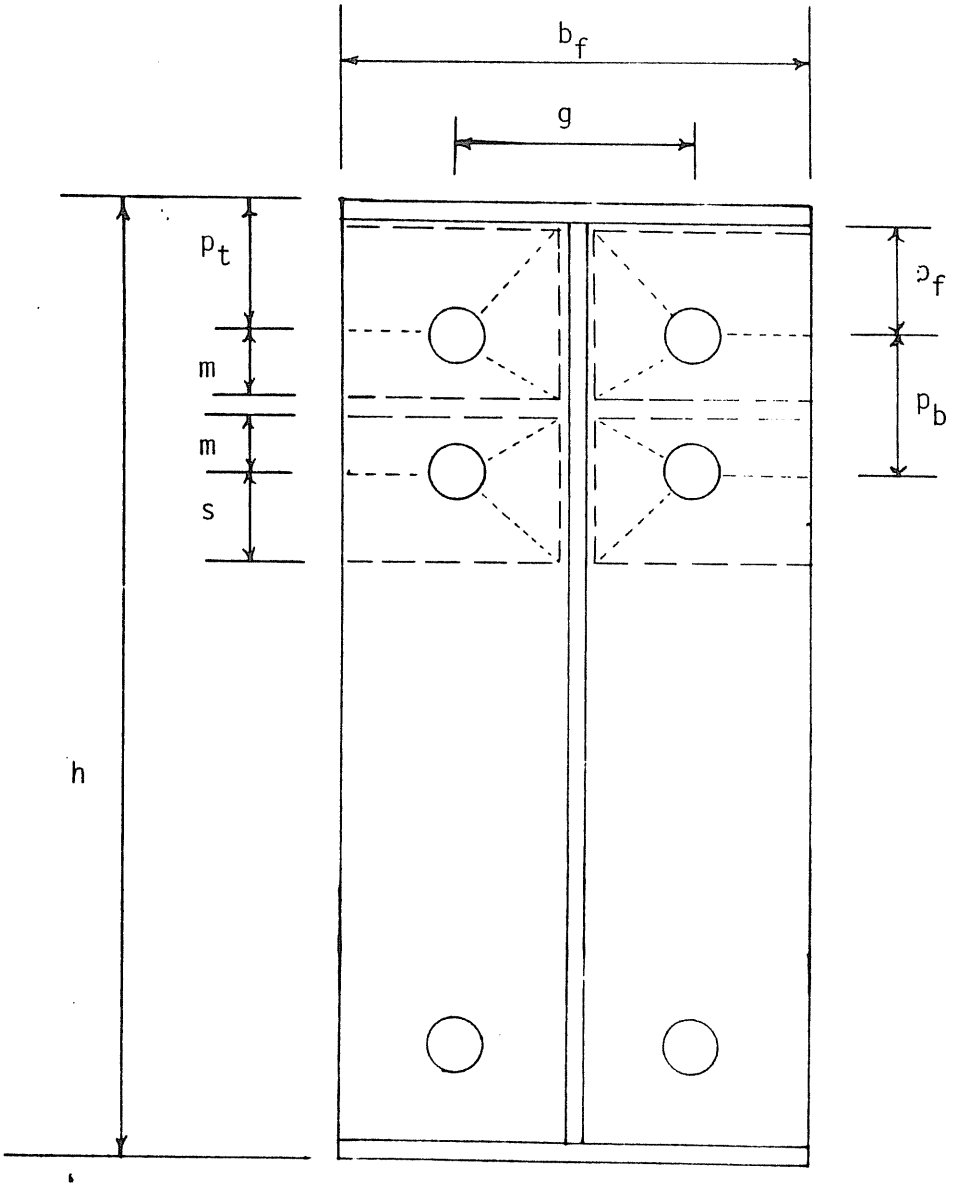

Figure B8 Mechanism F2-2

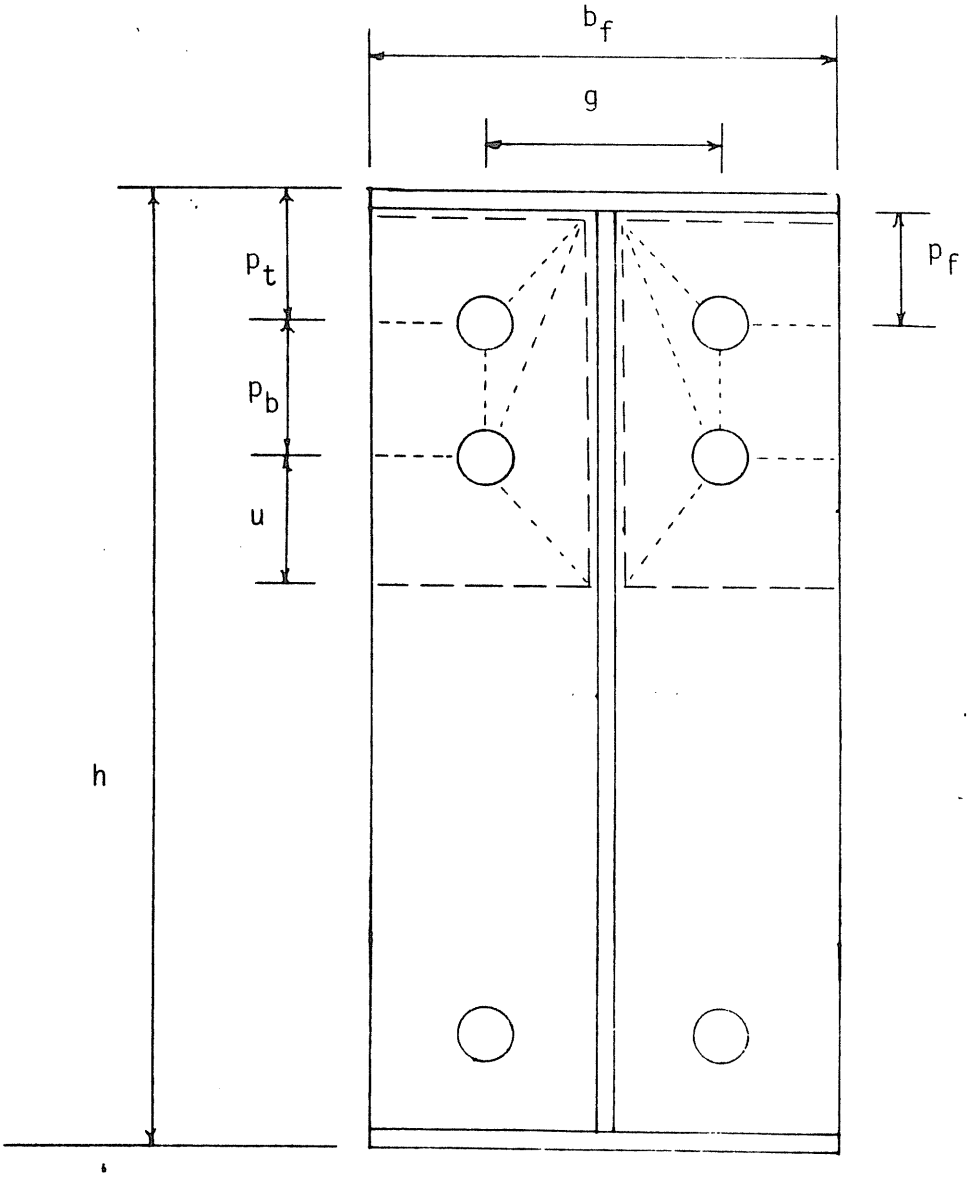

Figure B9 Mechanism F2-3

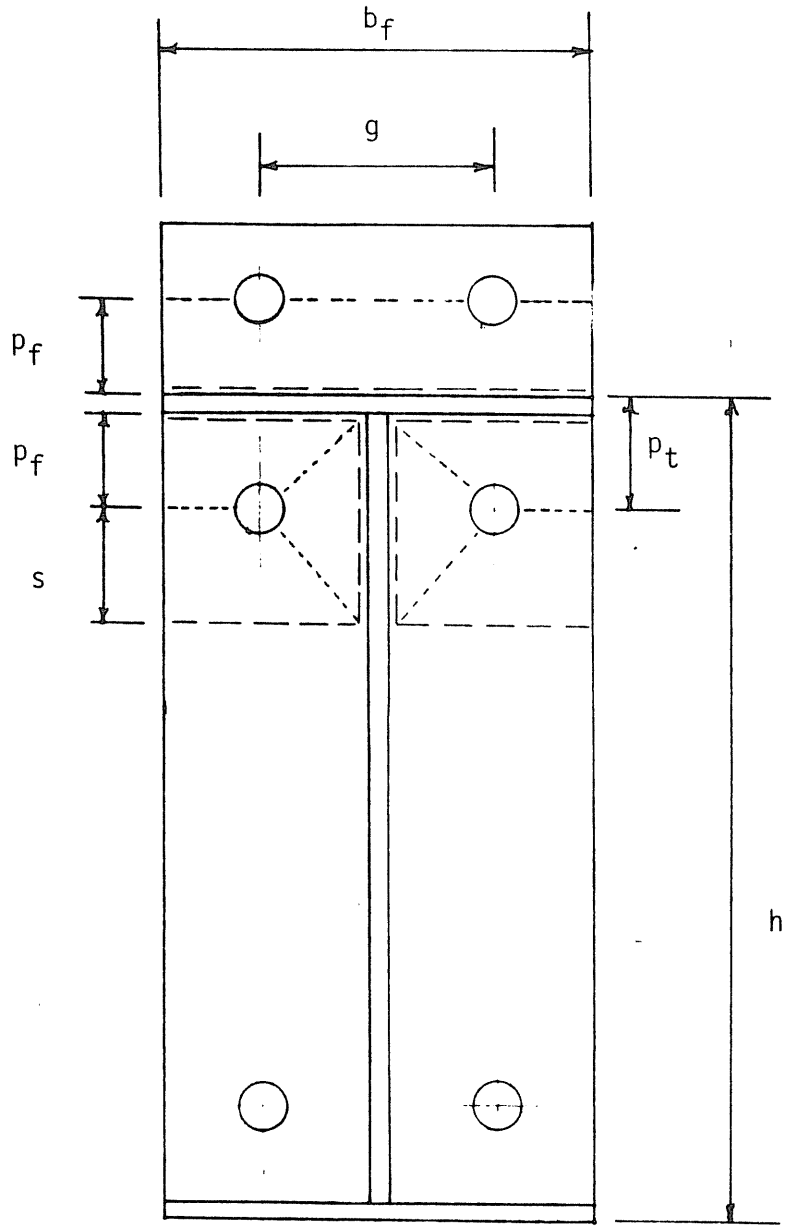

Figure B10 Mechanism UE-1

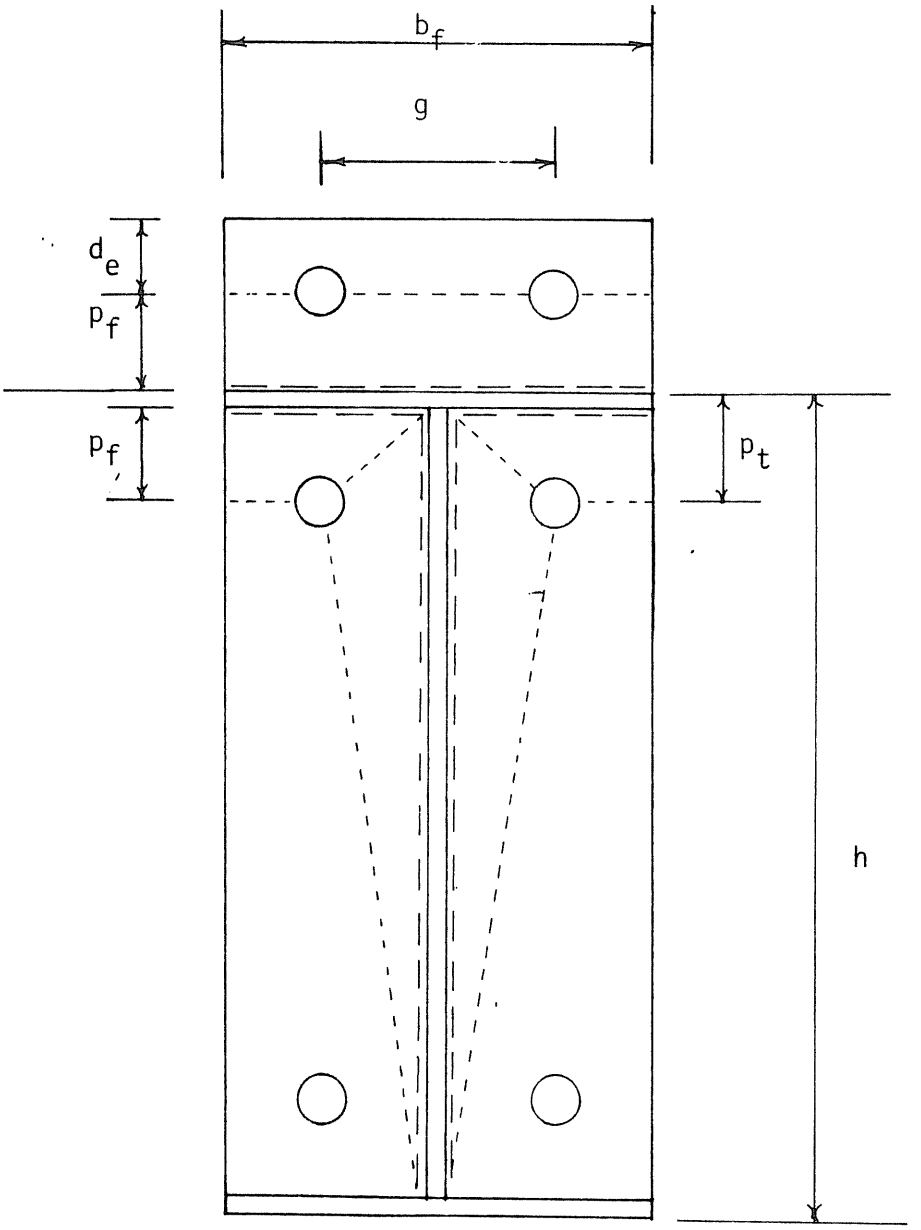

Figure B11 Mechanism UE-2

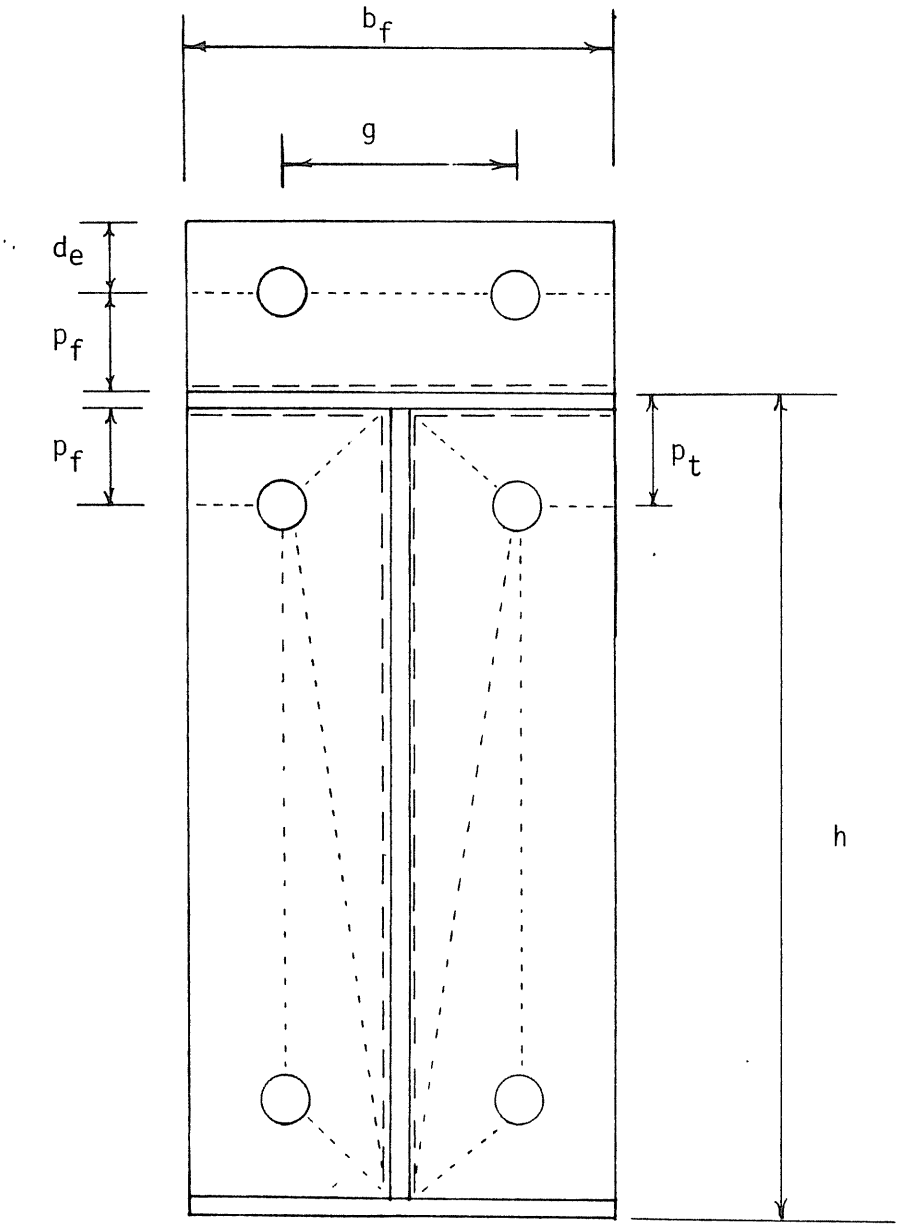

Figure B12 Mechanism UE-3

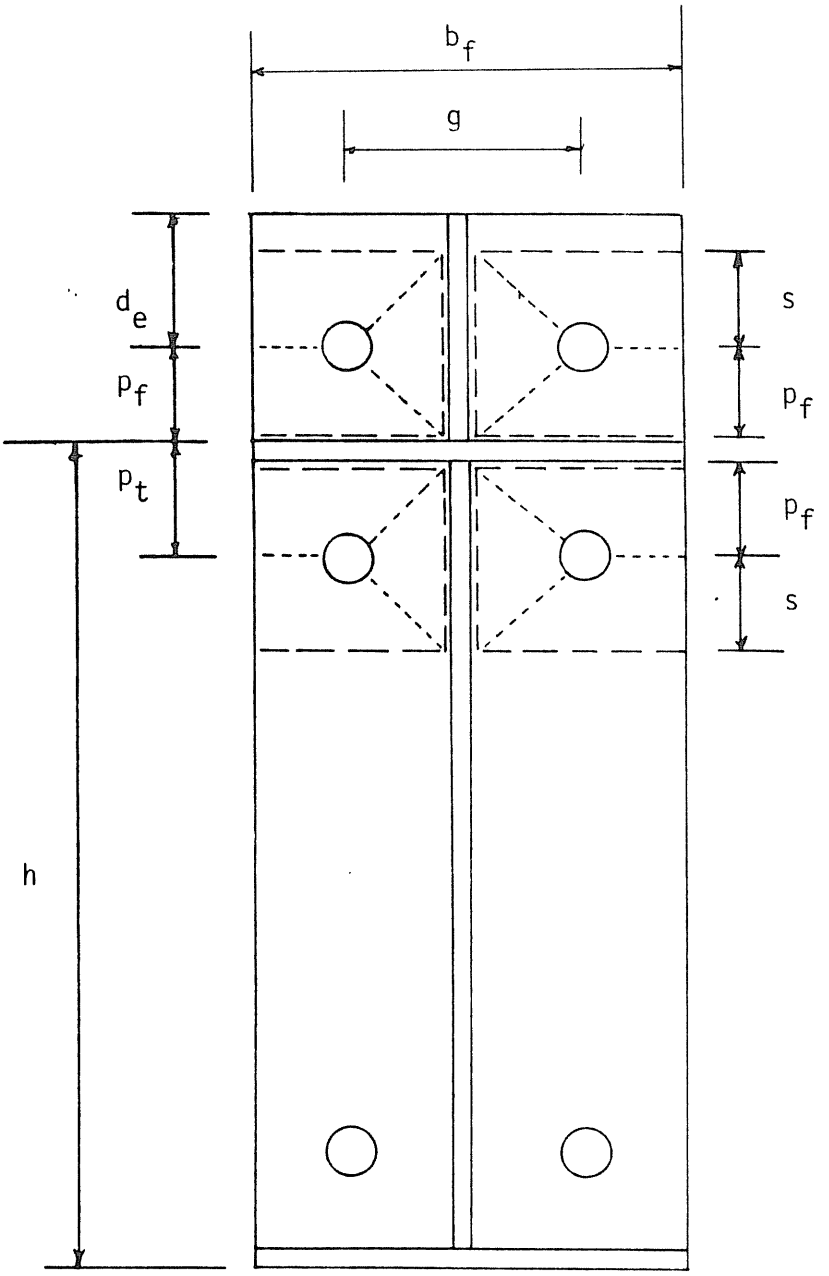

Figure B13 Mechanism SE-1

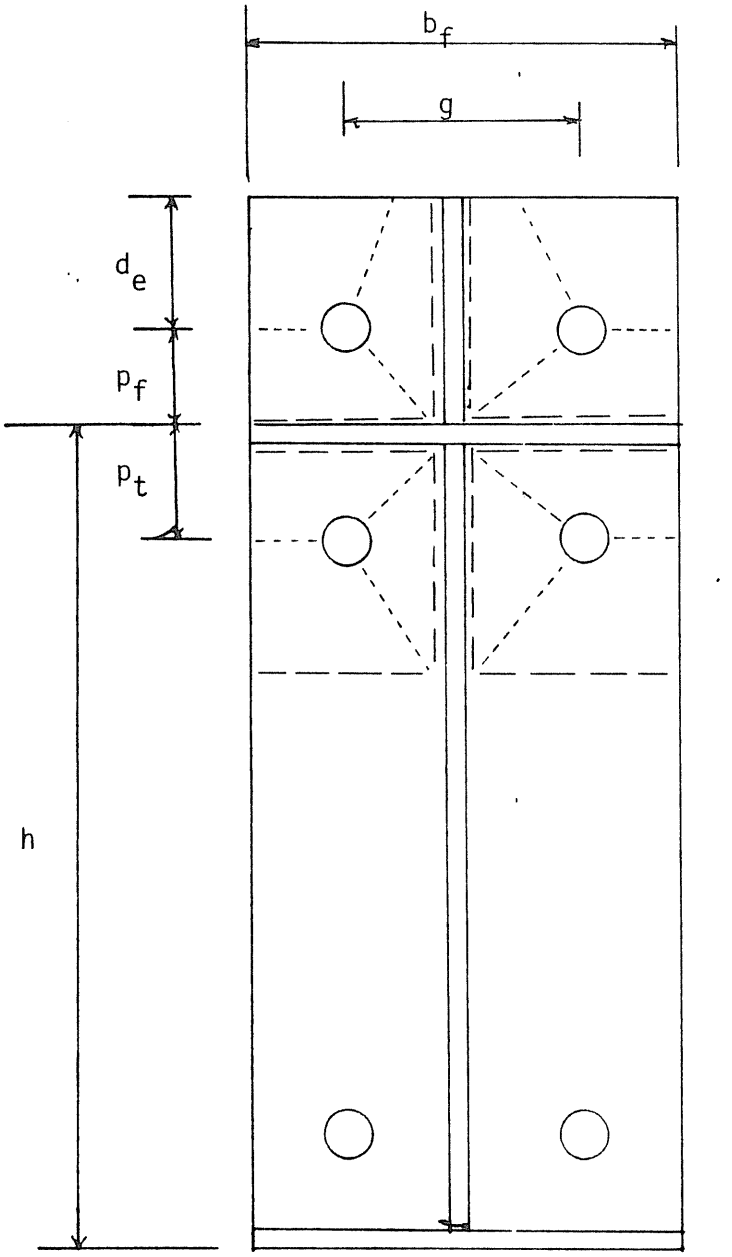

Figure B14 Mechanism SE-2

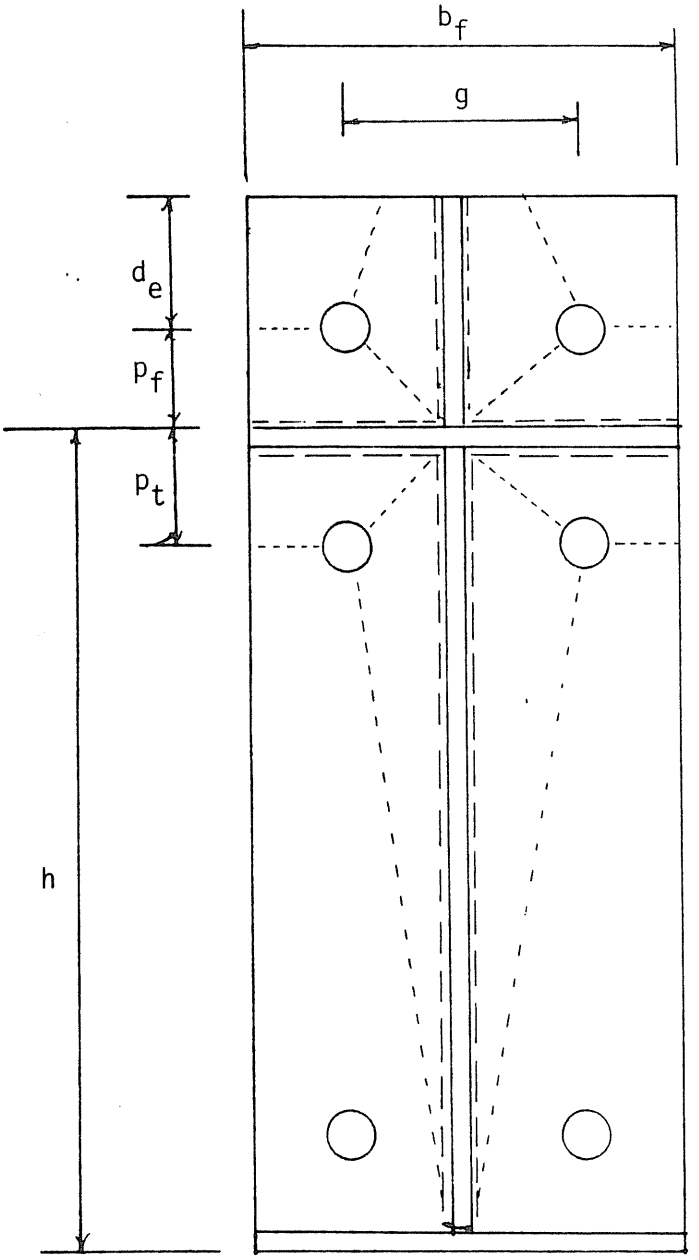

Figure B15 Mechanism SE-3